UNIVERSITÀ DEGLI STUDI DI PARMA

DIPARTIMENTO DI FARMACIA

Dottorato di ricerca in BIOFARMACEUTICA-FARMACOCINETICA

CICLO XXVII (2012-2014)

STUDY OF DRUG-MACROMOLECULE INTERACTIONS FOR THE DEVELOPMENT OF NEW ORAL CONTROLLED DELIVERY SYSTEMS

Coordinator: Chiar.mo Prof. PAOLO COLOMBO

Supervisor: Chiar.mo Prof. RUGGERO BETTINI

PhD Candidate: SIMONA DE ROBERTIS

INDEX

I. INTRODUCTION

I. INTRODUCTION

1. CONTROLLED DRUG DELIVERY

The 8th edition of European Pharmacopoeia defines a controlled drug delivery system as "a preparation where the rate and/or place of release of the active substance(s) is different from that of a conventional-release dosage form administered by the same route. This deliberated modification is achieved by a special formulation design and/or manufacturing method" [1].

The concept that the form of a medicament could be used to influence the drug effect firstly appeared in the 1924 edition of the Martindale and Wescott's *The Extra Pharmacopoeia*. The dissertation was about enteric coated pills and their effect in minimizing the adverse effect of drugs on mucous barriers. The German dermatologist Dr Paul Unna marketed keratin-coated pills in 1921, even though the use of these systems were reported in a *Lancet* paper of 1893. However, the basis of the modern idea for controlled drug delivery were established in 1960, when the first polymeric delivery devices, such as Ocusert® and Progestesert®, were developed by the Alza company [2]. Since then, academia and industry focused their efforts in this novel field of pharmaceutical research, leading to a massive and differentiated development of original products. Currently, there are more than 1400 controlled release systems approved all around the word [3]. The market of these medicaments is rated to be about $70 billion worldwide, with sales volume in the oral controlled drug delivery expected to increase of 9% every year [4].

The reason of the success of controlled delivery systems is related to the numerous advantages that they can offer. Systems providing constant drug release rate can reduce drug level fluctuations in blood and maintain a steady state concentration over a prolonged period of time. Thus, drug plasma levels are kept within a narrow window with no sharp peaks, with a subsequent reduction of adverse side effects, of the dose frequency and a general improvement of patient compliance. Furthermore, it is possible to target the drug delivery to its site of absorption or action, reducing unwanted side effects.

Besides these aspects, the development of controlled release dosage forms are attractive economical options for pharmaceutical companies. The introduction of new molecular entities is currently weak and Regulatory Agencies are demanding more cautious review processes and a greater number of complex clinical trials to authorise new drugs in the market. In addition, in the last few years, at least 20 blockbusters lost their patent protection. Therefore, the re-patentability of existing conventional release products as controlled delivery

formulation is a valuable possibility to overcome the difficulties in the drug market that companies are facing [4].

1.1 Oral controlled drug delivery

The oral route is the most common administration of drugs due to ease of ingestion and pain avoidance. In addition, solid dosage forms are versatile, being able of accommodating various drug candidates, do not require sterile operative conditions and are less expensive to manufacture. Therefore, it is not surprising that they represent a large part of the portfolio of pharmaceutical companies.

The main purpose for oral controlled drug delivery systems is to achieve a constant release rate of the active with a consequent constant rate of absorption, so that plasmatic steady levels can be assured.

Oral controlled drug delivery can offer other advantages simply by targeting the system to a particular zone of the gastro-intestinal tract. For example, gastric retentive forms can be used to target the release of the active to the stomach for the treatment of local diseases, to promote the absorption of drugs poorly soluble or chemically instable in the upper and large intestine [5].

Colonic delivery can improve the bioavailability of drugs substrate of efflux pumps or cytochromes, since their levels are particularly low in the lower intestine. Chronotherapy is a novel strategy to treat diseases showing exacerbations in particular moments of the day. Diseases such as angina pectoris, rheumatoid arthritis, which are worse in the morning, could benefit from colonic delivery, by taking at night a system that reach the colon and deliver the dose before awakening [6].

The principal dosage forms used to obtain oral controlled drug delivery are reservoir systems and matrix monolithic systems [7].

Reservoir systems consist of a drug-containing core coated by a polymeric membrane. In the classical reservoir system, the core is surrounded by a hydrophilic or water-insoluble coating and drug release is obtained by diffusion of drug through the membrane. Osmotic pumps can be considered a special class of reservoir systems. In these products, the coating is a semipermeable membrane with a mechanical or laser-drilled hole. The drug core usually contains osmotic agents to generate, within the system, the osmotic pressure necessary for the release of the drug as a saturated solution from the hole.

Monolithic matrix systems consist of a release-rate controlling polymer where the drug is dissolved or dispersed. Again, depending on the nature of the polymer, it is possible to distinguish between inert matrices and hydrophilic matrices.

Inert matrix systems are made of water-insoluble polymers. Drug release occurs by liquid penetration through pores present in the matrix, leading to the dissolution of the drug embedded and its diffusion through the matrix. In hydrophilic matrix systems, known also as swellable matrices, the drug is dissolved or dispersed in a water-soluble polymer. The drug is released via diffusion through the gel layer generating after hydration of the polymer. Hydrophilic matrices are extensively discussed in the following section.

2. HYDROPHILIC MATRIX SYSTEMS

Hydrophilic matrix systems, also known as swellable matrices, are generally solid oral formulations made of drug dissolved or dispersed in a water-soluble polymer. They are commonly manufactured by direct compression, wet or dry granulation and hot melt extrusion.

The polymers more frequently used are some cellulose esters (hypromellose, hydroxypropyl cellulose and sodium carboxymethylcellulose), polyethylene oxide, carbomers, sodium alginate and xantham gum [7].

Drug release from these delivery systems is basically regulated by solvent-polymer interaction and solvent-drug interaction.

The presence of solvent in contact with the matrix determine a reduction of the glassy-rubbery transition temperature of the polymer, whose chains gradually start to disentangle and hydrate. The macroscopic evidence of the polymeric transition is the formation of a superficial layer of gel, which acts as barrier for the drug release. As the solvent penetrates the matrix, the drug gradually dissolves and reaches the external receiving medium by diffusing through the gel layer. With the ongoing hydration of the matrix, the superficial gel weakens and the polymer gradually dissolves. The progressive erosion of the matrix surface leads to the reduction of its size, until the system is completely dissolved [8].

Changes in the matrix structure, during a typical study of dissolution in vitro, can be described by the position of the so-called “moving fronts”. A front is a boundary between two areas in a different physical state within the matrix. Usually, starting from the centre of the matrix, three fronts are observed (Fig. 1):

- SWELLING FRONT: boundary between the dry core and the swelled matrix;
- DIFFUSION FRONT: boundary between the undissolved solid drug and the drug in solution within the gel layer. It is more common to observe the diffusion front if the drug has a limited solubility in water;
- EROSION FRONT: boundary between the matrix and the dissolution medium [9].

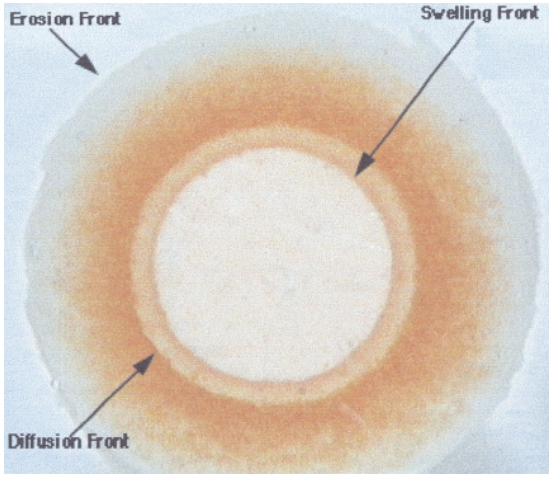

Figure 1. Image of a HPMC matrix containing buflomedil pyridoxal phosphate taken after 240 minutes of swelling [10].

The relative movement of erosion and swelling fronts determines the thickness of the gel layer and drug release rate and kinetics, since drug release occurs by diffusion through the gel layer.

First, the erosion front moves outwards upon contact with the solvent, while the swelling front moves inwards as a result of water penetration. Thus, at the early stage of the dissolution process, the gel thickness increases. As the hydration process continues, the erosion front moves inwards, in the same direction of the swelling front, because of the progressive dissolution of polymer chains in the medium. If the rate of movement of both fronts is the same, the gel thickness is constant. In this phase, the synchronization of the two fronts produces a constant drug release. Finally, when all the polymer is swollen, only erosion occurs and the gel thickness decreases until the matrix is completely dissolved [8].

The presence of a visible diffusion front depends on the drug solubility. If the drug is highly soluble, it easily dissolves in the small volume of water present in the gel layer. Therefore, undissolved drug is present only in the dry core of the matrix and the diffusion front coincides with the swelling front. For poorly soluble drugs, the diffusion front is observed within the swollen gel layer. The movement of this front depends on the drug solubility: it tends to be faster when the drug solubility is higher, providing also higher release rate. In addition, drug solubility affects also the thickness of the diffusion front and its rate of change. In systems where a diffusion front is present, the polymer relaxation near the swelling front may be reduced by the undissolved drug. Here the drug dissolution and its subsequent diffusion through the gel layer is more important in controlling drug release than the gel thickness [9].

It is evident, then, that the performance of a matrix system, in terms of drug release rate and release kinetics, is highly influenced by the nature of the drug and the polymer used in the formulation.

2.1 Mathematical modelling of drug release from swellable matrices

The diffusion of a solute between two solutions separated by a membrane is classically described the first Fick's law:

$$J = \frac{dM}{Sdt} = -D\frac{dC}{dx} \qquad \text{(eq. 1)}$$

Here, the flux J (g/cm^2 s) is the amount of solute (M) crossing a plane of unit surface area (S) normal to the direction of transport, per unit time (t). The equation 1 states that the flux of a solute is proportional to the gradient of concentration dC/dx in the diffusion distance x. The proportionality constant D (cm^2/s) is the diffusion coefficient, which is a characteristic property of each solute and indicates its capability to diffuse in a determined solvent at a determined temperature. The negative sign in the equation 1 means that the flux occurs in the direction of decreasing concentration. The first Fick's law is valid only when steady state conditions are assumed, which means that solute concentrations in the two compartments separated by the membrane do not change with time.

When such variations occur, as would be the case of a drug diffusing from a swellable matrix through the gel layer, dC/dx is known at the beginning of the experiment, but the mass flow will continually modify the concentration gradient. Thus, it is necessary to introduce time as variable:

$$J = -D(x)\left(\frac{\partial C}{\partial x}\right)_t \qquad \text{(eq. 2)}$$

Equation 2 is the second Fick's law, where the partial derivative indicates that the derivative with respect to x is taken at certain time t. Here the diffusion coefficient has been assumed to be independent of time but can depend on position, hence it is written $D(x)$ [11].

Higuchi's solutions of the second Fick's law has been one of the most used to describe drug release from matrix systems [12]:

$$\frac{M_t}{A} = \sqrt{D(2c_0 - c_s)c_s t} \qquad \text{(eq. 3)}$$

Where M_t is the cumulative absolute amount of drug released at time *t*, *A* is the surface area of the controlled release device exposed to the release medium, *D* is the drug diffusivity in the polymer carrier, and c_0 and c_s are the initial drug concentration and the drug solubility, respectively.

Clearly, the Higuchi's equation states that the fraction of drug released from a matrix system is proportional to the square root of time. The limitations of this model are in the assumptions that Higuchi made to derive the relationship. The model is valid if the initial drug concentration c_0 in the matrix is much higher than its solubility c_s, the concentration gradient must be kept constant with time and perfect sink conditions are maintained. In addition, the mathematical analysis is based on one-dimensional diffusion through a slab and swelling or erosion of the polymer are not taken into account [13].

Peppas' semi-empirical equation, also known as power-law, is a more comprehensive model, which takes into account also polymeric swelling and erosion in describing drug release from a matrix delivery system:

$$\frac{M_t}{M_\infty} = kt^n \qquad \text{(eq. 4)}$$

Here, M_t and M_∞ are the absolute cumulative amount of drug released at time *t* and infinite time, respectively; *k* is a constant related to the geometric and structural characteristic of the matrix, and *n* is the release exponent, indicative of the mechanism of drug release.

For system where the Fickian diffusion is the main mechanism of release, *n* has a value of 0.5. *n* takes a value of 1 if the drug is released upon relaxation of the hydrated polymeric chains. This case corresponds to zero-order release kinetics. Values of *n* between 0.5 and 1 are typical of a particular kinetics, defined anomalous-Fickian, where both diffusion and relaxation mechanism contribute to drug release. The extreme values of 0.5 and 1 are valid only for matrices with the geometry of a thin film. For cylindrical matrices *n* takes the value of 0.45 for diffusion-controlled release and 0.89 for relaxation-controlled release [14, 15].

Another interesting model was developed by Peppas and Sahlin [16]:

$$\frac{M_t}{M_\infty} = k_1 t^m + k_2 t^{2m} \qquad \text{(eq. 5)}$$

Where k_1 and k_2 and *m* are constants. The first term on the right hand side represent the Fickian contribution, *F*, whereas the second term the relaxation contribution, *R*. The ratio of both contribution can be calculated as follows:

$$\frac{R}{F} = \frac{k_2 t^m}{k_1} \qquad \text{(eq.6)}$$

The mathematical description of the entire process of drug release from a swellable matrix remains rather complex, because of the number of physical process that must be taken in consideration, such as water penetration into the matrix, polymer swelling and erosion process, drug dissolution and diffusion, radial and axial transport in 3-dimensional system, moving fronts and changes in matrix dimension, porosity and compositions.

3. GEOMETRIC CONTROL OF DRUG RELEASE IN HYDROPHILIC MATRIX SYSTEMS

It has been established that, in a hydrophilic matrix, the release area which determines the release rate and kinetics, is the area of the swollen polymer comprised between the swelling and erosion front [8].

Colombo et al. [17] have demonstrated that geometric control of drug release can be obtained by coating with an impermeable polymer different areas of a hypromellose cylindrical matrix (Fig. 2). The shape of swollen matrices was different depending on the location of the impermeable coating:

- Case 0 was the uncoated matrix which showed swelling in the axial and radial direction.
- Case 1 had one coated base. The coated base showed a minor swelling than the uncoated one.
- Case 2 had two coated bases: swelling was mainly radially oriented.
- case 3 had the lateral surface coated which permitted only axial swelling.
- case 4 had one base and lateral surface coated. It exhibited a one-direction axial swelling.

Figure 2. Schematic representation of partially coated matrices. *From the top*: case 0; case 1; case 2; case 3; case [18]

Drug release rate decreased with the increasing area of impermeable coating (case 4 < case 2 < case < case 1 < case 0). Also the kinetics of delivery changed: by calculating the *R/F* ratio, according to eq. 6, the contribution of relaxation mechanism increased with the increasing coating of the matrix. It was found that the amount of drug released per unit of releasing area was greater as the coating coverage was increased. The linear relationship found between the swollen releasing area and the amount of drug released suggests that matrix swelling kinetics determines the release kinetics. Thus, the modification of the

releasing area, in other words the geometry of the matrix, permits to obtain different release rates and kinetics without changing the composition of the formulation.

Geomatrix™ and Dome Matrix® technologies exploit the modification of the matrix system geometry to control drug release profile.

Geomatrix™ technology consists of a hydrophilic matrix core, containing the active principle, and one or two layers of a polymeric coating which delay the core hydration and drug diffusion. The system is easily produced with a multi-layer compression process [19].

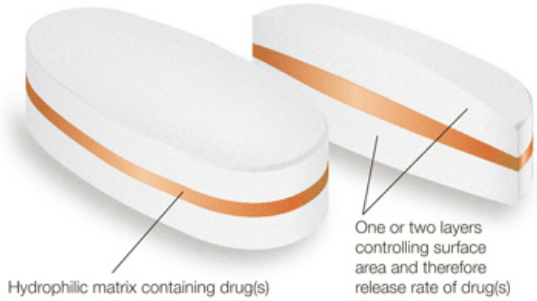

Figure 3. Geomatrix™ Technology [20].

Geomatrix™ can provide extended zero-order kinetics [21], bimodal and timed/delayed release [22], depending on the polymer used in the barrier layers. Currently, this versatile platform is applied in the sustained release formulations of paroxetin (Paxil CR™, GlaxoSmithKline), ropinirole (Requip® Once-a-day, GlaxoSmithKline), molsidomine (Coruno®, Therabel), alfuzosine (Xatral® OD, Sanofi), levodopa/benserazide (Madopar® DR, Roche), zileuton (Zyflo® CR, Cornestone Therapeutics Inc) and for the bimodal release of diclofenac (Diclofenac-ratiopharm, Teva).

Dome Matrix® is a release module with the shape of a disc with curved bases, one convex and the other concave. Since its axial section recalls a cupola (Fig. 4), the name Dome Matrix® has been given. Each individual bases of the module exhibits different swelling behaviour and drug release, confirming again the effect of geometry on drug release [23].

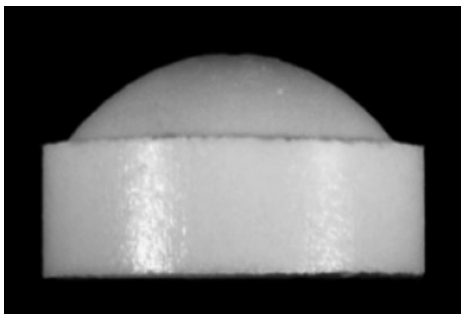

Figure 4. Dome Matrix® Technology [18].

The unusual shape allows the assemblage of numerous modules in one unit system. Each module is designed to have a particular characteristics in terms of type of drugs contained, dose and release profile. Two or more modules are then assembled in a single dosage form.
The first generation of Dome Matrix® modules were assembled by ultrasounds soldering. A second generation of differently shaped modules was designed to facilitate the assembly: the "male" module is fitted with a protrusion which perfectly allocates in a complementary recession in a "female" module, so that the assembly is obtained by clicking the modules.
It is possible to assembly modules in two different configurations, as shown in Fig. 6. The insertion of the convex base of a module into the concave base of the another one provides a unit in a "piled" or "stacked" configuration. Two modules joined by their concave bases have a void internal space within the assembled unit. The modules, assembled in the void configuration, have an apparent density lower than water and can float when immersed in an aqueous medium and show gastric retention *in vivo* [24]. The type of modules assembly play a role in the drug release profile obtained. Void configuration provides a slower release rate compared to the not assembled modules but is slightly higher with respect to the piled assembly because of the different volume/area ratio.

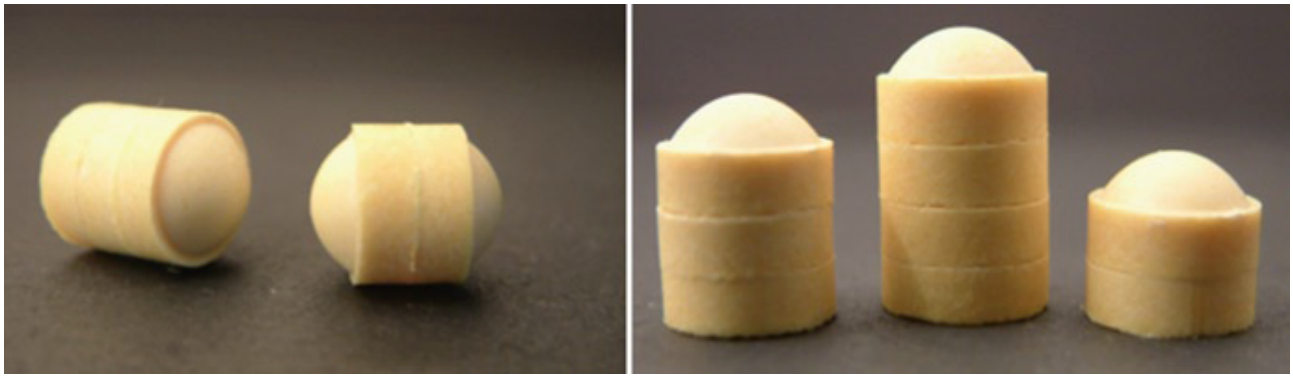

Figure 5. Void (left) and piled (right) configuration of Dome Matrix® assembled modules [18].

The main advantage of this technology is its versatility. In fact, it is possible to administer different drugs in the same dosage unit, solving possible incompatibility issues simply formulating each drug in a different module, or formulate the same drug with different release rate by assembling controlled release and conventional release modules [25]. Therefore, the Dome Matrix® technology is a promising platform, especially in those areas where personalized treatment regimen is required.

4. THE ROLE OF NON COVALENT DRUG-POLYMER AND INTERPOLYMER INTERACTIONS IN ORAL CONTROLLED DRUG DELIVERY

The scientific research about the influence of geometry on drug release from matrix systems has significantly contributed to a better understanding of the mechanisms involved in controlled drug delivery. Geometric release systems have been and still are a success in the market, as demonstrated by the wide application of the Geomatrix™ technology to obtain sustained release of different drugs.

However, a new approach in controlled drug delivery has emerged in the last decades. The new trend consists in the development system where drug-polymer interactions are the element controlling the release, with advantages in terms of drug-sustained release, linear kinetics and reduced sensitivity to the external environment.

In 1957 excipients were defined as "the substances used as a medium for giving a medicament" [26]. They are usually added to the formulation to aid manufacture, administration and/or absorption. The concept that excipients are "inert" ingredient, since they do not produce any pharmacological effect, has been lasting for decades. Nevertheless, excipients may interact with the active substance, promoting negative occurrences that might compromise quality and/or performance of products. Chemical interactions could cause degradation of the active, with a subsequent reduction/lack of efficacy or increased toxicity, if degradation products are unsafe. Physical interactions could affect drug solubility, rate of dissolution, uniformity of dose and ease of administration. Generally, a thorough investigation of potential drug-excipient and excipient-excipient incompatibility must be carried out during pharmaceutical development, in order to produce high-quality dosage form that are stable and safe during their shelf life.

Despite these premises, it is evident that the concept of such interactions has gradually evolved in the past years, in particular concerning drug-polymer interactions. Nowadays, polymer-polymer and drug-polymer interactions are considered a new promising tool to control drug delivery from numerous systems, mainly represented by matrices and films.

4.1 Interpolymer complexes

Polymer-polymer interactions are used to produce interpolymeric complexes. Interpolyelectrolyte complexes (IPECs) are obtained by ionic interaction occurring between oppositely charged polymers [27, 28], whereas hydrogen bonded interpolymer complexes

(IPCs) result from hydrogen bonding interactions between the carboxylic moieties of polyacrylic acis (PAA) or polymethacrylatic acid (PMMA) and non ionic polymers [29]. Both types of complexes are novel individual compounds and their properties are entirely different from the properties of their component polymers.

Moustafine et al. investigated the employment of different types of oppositely charged Eudragit, obtaining both complexes with pH-independent [30, 31] and pH-dependent swelling ratio [32, 33]. The authors proposed the pH-independent swelling complexes for colonic-specific drug delivery, while pH-dependent swelling IPECs were thought for drug release in the upper part of the gastro-intestinal tract. The same group investigated the possibility to obtain IPECs using cationic Eudragit and natural anionic polymers, such as sodium alginate [34] and kappa-carrageenan [35], producing a matrix system suitable for colonic drug delivery in the first case and a complex showing linear drug release profiles in the second one.

Polyionic complexes of chitosan and polyacrylic acid (PAA) were developed for the controlled release of amoxicillin trihydrate in the stomach [36-38]. The complexes with polymers ratio 2.5:1 and 5:2.5 respectively exhibited swelling behaviour and drug release profiles appropriate to ensure the maximum availability of the drug in the stomach, where it is mainly absorbed. The complex showed also a protective effect on the drug, reducing its degradation in acidic environment, and a more prolonged residence time in the stomach than the commercial available formulation [39].

Clausen and Bernkop-Schnurch developed a new directly compressible IPC, based on hydrogen bonding interactions between the carboxylic moieties of polymethacrylatic acid (PMMA) and hydroxyl groups of starch. The complex, insoluble at gastric pH, protected acid-labile drugs and peptide, affording their release in the upper intestine. In fact, as the pH changed, the number of unionized carboxylic groups of PMMA decreased with a lower interaction of starch, so the complex was more soluble and permitted a controlled release of drugs tested [40]. Similar pH-sensitive behaviour was shown by an IPC made of sugar-containing copolymers of poly(methacrylic acid-*co*-methacryloxyethyl glucoside) [41] or graft-copolymers of PEG and PMMA, in which the complex was formed by interactions within the copolymer network [42-44].

In conclusion, interpolymer complexes are more advantageous, in terms of time or site-specific drug release, than each component polymer alone. However, in these systems, the role of polymer-polymer interactions is to determine the new physical-chemical properties of the complex. Thus, time or site-specific drug release profile observed are not a direct

consequence of the interaction, but of the different solubility or swelling behaviour from the original polymers.

4.2 Drug-polymer interactions

As opposite to previously described polymer-polymer interactions based complexes, drug can effectively interact with polymer via non covalent bonds. In this case, the said interaction is the key factor influencing drug release profile.

4.2.1 Hydrogen bond and hydrophobic interactions

Among the different types of non covalent interactions, hydrogen bond and hydrophobic interactions are more difficult to exploit and therefore less studied [45].

Hydrogen bond with polymers can be used to stabilise unstable drugs and/or to provide sustained release rates.

Fluvastatin exhibits interconversion in various inactive forms during storage. Papageorgiou et al. investigated solid dispersions of fluvastatin with chitosan, Eudragit RS 100 and polyvinylpyrrolidone. They found that amorphous fluvastatin was more stable in chitosan solid dispersion rather than the other polymers studied. In addition, prolonged released for more than 8 hours was achieved from chitosan. They identified hydrogen bonds between the drug and chitosan by FT-IR, while no interactions with the other polymers were found. The authors suggested the solid dispersion fluvastatin-chitosan as a valid formulation to obtain sustained release and drug stabilization at the same time [46].

The presence of hydrogen bonds in a complex between naltrexone hydrochloride and Eudragit L [47] afforded a biphasic release of the drug. *In vitro* drug release showed that 60% of the dose was release in 2 hours with a zero-order kinetics and the remaining part was gradually released in the following 6 hours. The bimodal release profile obtained was ideal for the treatment of the opioid-free state in detoxified, formerly opioid-dependant, individuals. In the same research frame, a coprecipitate of morphine and Eudragit L was obtained again exploiting hydrogen bonding interactions between the two components [48]. Tablets, consisting of a mixture of pure drug and complexes, afforded a biphasic release, with an immediate release of 40% of morphine dose followed by a prolonged release over 8 hours [49].

Although less investigated, hydrophobic interactions are promising to provide drug release profiles suitable for controlled release. Poly(N-isopropylacrylamide) (PNIPA) is a thermoresponsive material which swells below a critical temperature and shrinks above. Since its critical temperature is around 32-34°C, it has been studied to obtain a pulsatile on-

off drug release. Coughlan et al. evaluated the effect of drugs, having different solubility, molecular weight and chemical nature, on release performances from PNIPA hydrogels [50, 51]. They found that low soluble and hydrophobic drugs, such as benzoate esters, highly affected the swelling rate of the hydrogel. Aromatic ring and side ester chains of benzoates, strongly interacting by non-polar forces with hydrophobic portions of PNIPA, caused lower than expected swelling rates. Interactions with hydrophilic drugs were negligible and the greater swelling observed was due to an osmotic effect. After the temperature switch, the gel contraction resulted in a drug pulse, due to the presence of a certain amount of drug dissolved in the gel prior the temperature increase. As a consequence of the different swelling rate, hydrogels containing hydrophilic drugs resulted in a greater pulse, while hydrophobic drug pulse was not effective. In conclusion, only hydrophilic drugs, poorly interacting with the polymer, were the best candidates to obtain a pulsatile release.

Hydrophobic chitosan was obtained by N-acylation with fatty acid having different chain length [52]. N-acylated chitosan was more crystalline and resistant to crushing forces than the native one, because interactions among the hydrophobic chains of fatty acid promoted a more compact and orderly structure. Formulations based on acylated chitosan with degree of substitution between 40 and 50% showed release rate appropriate for oral drug delivery. The release of acetaminophen persisted for up to 30 h, with no dependence from drug loading. In this case the release kinetics was based on diffusion and controlled by the low water penetration in hydrophobic matrices.

4.2.2 Ionic bonds

The most investigated and exploited interaction is certainly the ionic bond occurring between drugs and polymers oppositely charged. A large number of papers deals with the exploitation of electrostatic forces to obtain linear sustained release [53], to improve the stability of unstable drugs [54] and to perform the oral delivery of peptides [55]. Polyionic complexes have shown also the capability to enhance the permeability of drugs belonging to the class III of the Biopharmaceutical Classification System (BCS) [54], such as trospium chloride [56] and enalapril maleate [57], complexed with λ-carrageenan and Eudragit, respectively.

Electrostatic interaction depends on the ionization of both species involved, namely on their pK_a and on the medium pH and composition.

Jimenez-Kairuz et al. studied the mechanism of drug release from a swellable drug-polyelecrolyte matrix, made of Carbopol and different basic drugs [58]. Although the matrix showed the swelling typical of hydrophilic matrices, they found an additional mechanism that

contributed to the overall drug release. In a polyelecrolyte-drug complex the following equilibrium is established:

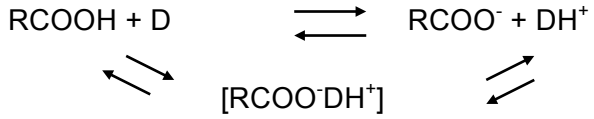

(eq. 7)

where $[RCOO^-DH^+]$ represents an ionic pair between the protonated drug (DH^+) and a carboxylate group ($RCOO^-$) of Carbopol.

They clarified that the limiting step in delivery is the dissociation of ionic pair, once the gel layer has formed. In such conditions, drug release takes place by the diffusion of the protonated specie and the non-protonated one (D) through the gel layer. Moreover, they found that the presence of high concentration of hydrogen ions in the dissolution medium increased drug delivery rate, by enhancing the ionic exchange with the protonated drug, according to the following equilibrium:

$$[RCOO^-DH^+] + H^+ + Cl^- \rightleftharpoons [RCOOH] + Cl^- + DH^+ \qquad \text{(eq. 8)}$$

Thus, any salt added to the releasing medium, namely the increase of the ionic strength, should promote the ionic exchange with the complex and, as a consequence, increase the release rate of the drug. Surprisingly, the authors found that the presence of NaCl in the medium did not significantly raise delivery rates. A different release kinetics and reduced thickness of the gel layer were instead observed. They explained that the overall delivery rate obtained resulted from the contribution of two mechanisms: on one hand the ionic exchange between ions in solution and the polyelecrolyte complex, on the other hand the presence of NaCl reduced the chain repulsion of the macromolecular complex, decreasing hydration, relaxation and ion pair dissociation. In the same research frame, the authors characterized polyelectrolytic complexes consisting of alginic acid and different basic drugs, founding that, the main release mechanism in these system was the erosion of the matrix, independently from the ionic strength of the dissolution medium [59]. In polyionic complexes made by Eudragit and acidic drugs, instead, drug release was mainly controlled by the electrostatic interaction, since the presence of NaCl in the dissolution medium promoted higher release rates. However, different kinetics depending on the drug used were observed, indicating that other factors affected the release [60]. These different results highlight the difficulty in separating the specific contribution to the release mechanism provided by the interaction from the contribution given by the particular behavior of the polymer employed in the complex.

The research carried out by Bonferoni et al. contributed to add new insights for a better understanding of the role of ionic interactions in drug controlled delivery. They investigated the possibility to exploit electrostatic forces to obtain release rates independent from the environmental pH conditions. In a study where different polymers were evaluated, such as sodium carboxymethylcellulose, xanthan gum and λ-carrageenan, they found that only λ-carrageenan-salbutamol matrix provided pH-independent release profiles, since the polymeric sulfate groups, more acidic than carboxylic groups of xanthan gum and sodium carboxymethylcellulose, allowed the drug-polymer interaction to be maintained also at low pH value, typical of the gastric environment [61]. Moreover, they put in evidence that, when ionic interactions occurs between oppositely charged drugs and polymers, the solubility of the complex obtained affect drug release, together with the ion exchange equilibrium previously described and the erosion sensitivity of the formulation [62]. λ-carrageenan formed polyionic complexes having different solubility values with diltiazem [63, 64] and metoprolol [62], the former slightly soluble in water, the latter freely soluble. The distinct solubility resulted in different water uptake and gelation properties. Diltiazem-carrageenan complex showed an immediate water uptake by capillarity followed by an equilibrium without any further gelation. Metoprolol-carrageenan complex exhibited slow and continuous water uptake, leading to the formation of a superficial gel layer which explained the diffusive kinetics observed. A further investigation on the different properties of the previously described complexes permitted to highlight the influence of the strength of interaction drug-polymer. Release profile curves obtained by matrices consisting of diltiazem-carrageenan complex and their drug-polymer physical mixture were different, with a slower drug release rate for the complex containing matrix. Also distinct kinetics were observed: the diffusional exponent *n*, calculated according to the eq. 4, was 0.61 in the first case, indicating a diffusion-controlled release, but assumed the strangely low value of 0.22 in the physical mixture matrix [65]. The particular value reflected the unusual shape of the release curve obtained. In fact, first a fast release was observed, followed by a phase where the release profile was more similar to the complex one. The shape of the release profile was attributed to a different state of the drug in the matrix. The initial faster release was due to the dissolution of the drug present on the matrix surface; as the water penetrated the matrix, the formation of the insoluble diltiazem-carrageenan complex *in situ* was promoted, so that the following release resembled the one obtained with the matrix containing the drug-polymer complex. As opposite, release profiles of metoprolol from matrices made of drug-polymer complex and of their physical mixture of drug were linear and superimposable, suggesting a lower extent of interaction. The observation of the fronts position during the dissolution of

matrices clamped between two Plexiglass disks, according to the procedure described by Bettini et al. [66], showed that, in the matrix containing the diltiazem-carrageenan, the complex itself was the diffusing species, while the precipitation *in situ* of the complex after the water penetration was confirmed in the matrix containing the physical mixture. On the contrary, metoprolol-carrageenan complex matrix demonstrate a progressive dissolution, behaving as a typical soluble matrix tablet. The authors concluded that the differences observed between the two complexes were due to different drug-polymer interactions strength. Diltiazem interacts strongly with λ-carrageenan, giving rise to an insoluble complex, whose own dissolution controls the release of the drug. In this case the tablet has to be considered as a monolith constituted by a unique insoluble compound rather than a matrix system. Metoprolol-λ-carrageenan interaction is weaker and therefore permits a better interaction with the dissolution medium, with the subsequent hydration of the polymer and drug release upon ionic pair dissociation, as a classical swellable matrix.

4.3 Concluding remarks

The comprehensive understanding of the specific role of non-covalent interactions in controlled drug release is still an ongoing process.

The principal factor emerging from the literature available is the difficulty to identify and quantify the contribution of the interaction on the overall drug release observed.

Hydrogen bond and hydrophobic interactions are basically an unexplored field. So far, the research has been focusing on the evaluation of the feasibility of controlled release systems based on these kinds of interactions. The thorough understanding of how they affect release rates and kinetics is an open field for investigation.

Although ionic interactions are much more investigated, the comprehension of their role of in controlled delivery systems still presents some unclear aspects. It is well known that the mechanism controlling drug release in polyionic complexes is the ionic exchange equilibrium due to the presence of competing counterions in the dissolution medium. However, in the majority of the published works, drug release profiles obtained are always influenced somehow by the properties of the polymer involved, i.e. erosion or swelling properties. Very recently, Bettini et al. have shown that the strength of interaction between the drug and the polymer of interest might have a role in producing complexes where the interaction is the only factor controlling the release [65].

It is evident that the investigation at molecular level of such features would provide better knowledge of the matter. In particular, the study of the influence of the various functional groups in establishing certain types of interactions could provide a predictive model, useful

for the selection *a priori* of the best molecules to obtain the desired performance. In this perspective, computational molecular modeling would be a powerful instrument.

Moreover, new and accurate methods to detect and quantify interactions are needed, since the classical techniques used, such as Fourier Transform InfraRed (FTIR) analysis and nuclear magnetic resonance (NMR), often require complicated protocols of validation and/or long analysis acquisition times. For example, Pavli et al. [67] proposed an ion selective electrode for doxazosin to investigate and quantify its interactions with different types of carrageenan [68].

Lastly, the effective development of controlled release systems based on interactions requires the availability of mathematical models to evaluate the drug release kinetics.

Peppas' power law (eq. 4) is a useful tool massively exploited to describe release kinetics form polymeric network undergoing significant relaxation upon contact with a solvent, thus accounting from deviation from to pure diffusion transport mechanism (n value > 0.5), as explicitated by the Peppas and Sahlin equation (eq. 5). This mathematical model has been applied to different polymeric systems, including eroding matrices. Erosion, not initially included in the original model, has been considered an additional contribution to drug transport affording linear kinetics. Similarly, the contribution of interactions should be taken in account, considering that it would be not an additive contribute but an element contrasting the drug diffusion

II. AIM OF THE WORK

II. AIM OF THE WORK

The present research work has been focused on a thorough and comprehensive investigation of the role of non covalent interactions between drugs and polymer in oral controlled drug delivery with the aim to present a more systematic approach for the prediction of desired release profile, depending on the chemical functions and the interactions involved.

The research has been structured in three parts.

Firstly, non covalent interactions between a model basic drug, atenolol, and polymers having different functional groups, such as chondroitin sulphate, sodium alginate, chitosan and λ-carrageenan, were characterized by classical techniques, i.e. FTIR and NMR. In addition, desorption electrospray ionisation high-resolution mass spectrometry was proposed as a technique for a fast evaluation of interactions between the molecules selected. The effect of interactions on drug release in *in-vitro* dissolution studies was then evaluated.

The second part of the work focused on an accurate investigation of the factors involved in atenolol release from λ-carrageenan matrices. In particular, the effect of ionic strength and polymer solubility was taken in account. Since a role of drug-polymer-salt interactions was put in evidence, ternary matrices were prepared and the effect of different salt on the release was studied.

Finally, the last part of the work, carried out at the UCL School of Pharmacy in London, under the supervision of Prof. Duncan Craig ant Dr. Min Zhao, involved the evaluation of the possibility to produce ionic liquid-like systems from oppositely charged drugs and polymers by hot melt extrusion. The molecules selected were sodium ibuprofen and Eudragit RS 100.

III. FIRST PART

III. FIRST PART

The first part of the research involved the investigation of interactions occurring between a model drug with basic characteristics, atenolol (ATN), and selected polymers carrying different functional groups, such as chondroitin sulphate (CDS), sodium alginate (ALG), chitosan (CHT) and λ-carrageenan (CAR). The influence of the interactions found on drug release from matrix tablets was then investigated, by conducting *in vitro* dissolution studies on drug-polymer matrices. In this frame, the desorption electrospray ionization high-resolution mass spectrometry technique was evaluated as a rapid and sensitive method for the investigation *in situ* of mechanisms involved in drug release from the matrix systems produced.

1. MATERIALS AND METHODS

1.1 Materials

1.1.1 Chemicals

- ATENOLOL (Figure 6) was kindly donated by Lisapharma S.p.A (Italy). The drug has a molecular mass of 266.34 g/mol and a pK_a value of 9.6. It belongs to the third class of the Biopharmaceutical Classification System, having a high solubility and low intestinal permeability [54]. The drug is a cardioselective beta-adrenoreceptor antagonist, inhibiting selectively beta-1 receptors with a lower affinity for beta-2 subtype. Atenolol is used to treat many cardiovascular disorders such as hypertension, arrhythmias, angina, myocardial infarction and heart failure [69]. Its use in such chronic diseases appoints atenolol as a good candidate for oral controlled drug delivery.

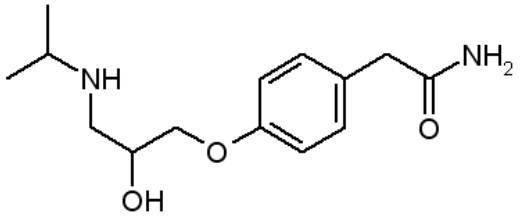

Figure 6. Molecular structure of atenolol.

- CHONDROITIN SULFATE (Figure 7) was supplied by ACEF S.p.A. (Italy). It is a glycosaminoglycan containing sulfate groups widespread on cell surface and within extracellular matrix in the form of proteoglycans. The linear polysaccharide consists of repeating disaccharide units composed by uronic acid and 4/6-sulfated N-acetylhexosamine, linked alternatively by β-1,4 and β-1,3 bonds [70].

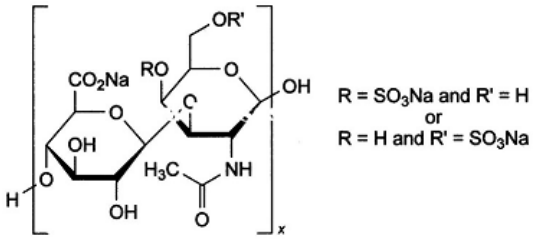

Figure 7. Base structure of chondroitin sulfate.

- SODIUM ALGINATE (Figure 8) was. supplied by Carlo Erba Reagents (Italy). It is the sodium salt of alginic acid, an anionic polymer consisting of a mixture of polyuronic acids composed of residues of D-mannuronic and L-glucuronic acid [71]. The polymer may establish ionic and hydrogen bonds because of carboxylic and hydroxyl groups present in its structure.

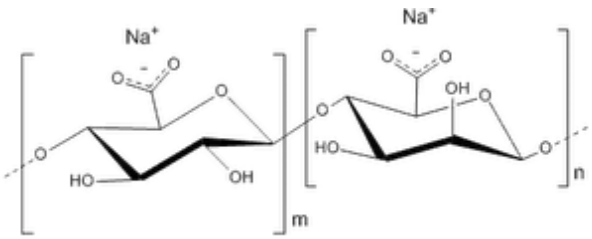

Figure 8. Base structure of sodium alginate.

- CHITOSAN 95/50 (Figure 9) was provided by Heppe Medical Chitosan GmbH (Germany). It derives from the partial deacetylation of chitin, which makes available free amine groups, able to establish ionic or hydrogen bonds with opportune molecules. The ratio of glucosamine and N-acetylglucosamine monomers depends on the degree of deacetylation [72]. The polymer used in this work had a degree of deacetylation of 92.6-97.5%.

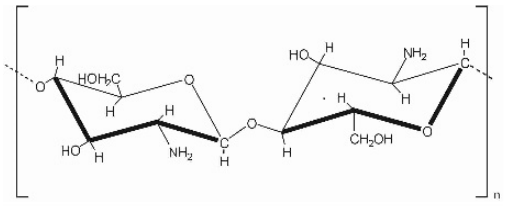

Figure 9. Base structure of chitosan.

- λ-CARRAGEENAN (Figure 10) Viscarin® GP 209 NF was kindly donated by FMC Biopolymer (USA). It consists mainly of the alternating monomeric units D-galactose-2-sulfate (1,3-linked) and D-galactose-2,6-disulfate (1-4 linked) [73]. The presence of three sulfate groups for each dimeric unit imparts a strong acidic character.

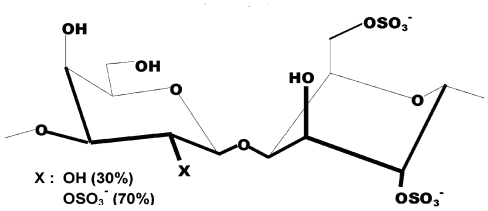

Figure 10. Base structure of λ-carrageenan.

- Other chemicals used were: methanol HPLC grade, deuterium oxide, dibutylamine (Sigma Aldrich, Germany), 1-heptansulphonic acid sodium salt (Alfa Aesar, Germany), anhydrous dibasic sodium phosphate (Riedel-de haën, Germany), potassium dibasic phosphate, potassium monobasic phosphate, hydrochloric acid 37% (Carlo Erba, Italy), phosphoric acid 85% (ACEF, Italy), sodium hydroxide pellets (Prolabo, France).

1.1.2 Buffer solutions

The following buffers solutions, prepared as described in the Italian Pharmacopoeia [74] were used.

- Phosphate buffer solution pH 4.5 (0.1 M): 13.61 g of potassium dihydrogen phosphate were dissolved in 1000 mL of water. pH was eventually adjusted with hydrochloric acid 0.1 M or sodium hydroxide 0.1 M.

- Phosphate buffer solution pH 4.5 (0.01 M): 1.361 g of potassium dihydrogen phosphate were dissolved in 1000 mL of water. pH was eventually adjusted with hydrochloric acid 0.1 M or sodium hydroxide 0.1 M [74].
- Phosphate buffer solution pH 7.4 (0.1 M): 250 mL of potassium dihydrogen phosphate 0.2 M were mixed with 195.5 mL of sodium hydroxide 0.2 M. The volume was then made up to 1000 mL [75].
- Phosphate buffer solution pH 7.4 (0.1 M): 1.7418 g of dipotassium hydrogen phosphate were dissolved in 1000 mL of water. pH was then adjusted with phosphoric acid (modified from 0.03 M phosphate buffer solution pH 7.0 [74]).

1.2 Methods

1.2.1 Attenuated Total Reflectance - Fourier Transform Infrared (ATR-FT-IR) analysis

Infrared spectroscopy was performed on atenolol, polymers and their mixtures using a FT-IR spectrometer Thermo Nicolet 7500 (Thermo Scientific, USA) equipped with a Thermo Smart Orbit ATR diamond accessory. Spectra were recorded by collecting 32 scans in the 4000-400 cm^{-1} wave number range at a resolution of 2 cm^{-1}. In order to promote a more intimate contact between the two components, mixtures were prepared by evaporating suspensions of different amount of each polymer wetted with an ethanolic solution of atenolol. The final atenolol-polymer weight ratios were 1:1, 1:2, 1:4. Solids obtained were then analysed. Atenolol alone was analysed after solvent evaporation of its ethanolic solution, while polymers powder were wetted with ethanol prior the analysis.

1.2.2 H^1 Nuclear Magnetic Resonance (H^1 NMR)

H^1 NMR characterization was performed with a nuclear magnetic resonance spectrometer Bruker Avance 300 (Bruker Corporation, USA). Analyses were carried out on solutions of pure atenolol and of its mixtures with polymers (1:1, 1:2, 1:4 w/w ratio) in deuterium oxide (D_2O) and in a 1% v/v acidic solution of CD_3COOD in D_2O. Atenolol-chitosan mixtures were analyzed only in the CD_3COOD/D_2O solution, since chitosan is not soluble at neutral pH. H^1 NMR spectra of each polymer were acquired in the same conditions in order to detect potential overlapping of their signals with those belonging to atenolol.

1.2.3 Analytical methods for the quantification of atenolol and system suitability

The quantitative determination of atenolol was carried out by High Performance Liquid Chromatography (HPLC) according to the atenolol assay described in USP 34 [76]. The

analysis was performed on a 10AT VP LC system (Shimadzu Corp., Japan) coupled online with a diode-array detector (SPD-M10A VP, Shimadzu). Chromatographic separation was performed on a Nova-Pack C-18 silica-bonded stationary phase column (150 x 3.9 mm, 4 µm; Waters, USA) using an isocratic solvent system composed of a 30:70 v/v mixture of methanol and an aqueous solution of sodium-1-heptansulfonate 0.005M, sodium phosphate anhydrous 0.005 M and dibutylamine 0.28% v/v at pH 3, delivered at a flow rate of 0.6 mL/min. The detector was set at 226 nm and data were analyzed using the Class VP v. 3.4 software (Shimadzu).

The performance of the chromatographic system used was verified by system suitability. Relative standard deviation, number of theoretical plates, tailing factor, signal-noise ratio were calculated from a chromatogram obtained from the analysis of a solution 0.01 mg/mL of atenolol in mobile phase. Limit of detection (LOD) and limit of quantification (LOQ) were also determined using the signal-to-noise (S/N) approach, considering said limits the concentrations of analyte providing S/N ratios of 3 and 10, respectively [77].

The linearity of the method was verified by plotting the areas obtained from chromatograms of 5 solutions of atenolol, in the concentration range 0.001 – 0.1 mg/mL, as a function of their concentration. Linearity was verified for the following solvents: distilled water, buffer phosphate pH 4.5 and 7.4, at both ionic strength (µ), 0.1 and 0.01 M.

1.2.4 Solubility

Atenolol solubility was evaluated in different solvents: distilled water, phosphate buffer pH 4.5 and pH 7.4. Both phosphate buffers were prepared at two different ionic strengths (µ), 0.01 M and 0.1 M. Saturated solutions of atenolol were equilibrated at 37°C for 24 hours. After centrifugation at 15000 rpm at room temperature for 10 minutes, supernatant was withdrawn from each solution, filtered, diluted and then analysed by HPLC-UV. Drug solubility was calculated based on calibration curves prepared in each solvent tested. Drug solubility was measured in three replicates.

1.2.5 Tablets preparation

Polymer and drug powders were initially sieved (Endecotts Limited, UK) in order to obtain powders with particle size ranging between 180 and 125 µm. Then, the powders of the active substance and the polymer were mixed in 1:1, 1:2, 1:4 ratio w/w in Turbula® (WAB, Switzerland) for 15 min before compression. Tablets were prepared by direct compression of 150 mg of powders mixtures using 7 mm diameter flat faced punches and a fixed cylindrical die, mounted on a reciprocating tablet press Korsch Mod. EKO (Germany) instrumented for

the registration of applied compression force (Kistler, Italy). Compression force was maintained in the range of 12-15 kN.

1.2.6 In vitro dissolution studies

Release rate of ATN from tablets were studied for up to 12 h. The experiments were conducted at 37 ± 0.5 °C on a USP dissolution apparatus II (Agilent VK 7025, Agilent Technologies, USA) equipped with a peristaltic pump (Agilent 810, Agilent Technologies) and an autosampler (Agilent 8000, Agilent Technologies) for automatic sampling. Dissolution studies were performed at 50 rpm in 1000 mL of different dissolution media: distilled water, phosphate buffer pH 4.5 and 7.4 at both ionic strength of 0.01 M and 0.1 M. Samples of 1.5 mL were withdrawn at defined time intervals and the amount of the released drug was quantified by HPLC-UV. All experiments were done in triplicate. Peppas' empirical power law (eq. 4) was used to characterize drug release mechanism from the matrix tablets prepared [14, 15].

1.2.7 Desorption electrospray ionization high-resolution mass spectrometry (DESI-HRMS) technique

DESI technique combines features of electrospray ionization (ESI) with those of the desorption ionization (DI) methods. In fact, an electrospray emitter is used to produce gas-phase solvent ions, ionic clusters and charged microdroplets to be directed to the sample at atmospheric pressure. An electrical potential is applied to the spray solution and pneumatic nebulisation is used to assist in de-solvation. As all the DI methods, DESI technique involves the impact of droplets on condensed phase-samples. The microdroplets act as projectiles and desorb ions from the sample surface as a result of electrostatic and pneumatic forces. The sample can be moved continuously and/or reoriented in space while MS analysis proceeds. The ions released are transferred to the distant mass-spectrometer via an atmospheric pressure ion-transfer line. DESI ion sources are easily connected to any mass spectrometer equipped with an atmospheric pressure interface. The sample remains fully accessible to observation or to any additional processing step during analysis [78, 79]. A typical DESI-HRMS experimental set up is showed in Figure 11.

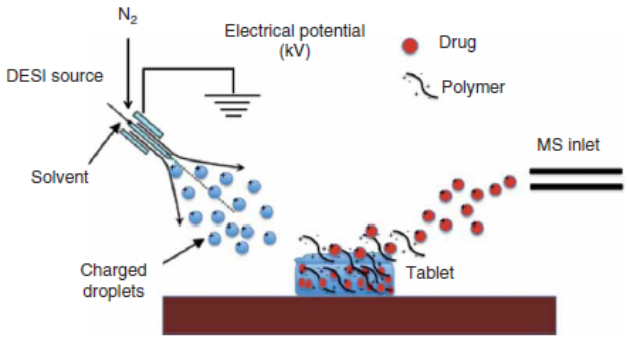

Figure 11. Schematic representation of the experimental set up for DESI-HRMS measurements on tablets [45].

Samples do not require treatment and analysis is carried out at atmospheric temperature, which represents the principal advantage of the technique. The main applications are high-throughput analysis of pharmaceutical preparations, detection of metabolites in biological fluids for diagnosis and pharmacokinetics studies, forensic analysis.

In the present research frame, the DESI-HRMS technique was evaluated as a tool for investigating potential interactions between the drug and polymers selected, as well as its applicability to study *in vitro* release kinetics of atenolol from polymeric matrix systems.

Experiments were carried out on a LTQ-Orbitrap XL hybrid linear ion trap Orbitrap mass spectrometer (Thermo Scientific, USA) equipped with a DESI Omni Spray ion source (Prosolia, USA), tuned for optimum detection of the ion of interest. The DESI source was fitted with a sample platform and two cameras to assist in the positioning and monitoring of the spray and surface. The spray tip for the solvent was positioned 2 mm from the surface at an incident angle of 55°. The tip-to-inlet distance and the surface-to-inlet distance were 4 and 0.5 mm, respectively. The same configuration was used for all the experiments. Nitrogen was used as nebulising gas at pressure of 8.3 bar. The main experimental parameters were: spray voltage 3,5 kV; capillary voltage 8 V; capillary temperature 200°C; tube lens voltage 40 V. MS analyses were performed in positive ion mode, observing the $[M+H]^+$ ion at *m/z* 267.17 and using a fixed spray position. The resolving power was 20,000 (at *m/z* 400).

DESI-MS observation were performed directly in the centre and at the edges of each tablet by spraying different aqueous solutions in the fixed positions at 1 µL/min for 20 minutes. The solutions used were ammonia aqueous solution at pH 7.4, acetic acid solution at pH 4.5 and formic acid solution at pH 1.2. All the solutions had the same ionic strength of 0.01 M. The atenolol desorbed amount was estimated by using calibration curved built by analysing

known amount of drug in the range 5-200 ng at the three pH values selected for the experiments.

2. RESULTS AND DISCUSSION

2.1 ATR-FT-IR analysis

ATR-FT-IR spectra of atenolol (Figure 12) and the polymers selected (Figure 13) showed characteristic peaks over the entire wave number range scanned (4000-400 cm^{-1}) [80, 81].
Atenolol bands associated with stretching of hydroxyl (1) and amine (2) groups at 3353 and 3176 cm^{-1}, respectively, as well as the signal at 1636 cm^{-1}, related to the stretching of carbonyl group (3) and the peak at 1417 cm^{-1}, attributed to the vibration of C-OH bond (4), were observed to detect potential ionic and/or hydrogen bonds with polymers. However, peaks related to C-C stretches in the region 2960-2900 and at 1515 cm^{-1} that may be used to put in evidence eventual hydrophobic interactions were not observed.

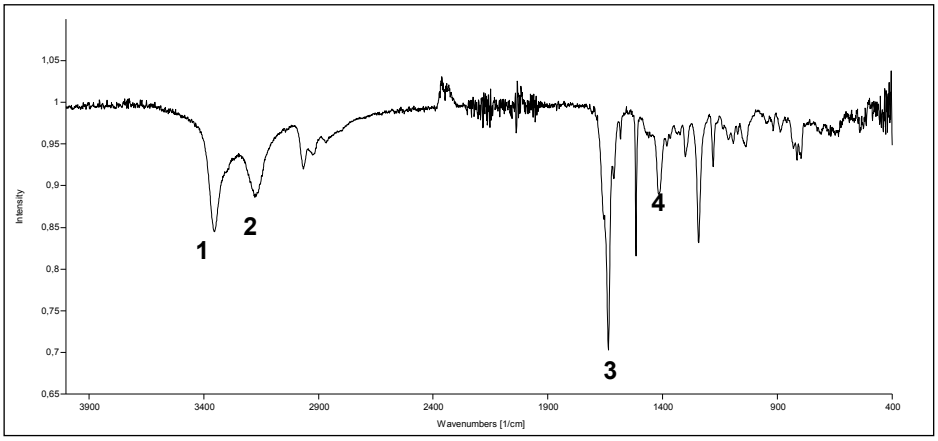

Figure 12. ATR-FT-IR spectrum of atenolol.

Chondroitin sulfate spectrum (Figure 13, panel A) showed bands associated with the stretching of hydroxyl group at 3328 cm^{-1} (band 1), carboxylate group at 1608 cm^{-1} (band 2) and sulfate groups at 1220 cm^{-1} (band 3) [82].
Sodium alginate spectrum presented 7 characteristic bands (Figure 13, panel B). The strong band 1 at 1600 cm^{-1} was assigned to the stretching of the carboxylate anion. Band 2 at 1406 cm^{-1} was attributed to the C-OH deformation vibration with contribution of O-C-O symmetric stretching of carboxylate group. Bands 3 (1083 cm^{-1}) and 4 (1024 cm^{-1}) were related to the C-O and C-C stretching of pyranose ring. Band 5 at 948 cm^{-1} was indicative of vibration of

uronic acide residues, while band 6 and 7, at 878 and 817 cm^{-1} were related to mannuronic acid residues [83].

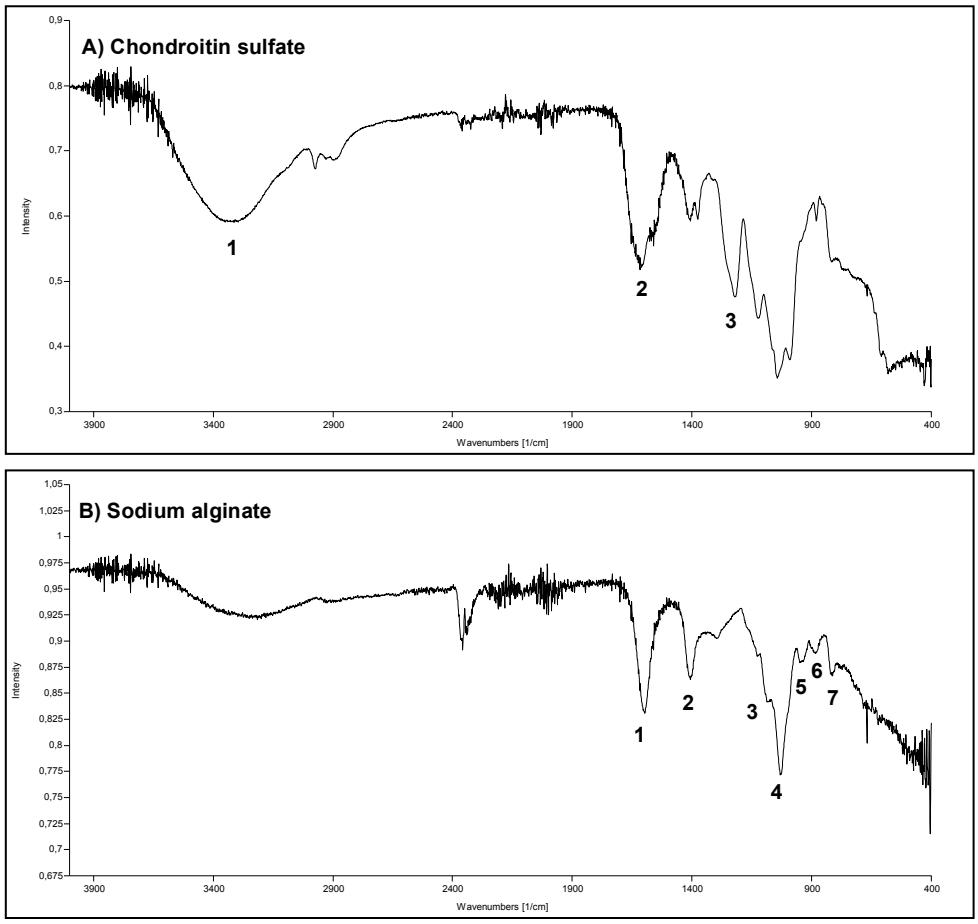

Figure 13. ATR-FT-IR spectra of chondroitin sulfate (A) and sodium alginate (B).

Chitosan spectrum (Figure 14, panel A) presented bands associated with hydroxyl and amine groups at 3355 (band 1) and 3289 cm^{-1} (band 2), respectively. Band 3 at 1592 cm^{-1} was related to the stretching of carboxylate group and the strong peak centred at 1023 cm^{-1} (band 4) was attributed to the vibrations of C-O-C groups in the glycosidic linkage [84].

λ-carrageenan spectrum (Figure 14, panel B) displayed the very strong bands 1 and 2 at 1215 and 1110 cm^{-1}, characteristic of the sulfate group and the glycosidic linkage, respectively. Band 3 at 930 cm^{-1} was related to the 3,6-anhydrogalactose residues, while the band 4 at 838 cm^{-1} to the 2-sulfate group [85].

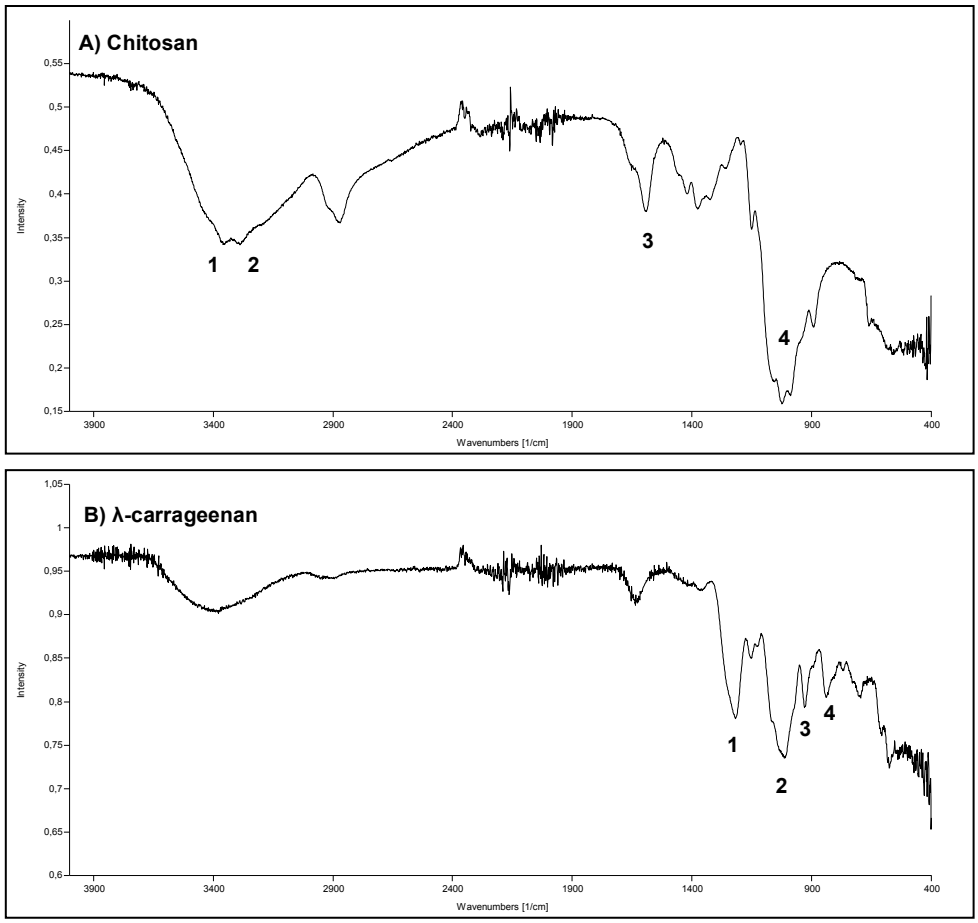

Figure 14. ATR-FT-IR spectra of chitosan (A) and λ-carrageenan (B).

Strong shifts involving the bands associated with hydroxyl and amine groups of atenolol at 3353, 3176 and 1417 cm^{-1} were observed in all its mixtures with the polymers selected, whereas no variations in signals related with carbon-carbon bonds were detected. Unfortunately, it was not possible to detect any change in polymers signals position due to the overlapping of their characteristic peaks with those of atenolol. Nevertheless, the results obtained were consistent with the occurrence of electrostatic interactions and hydrogen bonds between the drug and the polymers. Shifts observed in the mixtures atenolol-polymer 1:1 w/w are reported in Table 1. Surprisingly, the variations observed were not dependent on the amount of polymer contained in the mixture. This could be due to the method of preparation of the mixtures analyzed. Each polymer was, in fact, wetted with an atenolol solution in ethanol and then analyzed after the complete evaporation. Likely the time of contact between the molecules was not sufficient to assure the maximum extent of interactions.

Table 1. Shifts of atenolol peaks in mixtures with polymers (1:1 w/w) observed in ATR-FT-IR analyses.

	Wavenumber (cm^{-1})				
	ATN-polymer mixtures 1:1				
FUNCTIONAL GROUP	ATN	ATN-CS	ATN-ALG	ATN-CHT	ATN-CAR
v OH	3353	3349	3347	3347	3349
v NH_2	3176	3164	3159	3159	3158
v CO	1636	1635	1635	1635	1635
v COH	1417	1412	1413	1413	1413
δ $OCNH_2$	1301	1300	1301	1301	n.d.*
* not detected					
v: stretching; δ: bending					

2.2 H^1 NMR

H^1 NMR spectra of all the polymers did not show significant overlapping with atenolol signals both in D_2O and CD_3COOD/D_2O. In H^1 NMR spectrum of atenolol only the 18 of the 22 hydrogen atoms of the molecule were detected in both solvents, because of the rapid exchange of the hydrogen atoms of the hydroxyl and amine group with D_2O. Atenolol H^1 NMR spectrum and the assignation of the signals detected are reported in Figure 15.

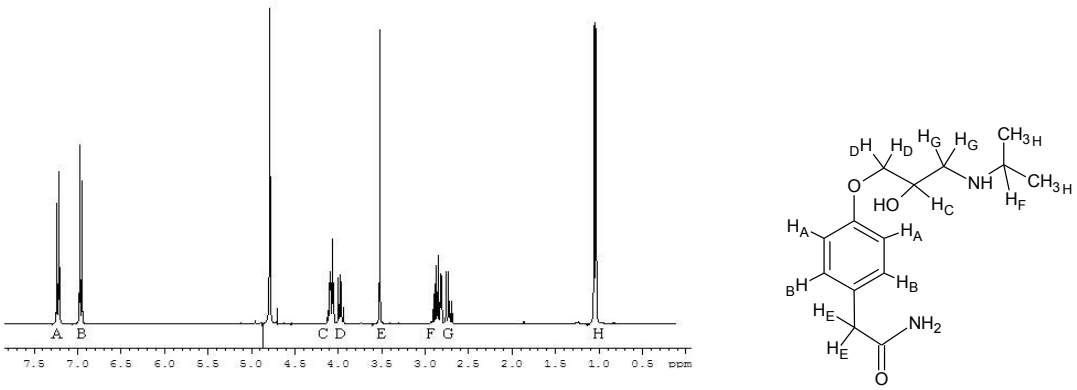

Figure 15. H^1 NMR spectrum in D_2O of atenolol and relevant assignations.

Table 2. H^1 NMR chemical shifts acquired for atenolol-polymer mixtures in D_2O.

		δ (ppm)		
		ATN-CDS		
H ATOM	ATN	1:1	1:2	1:4
A	7.23	7.23	7.23	7.23
B	6.97	6.97	6.97	6.97
C	4.09	4.11	n.d*	n.d
D	3.97	3.98	n.d	n.d
E	3.52	3.53	3.53	3.53
F	2.86	2.96	3.05	3.29
G	2.78	2.84	2.92	3.09
H	1.04	1.09	1.12	1.22
		ATN-ALG		
H ATOM	ATN	1:1	1:2	1:4
A	7.23	7.22	7.23	7.22
B	6.97	6.96	6.96	6.97
C	4.09	4.09	n.d.	n.d.
D	3.97	3.97	n.d.	n.d.
E	3.52	3.52	3.52	3.52
F	2.86	2.94	2.99	3.15
G	2.78	2.85	2.90	3.05
H	1.04	1.09	1.14	1.18
		ATN-CAR		
H ATOM	ATN	1:1	1:2	1:4
A	7.23	7.23	7.23	7.24
B	6.97	6.96	6.96	6.97
C	4.09	4.08	4.09	4.04
D	3.97	3.97	3.97	n.d.
E	3.52	3.52	3.52	3.52
F	2.86	2.92	2.97	3.06
G	2.78	2.81	2.87	2.94
H	1.04	1.06	1.09	1.13

*n.d.: not detected

H^1 NMR spectra of atenolol-polymers mixtures in D_2O displayed variations of the chemical shift (δ) of drug signals (Table 2). Peaks related to hydrogen atoms H_F and H_G, contiguous to the amino group, as well as hydrogen atoms H_H, showed downfield shift. Wider shifts toward more de-shielded regions of the spectrum were observed as the amount of polymer in solution increased. These findings suggested the occurrence of ionic interactions between the amino groups of the drug, protonated in aqueous solution, with the acidic groups of the polymers considered. In fact, ionic interaction reduced electronic density in the surroundings

of amino groups, with a consequent de-shielding of protons linked to contiguous carbons, which moved towards higher chemical shifts. When polymers amount increased, more interactions with the drug could be established, so that wider shifts were observed. Moreover, similar behaviour was observed with sodium alginate and carrageenan whereas, wider variations were observed in atenolol-chondroitin sulphate mixtures, implying stronger interactions with the latter polymer.

Atenolol peaks did not display any variations in their positions in H^1 NMR spectra obtained from mixtures with polymers in CD_3COOD/D_2O (Table 3), suggesting that no ionic interactions occurred in acidic environment with any of the polymers considered. The lack of interaction with chitosan was expected, as both drug and polymer contain basic groups. Carboxylic and sulfate groups of chondroitin sulfate have pK_a values of about 3-5 and 1.5-2 respectively [86]; in sodium alginate, mannuronic acid and guluronic acid residues have pK_a values of 3.38 and 3.65, respectively [87]; λ-carrageenan sulfate groups have a pK_a value of about 2 [88]. The measured pH value of the CD_3COOD/D_2O solution was of about 2.75. Therefore, atenolol did not interact with chondroitin sulphate, sodium alginate and carrageenan because their acidic groups were completely or partially protonated.

.

Table 3. H^1 NMR chemical shifts acquired for atenolol-polymer mixtures in CD_3COOD/D_2O.

	δ (ppm)			
		ATN-CHT		
H ATOM	ATN	1:1	1:2	1:4
A	7.22	7.21	7.21	7.22
B	6.95	6.94	6.94	6.95
C	4.25	4.24	4.24	4.26
D	4.07	4.07	4.06	4.07
E	3.52	3.51	3.51	3.51
F	3.45	3.44	3.44	3.45
G	3.24	3.23	3.23	3.23
H	1.30	1.29	1.29	1.30
		ATN-CDS		
H ATOM	ATN	1:1	1:2	1:4
A	7.22	7.22	7.22	7.22
B	6.95	6.96	6.96	6.96
C	4.25	4.26	4.26	4.25
D	4.07	4.07	4.08	4.08
E	3.52	3.52	3.52	3.52
F	3.45	3.46	3.46	3.46
G	3.24	3.24	3.24	3.24
H	1.30	1.31	1.31	1.31
		ATN-ALG		
H ATOM	ATN	1:1	1:2	1:4
A	7.22	7.21	7.22	7.22
B	6.95	6.94	6.95	6.94
C	4.25	4.24	4.26	4.25
D	4.07	4.06	4.06	4.08
E	3.52	3.51	3.51	3.51
F	3.45	3.45	3.45	3.45
G	3.24	3.23	3.23	3.24
H	1.30	1.30	1.30	1.30
		ATN-CAR		
H ATOM	ATN	1:1	1:2	1:4
A	7.22	7.21	7.22	7.23
B	6.95	6.95	6.95	6.95
C	4.25	4.25	4.26	4.25
D	4.07	4.06	4.07	4.07
E	3.52	3.51	3.51	3.51
F	3.45	3.45	3.45	3.45
G	3.24	3.23	3.24	3.25
H	1.30	1.31	1.30	1.30

2.3 System suitability of the assay method for atenolol

The chromatographic system used for the determination of atenolol described was suitable to assure a quality performance, as shown by the results obtained from system suitability tests, reported in Table 4.

The linear relationship between the chromatogram signals and the analyte concentration for each solvent tested was evaluated by calculating the regression line with the least square method. The correlation coefficient, y-intercept and slope of the regression line obtained are reported in Table 5. Data obtained showed a good linearity of detectability.

Table 4. Relative Standard Deviation (RSD), Number of theoretical plates, symmetry factor, ration signal to noise, Limit of Detection (LOD) and limit of Quantitation (LOQ) obtained from system suitability tests, in comparison with the USP 38 references.

PARAMETER	USP 34 SPECIFICATIONS	OBTAINED VALUE
RSD	≤2%	0.23%
Number of theoretical plates	> 5000	5500
Symmetry factor	≤2	1.28
Ratio S/N	-	220
LOD	-	$1.36\ 10^{-4}$ mg/mL
LOQ	-	$4.54\ 10^{-4}$ mg/mL

Table 5. Regression lines parameter obtained in different solvents.

SOLVENT	SLOPE	Y-INTERCEPT	R^2
Distilled water	1871.3	3.30×10^7	0.999
Phosphate buffer pH 4.5 µ 0.01 M	3960	3.10×10^7	0.999
Phosphate buffer pH 4.5 µ 0.1 M	8526.6	3.42×10^7	0.999
Phosphate buffer pH 7.4 µ 0.01 M	10301	3.04×10^7	0.999
Phosphate buffer pH 7.4 µ 0.1 M	11507	3.08×10^7	0.999

2.4 Equilibrium solubility

Solubility values of atenolol in each solvent studied are reported in Table 6. Atenolol has a similar solubility value of about 23 mg/mL in water and at pH 7.4 at both ionic strengths studied This result is in agreement with the datum reported by Wander et al [89] but higher than those reported by Etherson et al. [90] and Narasimham and Barhate [91]. In buffer phosphate pH 4.5 its solubility was greater at μ 0.1 M (46 mg/mL) than at μ 0.01 M, where it was comparable to the other solvents (26 mg/mL). The greater percentage of atenolol ionization at pH 4.5, since its pK_a has a value of 9.6, as well as a salting-in effect promoted by the higher concentration of phosphate ions present in the buffer at μ 0.1 M, might explain the solubility value found in this solvent.

Table 6. Solubility of atenolol in different solvents at 37 °C. Standard deviation in parenthesis (n=3).

SOLVENT	SOLUBILITY (mg/mL)
Distilled water	23.28 (2.68)
Phosphate buffer pH 4.5 μ 0.01 M	26.16 (0.58)
Phosphate buffer pH 4.5 μ 0.1 M	46.49 (1.45)
Phosphate buffer pH 7.4 μ 0.01 M	23.48 (0.55)
Phosphate buffer pH 7.4 μ 0.1 M	24.78 (0.60)

2.5 *In vitro* drug release studies

2.5.1 Effect of pH and drug-polymer ratio

In vitro dissolution studies were carried out in order to investigate how the interactions found influenced atenolol release from matrix tablets made by each polymer selected. ATR-FT-IR and H^1 NMR characterization of drug-polymers mixtures confirmed the presence of hydrogen and ionic bonds. In particular, H^1 NMR analyses put in evidence different grades of interactions, depending on the drug-polymer weight ratio and environmental pH. For these reasons, drug release from matrices having three different drug-polymer compositions, namely 1:1, 1:2, 1:4 w/w, was evaluated. *In vitro* dissolution studies were performed at two different pH values and at the same ionic strength (0.1 M). Phosphate buffer at pH 4.5 was

chosen to simulate the environment of the upper part of the small intestine, while phosphate buffer at pH 7.4 simulated the large intestine. Drug release profiles obtained from chondroitin sulfate, chitosan, sodium alginate and λ-carrageenan are reported in Figures 16, 17, 18, 19, respectively.

Atenolol-chondroitin sulfate tablets dissolved completely within 2 hours in both media, releasing the drug with a linear kinetics and similar release rate in the two tested solutions. Curiously, the slower release rate was obtained from the system containing the lower amount of polymer (1:1 drug polymer ratio).

Atenolol-chitosan tablets did not dissolve completely in both solvents, so atenolol was released mainly upon diffusion in the solvent penetrated the matrix. Drug dissolution profiles, effectively, showed an average diffusional exponent *n* of 0.56 ± 0.02 at pH 4.5 and 0.63 ± 0.03 at pH 7.4

Also in this case the drug release rate slowed down with the decrease of the polymer content.

At acidic pH the atenolol release was completed in 6 hours, whereas at pH 7.4 the drug was quantitatively released in about 12 hours. This difference can be ascribed to the different solubility of chitosan at the two pH values. Since the pKa of the polymer is around 6.3 [92], it dissolves quite easy at pH 4.5 while it is almost insoluble at pH 7.4.

Atenolol-sodium alginate tablets dissolved more slowly than chondroitin sulfate matrices. A thin gel layer formed on their surface and complete erosion was observed in 4 hours in both media. The atenolol release rate increased with time in the up to 80% of the dose delivery, indicating that the system dissolution was faster than the solvent penetration into the matrix [8]. It is worthy underlying that the pH of the dissolution medium as well as of the drug-polymer ratio did not affect the observed drug release profiles.

Finally λ-carrageenan matrix tablets showed the more extended atenolol release. The polymer swelled upon contact with both media forming a thick gel layer on the matrix surface. This situation afforded an unexpected linear release of atenolol for up to 10 hours. Also in this case the atenolol release was not affected by.

Furthermore, it is interesting to note that drug release rates from all atenolol-polymer matrices tested were unaffected by the pH value of the dissolution medium, despite the large difference in drug solubility at the two pH values (Table 6).

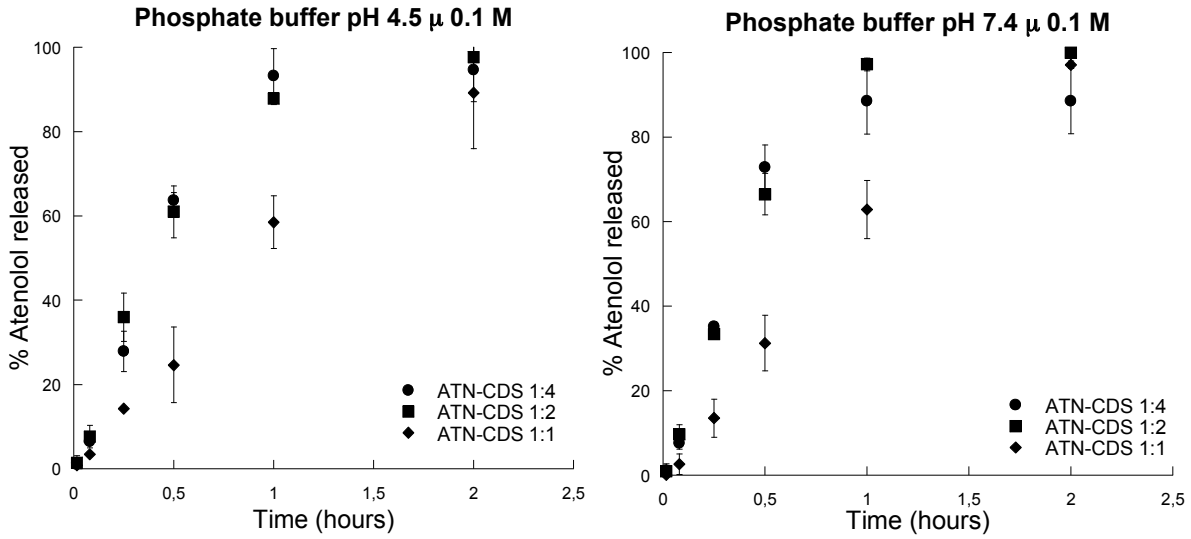

Figure 16. Atenolol release profiles obtained from chondroitin sulfate tablets containing different drug-polymer ratios.

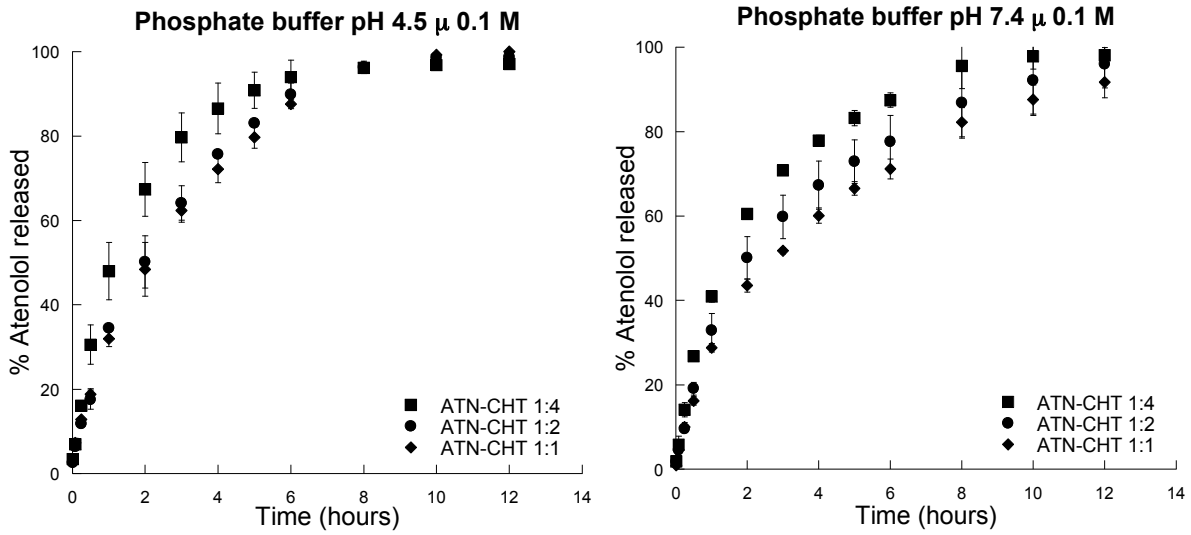

Figure 17. Atenolol release profiles obtained from chitosan tablets containing different drug-polymer ratios.

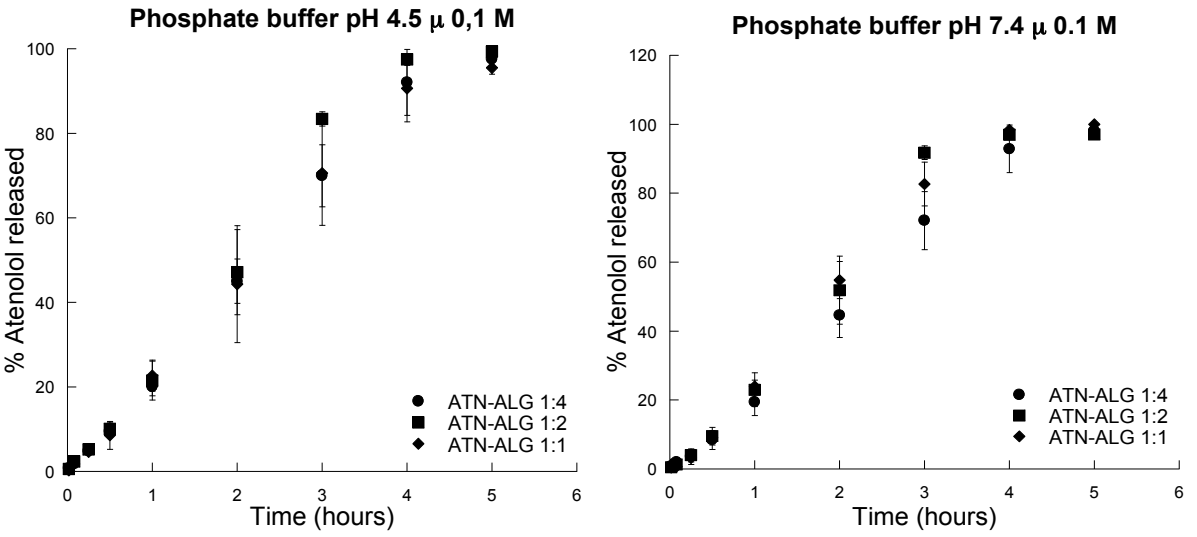

Figure 18. Atenolol release profiles obtained from sodium alginate tablets containing different drug-polymer ratios.

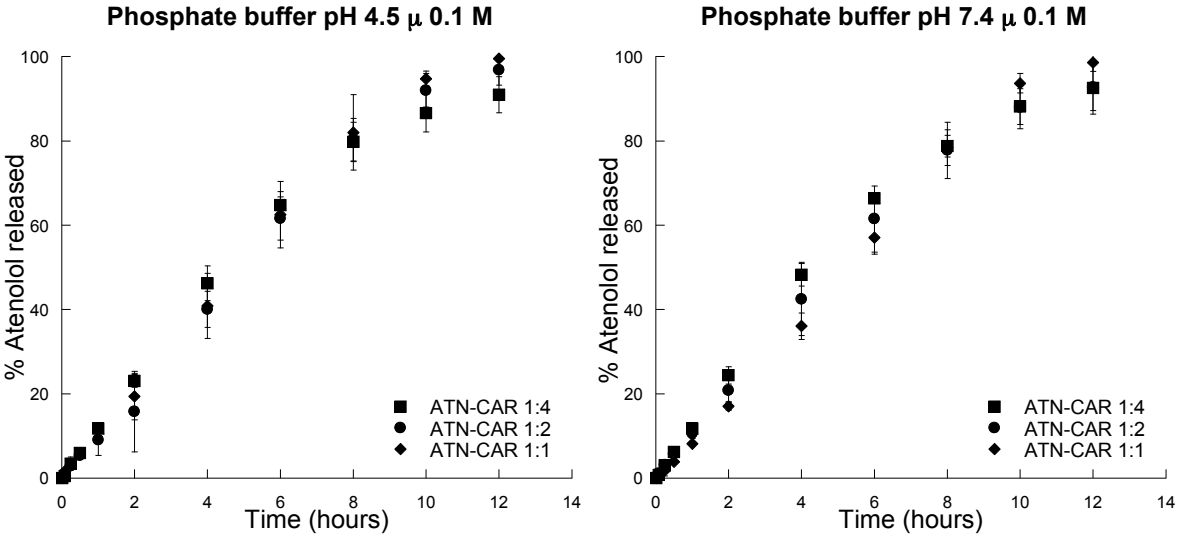

Figure 19. Atenolol release profiles obtained from carrageenan tablets containing different drug-polymer ratios.

As to chitosan, ATR-FT-IR analysis confirmed the occurrence of interactions with atenolol, which are likely hydrogen bonds, since both molecules contain basic groups and no significant changes in atenolol signals were detected in H^1 NMR analysis. As hydrogen bond

establishment depends on the availability of hydrogen bond donors and acceptors, changes in the environmental pH value are not expected to modify the strength of interactions between the two molecules and, as a consequence, similar drug release profiles were observed at pH 4.5 and 7.4. As opposite, when electrostatic interactions are involved, pH values of dissolution media are important to determine the interaction of ionic pairs, according to pK_a values of the molecules involved. Atenolol is positively charged at both pH values of 4.5 and 7.4, since its pK_a is 9.6. Chondroitin sulfate, λ-carrageenan and sodium alginate are negatively charged in the conditions tested, as pK_a values are 1.5-2 and about 3.5 for sulfate and carboxylic groups, respectively. Therefore, interactions occurring between atenolol and the said polymers did not change in the different media used and drug release profiles did not differ at acidic and neutral environment.

As stated, no significant differences in atenolol release profiles were observed among tablets containing different percentages of polymer for all the matrix systems produced, although increased drug release rates with decreasing amount of polymer are widely reported in the literature [93, 94], since the amount of drug released is proportional to its gradient of concentration, as stated by Fick's law. Moreover, many authors reported increased release rates with high soluble drugs [9, 95]. Since atenolol has a two fold higher solubility in 0.1 M phosphate buffer at pH 4.5, a faster drug release rate was expected than at pH 7.4. occurring with the polymers selected might prevent atenolol release, minimizing the effects of higher solubility and drug loading.

2.5.2 Effect of ionic strength

It has been demonstrated that drugs forming ionic complexes with oppositely charged polymers are released upon ionic exchange with ions of the same charge present in the releasing medium [58]. Thus, ionic strength of the dissolution medium is expected to influence drug release, which would be faster at higher ionic strength.

In vitro dissolution tests were carried out on matrix tablets, containing atenolol and each polymer in 1:1 weight ratio, in dissolution media at lower ionic strength, namely 0.01 M phosphate buffer at pH 4.5 and 7.4 and distilled water. The effect of ionic strength on drug release was then evaluated to eventually confirm the occurrence of ionic bonds in the systems.

As shown in Figure 20, atenolol release from chondroitin sulfate was not influenced by the different ions concentration of the dissolution medium. Atenolol dose was quantitatively released in 2 hours with a zero-order kinetics in all the solvents (Table 7), in conjunction with the matrix complete dissolution. This implied that, although strong ionic interactions are

present between atenolol and chondroitin sulfate, the main element controlling drug release was the dissolution of the polymer, very soluble in all the media tested.

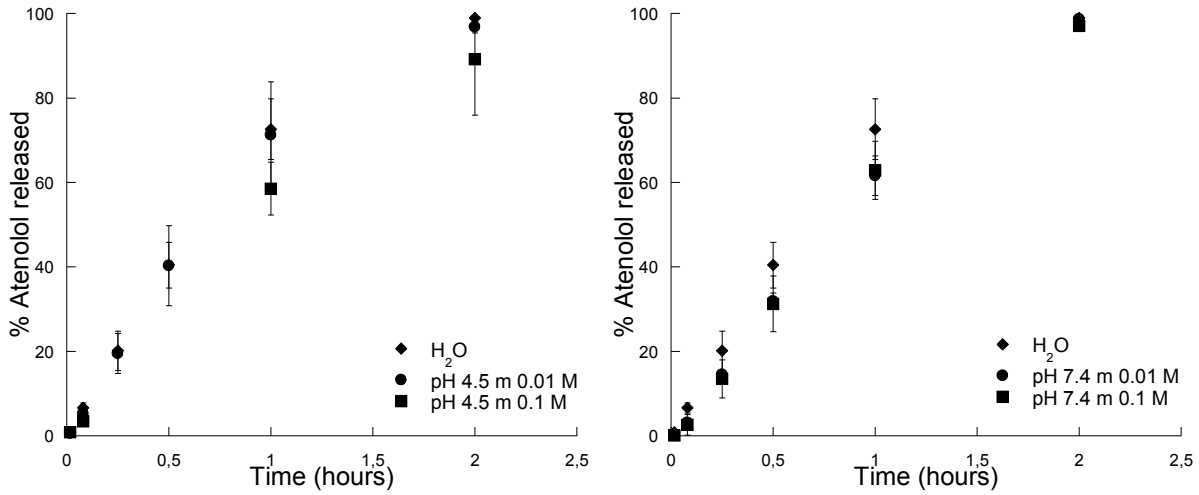

Figure 20. Atenolol release profiles obtained from chondroitin sulfate tablets containing in different dissolution media.

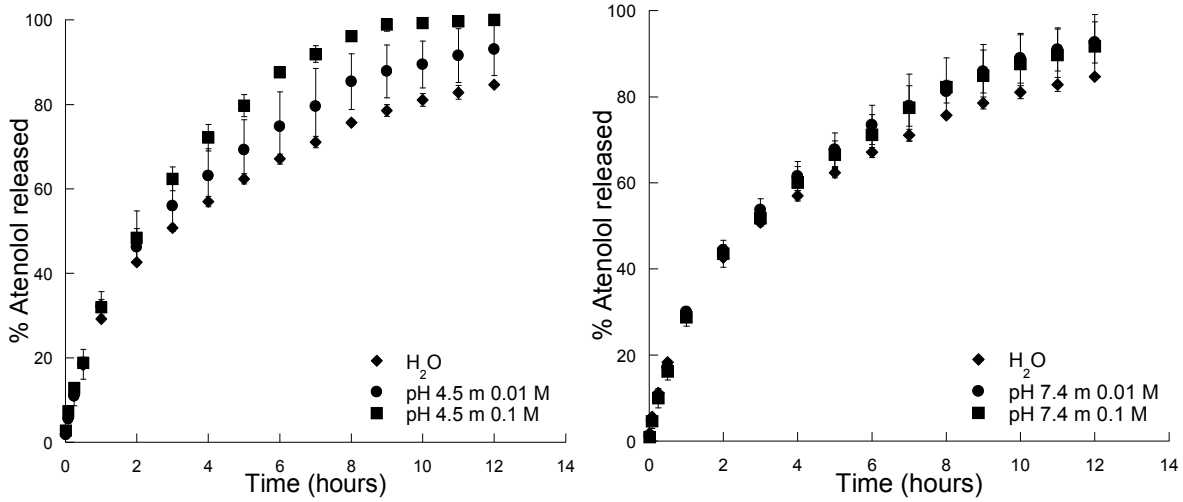

Figure 21. Atenolol release profiles obtained from chitosan tablets containing in different dissolution media.

Atenolol release from chitosan tablets did not appear significantly different in water, 0.01 phosphate buffers at both pH values and 0.1 M phosphate buffers at pH 7.4, while drug release rate was slightly increased in phosphate buffer at pH 4.5 and higher ionic strength,

as shown in Figure 21. These results were consistent with the different solubility of atenolol in the various dissolution media used, confirming that the diffusion of the drug in the solvent-penetrated matrix is the principal mechanism that controlled its release.

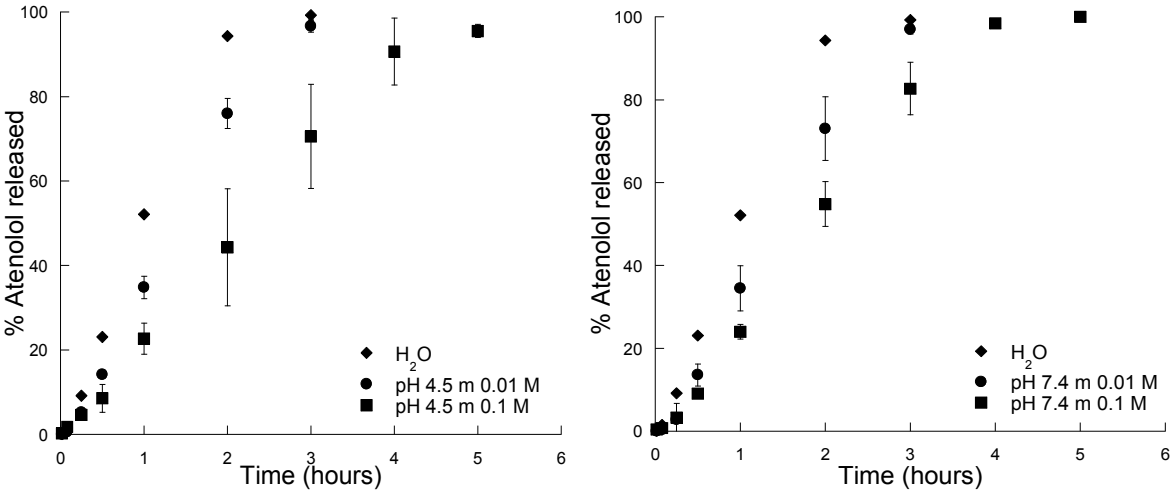

Figure 22. Atenolol release profiles obtained from sodium alginate tablets containing in different dissolution media.

In Figure 22 atenolol release profile from sodium alginate matrix tablets are reported. As opposite than expected, atenolol was released in 3 hours in water and in media at lower ionic strength and in 4-5 hours in media at higher ionic strength. Gradual erosion of tablets, affording super Case II release kinetics (Table 7), was observed during dissolution tests in all the media used. It is evident that the dissolution of sodium alginate controlled the atenolol release rather than drug-polymer interactions. The effect of ionic strength on drug release rates might be due to different sodium alginate properties, such as solubility or viscosity, in the different media used.

Similar results were obtained also for λ-carrageenan tablets (Figure 23). The faster release was obtained in water, where atenolol was quantitatively released in 4 hours. Drug release rates decreased as the medium ionic strength increased and atenolol was released in 6 hours in 0.01 M media and in 12 hours in 0.1 M. Tablets showed erosion in water and at lower ionic strength, which was consistent with the zero-order/super Case II release kinetics observed (Table 7). However, linear release profiles were exhibited also at higher ionic strength, where λ-carrageenan tablets swelled forming a thick layer of gel, as pointed out previously. As a matter of fact, polymer properties again had a leading role in determining

drug release, especially in water and at lower ionic strength. However, non-covalent interactions between atenolol and λ-carrageenan might prevent atenolol diffusion though the polymeric gel layer, formed upon contact with media at higher ionic strength, affording the quite unexpected linear release kinetics observed from a swelled matrix.

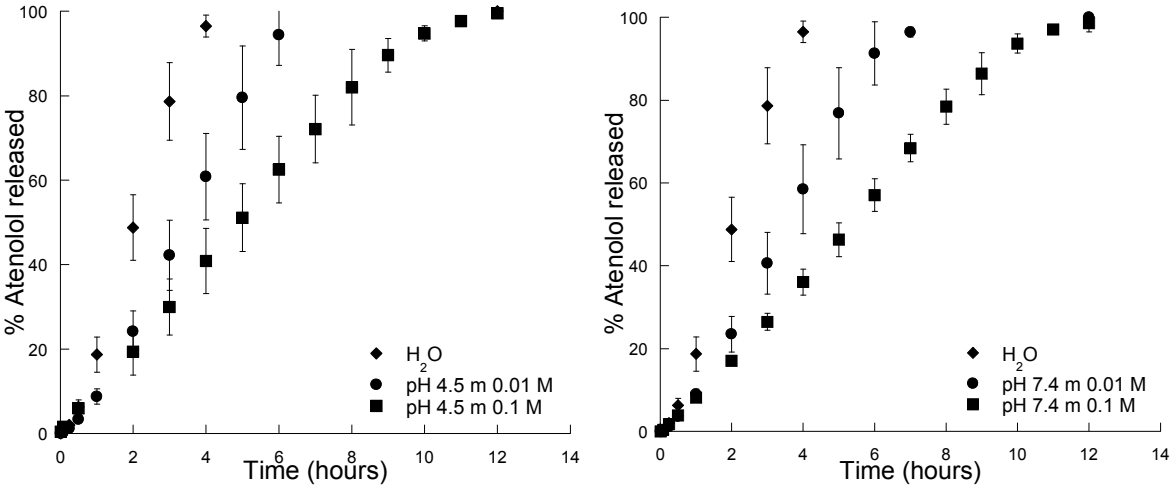

Figure 23. Atenolol release profiles obtained from λ-carrageenan tablets containing in different dissolution media.

Table 7. Diffusional exponent n, calculated by using Peppas' equation (eq. 4). Standard deviation in parenthesis (n=3).

Polymer	Distilled water	Phosphate buffer pH 4.5 μ 0.01 M	Phosphate buffer pH 7.4 μ 0.01 M	Phosphate buffer pH 4.5 μ 0.1 M	Phosphate buffer pH 7.4 μ 0.1 M
Chondroitin sulfate	0.96 (0.04)	1.04 (0.01)	1.18 (0.08)	1.10 (0.08)	1.17 (0.10)
Chitosan	0.57 (0.01)	0.62 (0.02)	0.66 (0.01)	0.60 (0.03)	0.66 (0.07)
Sodium alginate	1.30 (0.03)	1.50 (0.11)	1.27 (0.01)	1.21 (0.03)	1.42 (0.15)
λ-carrageenan	1.55 (0.10)	1.41 (0.07)	1.40 (0.14)	0.84 (0.09)	1.12 (0.19)

2.6 DESI-HMRS analysis

DESI is a process in which the analyte is extracted from the sample surface by a thin layer of solvent originating from primary droplets sprayed through a capillary and transported to the

mass analyzer by secondary droplets that have undergone electrospray ionization. In the present work, the surface of matrix tablets of atenolol-polymer was sprayed with solvents at constant ionic strength and different pH values (1.2, 4.5 and 7.4). The DESI technique permitted to study *in situ* the mechanisms involved in drug desorption, namely its release, from matrices made by each selected polymer.

The ion current registered in each sample was associated with the atenolol transport through the solvent spread on the matrix system surface. As shown in Figure 24, the shape of atenolol ion signal over the duration of the experiments was different, depending on the polymer tested. Tablets consisting of chondroitin sulfate exhibited an initial peak of atenolol signal, which collapsed to zero after 3 minutes (Figure 24, panel A). An initial atenolol peak from chitosan matrices was also observed, followed by a reduction of the current intensity, which remained constant over time (Figure 24, panel B). Ion current from both sodium alginate (Figure 24, panel C) and λ-carrageenan tablets (Figure 24, panel D) showed initial current peaks, followed by constant signals over time. The differences in the shape of the atenolol current signals were due to the various properties of polymers upon contact with the sprayed solvent.

As to chondroitin sulfate tablets, viscous gel ripples formed in front of the transfer capillary, leading to the downfall of atenolol signal after the initial peak. Chitosan matrices showed the formation of a hole where the solvent was sprayed. So, the initial atenolol peak observed was due to the dissolution of the amount of drug present on the surface, whereas the following reduced and constant signal was consequent to the dissolution of the drug contained in the gradually dug hole. Sodium alginate and λ-carrageenan swelled upon contact with the sprayed solvent, affording constant atenolol ion currents because of its diffusion through the gel layer.

To obtain information about the amount of drug release from each polymeric matrix, the atenolol ion current was converted into amount values by using calibration curves. The equations obtained by calculating the regression line with the method of least square are reported in Table 8.

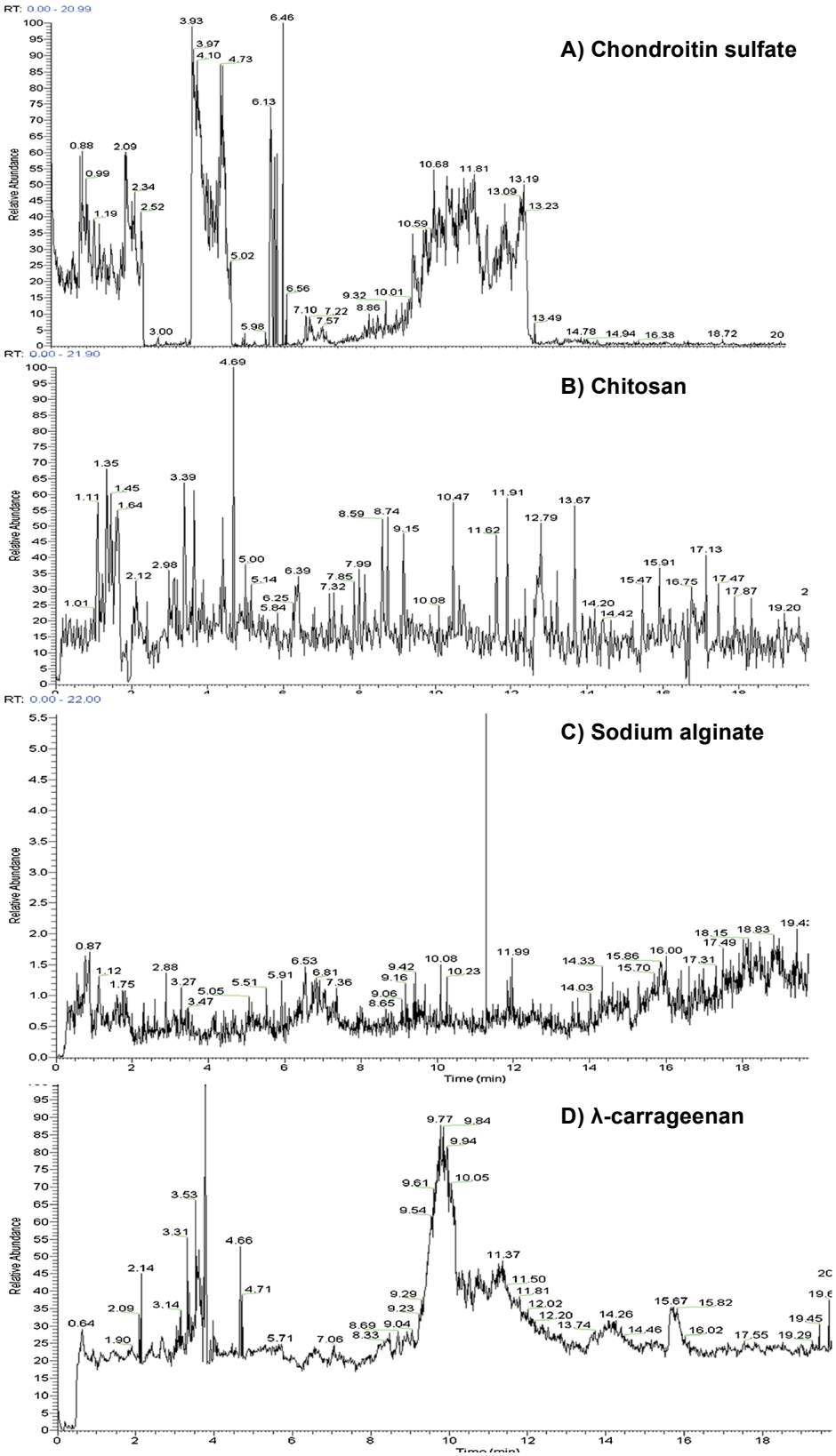

Figure 24. DESI-MS atenolol ion current recorded in the 0-20 minutes range for polymeric tablets sprayed with aqueous solution at pH 7.4.

Table 8. Parameters of the calibration curves for atenolol ion current in different solvents.

SOLVENT	EQUATION	R^2
pH 7.4	y = 3616x	0.998
pH 4.5	y = 4265x	0.991
pH 1.2	y = 7441x	0.995

Cumulative amounts of atenolol released at pH 7.4, 4.5 and 1.2 reported as a function of time are shown in Figure 25, 26 and 27, respectively.

A biphasic pattern was presented by all investigated polymers, indicating two different mechanisms controlling drug desorption. At very early stages of desorption, before the superficial gelation of the polymers, drug release was mainly influenced by drug-polymer non covalent interactions in the thin layer of solution present on the tablet surface as well as by the polymer solubility. After the formation of the gel layer, or of the hole in the case of chitosan, the specific characteristic of each polymer determined atenolol desorption.

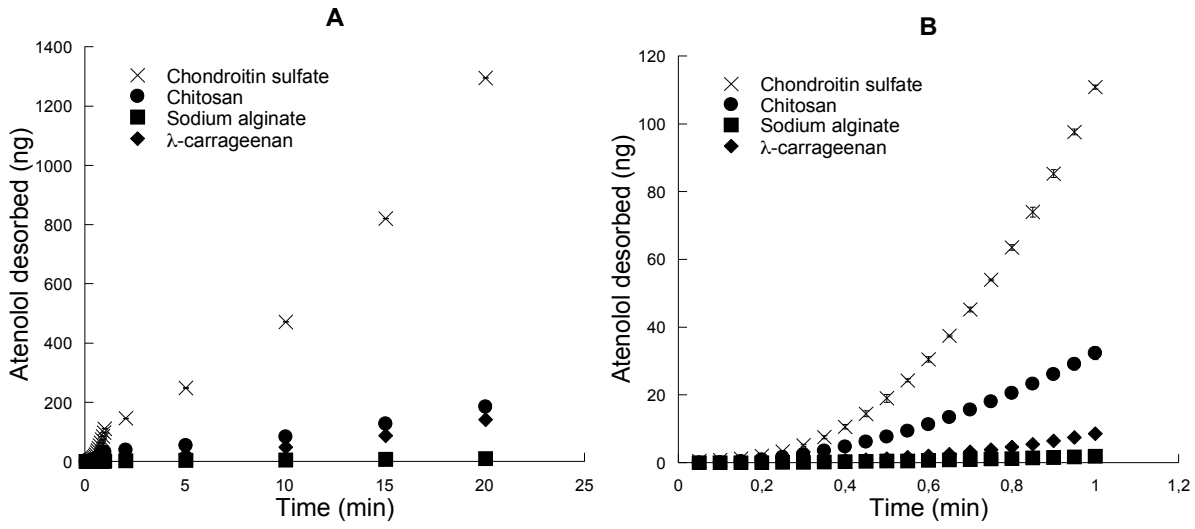

Figure 25. Desorbed atenolol amount at pH 7.4 from the four polymeric matrix systems investigated: A) 0-20 min and B) 0-1 min.

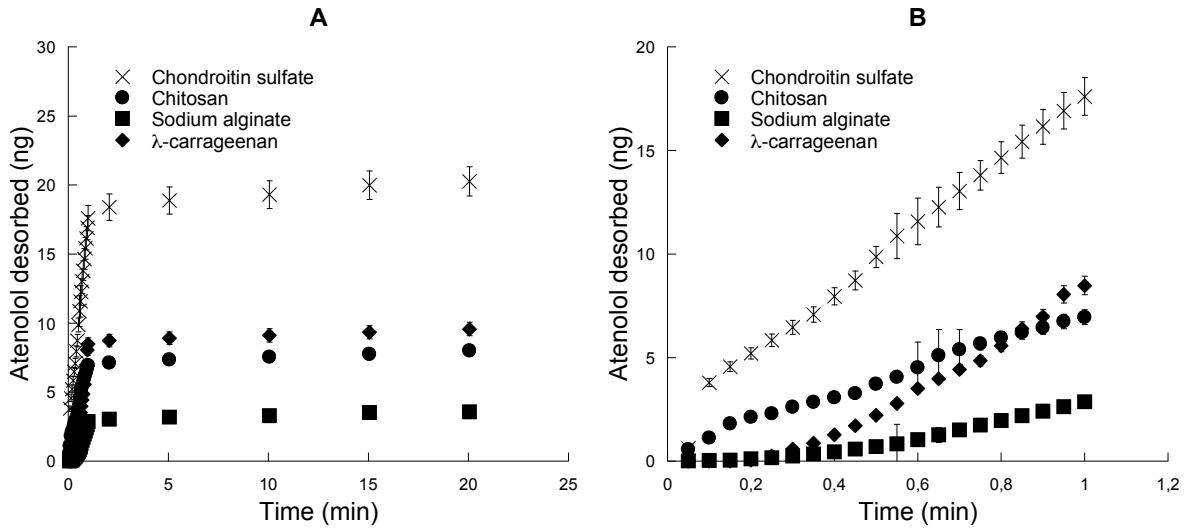

Figure 26. Desorbed atenolol amount at pH 4.5 from the four polymeric matrix systems investigated: A) 0-20 min and B) 0-1 min.

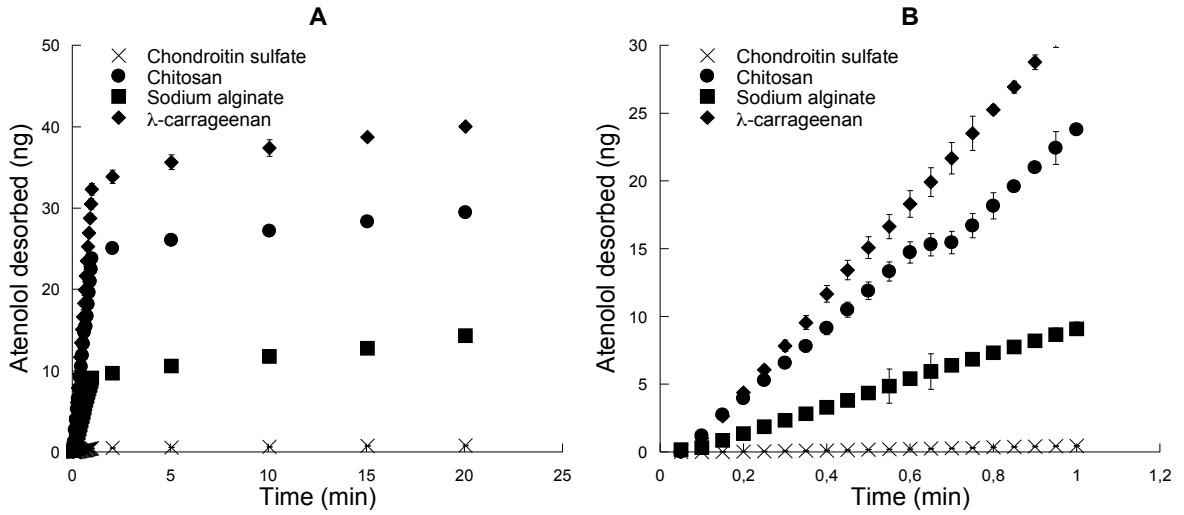

Figure 27. . Desorbed atenolol amount at pH 1.2 from the four polymeric matrix systems investigated: A) 0-20 min and B) 0-1 min.

In order to compare the extent of atenolol released from different matrices in the particular operative conditions of DESI experiments, the area under the curve (AUC) of the amount of drug dissolved in the same time interval was calculated. In particular, two time regions,

namely the intervals 0-1 minute and 1-20 minutes, were considered to better understand the mechanisms involved in each phase.

In the 0-1 minute interval, the highest amount of atenolol at pH 7.4 was released from chondroitin sulfate, followed by chitosan, λ-carrageenan and sodium alginate, as shown by AUC values reported in Table 9. The greater release of atenolol from chondroitin sulfate was determined by the high solubility of the polymer in water, which readily dissolved in the solvent allowing the efficient and rapid desorption of the drug. As to matrices made by chitosan, which is a polymer insoluble in the solvent used, the release of atenolol mainly occurred because of the high solubility of the drug in the thin layer of solvent deposited on the tablet surface. On the contrary, sodium alginate and λ-carrageenan tablets showed very poor desorption of atenolol. These two polymers are not very soluble in water, so at the very beginning of the experiments, atenolol interactions with polymers prevented its dissolution in the solvent layer and, as a consequence, its desorption.

At acidic pH values (4.5 and 1.2) a similar trends in AUC values, calculated over the first minute of the experiments, was observed. Atenolol drug release from chondroitin sulfate was the highest, in particular at pH 4.5, confirming that the key element controlling the desorption process was the polymer dissolution in the solvent. A negligible desorption was obtained, instead, at pH 1.2 because of the fast formation of a viscous gel layer on the tablet surface which reduced the drug transfer to the mass analyzer. Drug desorption from chitosan matrices was unaffected by the solvent pH, demonstrating that the mechanism involved in release was drug dissolution in the superficial solvent layer. Sodium alginate and carrageen showed the lowest drug release also at acidic pH values, and drug desorption increased as pH value was lowered. These results were consistent with the occurrence of ionic interaction of the anionic polymers with atenolol which controlled its desorption from the tablets surface. In fact, lower pH values of the solvent reduced the negative charges on the polymers, reducing also the extent of interaction with the drug, which was more easily released.

Table 9. Area under the curve values calculated in the 0-1 minutes time range.

Polymer	AUC (ng/mim)		
	pH 7.4	pH 4.5	pH 1.2
Chondroitin sulfate	1.30 ± 0.02	1.26 ± 0.09	0.017 ± 0.003
Chitosan	0.456 ± 0.01	0.272 ± 0.007	0.40 ± 0.02
Sodium alginate	0.028 ± 0.004	0.038 ± 0.004	0.19 ± 0.05
λ-carrageenan	0.096 ± 0.002	0.109 ± 0.05	0.638 ± 0.008

The analysis of the second time interval (1-20 minutes) revealed for all the polymers, in every pH tested, that the amount of drug desorbed was almost constant over time. The formation of the gel layer for chondroitin sulfate, sodium alginate and λ-carrageenan matrices and of a hole on the chitosan tablet surface reduced the transfer of the drug to secondary droplets, leading to the change of the drug desorption. Only chondroitin sulfate at pH 7.4 showed an increasing release of atenolol in the 20 minutes investigated, probably due to the polymer solubility in the solvent.

The DESI-MS technique provided the fast, reproducible and simple analysis of atenolol release from polymeric matrix tablets in a reduced area in contact with a small volume of solvent. These particular experimental conditions permitted to investigate the mechanisms involved in drug release, in particular during the first minute of analysis, when the properties of each polymer, not yet interacting with the solvent, were less crucial. Results obtained from DESI-MS experiments confirmed the observations resulting from *in vitro* dissolution studies, showing that atenolol release from chondroitin sulfate was mainly controlled by the polymer dissolution, whereas drug dissolution in the sprayed solvent was the mechanism involved in the case of chitosan tablets. Ionic interactions were responsible for the release of atenolol from sodium alginate and λ-carrageenan.

3. CONCLUSIONS

The model basic drug atenolol interacted with polymers carrying various chemical functions in different ways. ATR-FT-IR and H^1 NMR analyses confirmed the occurrence of electrostatic interactions between atenolol and chondroitin sulfate, sodium alginate and λ-carrageenan, while hydrogen bonds were established with chitosan.

In vitro dissolution studies carried out on matrix systems consisting of atenolol and each polymer selected, showed that both drug-polymer interactions and polymer characteristics have a key role in drug release.

Atenolol release was not affected by the different amount of each polymer in all the matrix systems studied. Moreover, although atenolol has a different solubility in the dissolution media used, drug release profiles obtained from all polymeric tablets was not influenced by drug solubility. Drug-polymer interactions play a role in determining these effects.

Atenolol release from chondroitin sulfate tablet was not appropriate for controlled drug delivery, since tablets dissolved completely within 2 hours in all the conditions of pH and ionic strength tested, suggesting that drug release was mainly controlled by polymer dissolution.

Chitosan tablets behaved as classical polymeric matrices, so that atenolol release was controlled by its dissolution/diffusion in the gradually solvent penetrated matrix.

Atenolol release from sodium alginate and λ-carrageenan tablets depended on the ionic strength of the solvents used. As opposite than expected, drug release rate was lowered by increasing ionic strength. In the case of sodium alginate matrix tablets, erosion was observed in all the media used, so that, again, polymer properties were more important than interactions in determining drug delivery rate and kinetics. λ-carrageenan exhibited different behaviours in each solvent used, showing erosion at lower ionic strengths and swelling at higher ionic strength. However, zero order or super Case II kinetics were observed in every dissolution medium. Atenolol-λ-carrageenan ionic interactions play a role in preventing drug diffusion through the swelled polymer at higher ionic strength, affording a linear kinetics rather than the expected Fickian kinetics.

The DESI-MS technique allowed studying the mechanisms involved in drug release from polymeric matrices in a localized area of the tablet surface in contact with a small volume of solvent. These particular operative conditions permitted to indentify an interval of time where polymer-solvent interactions were negligible, so that only the contribution of drug-polymer interactions on drug release could be evidenced and evaluated. DESI-MS data confirmed that non-covalent interactions were important in atenolol release only in the case of sodium

alginate and λ-carrageenan, while polymer-solvent interactions and drug-solvent interactions mainly controlled drug release from chondroitin sulfate and chitosan matrices respectively.

IV. SECOND PART

IV. SECOND PART

The second part of the research focused on the thorough characterization and comprehension of the factors involved in atenolol release from λ-carrageenan matrix tablets, which resulted the more suitable system for atenolol oral controlled drug delivery among those studied in the present research project.

In this system, erosion/swelling of tablets (Figure 28) as well as release kinetics were influenced by the ionic strength of the dissolution medium. The relative contribution of polymer hydration properties and of drug-polymer interactions on the observed release profiles was evaluated with various techniques, such as differential scanning calorimetry and the study of fronts movement of the matrix systems. In these studies, drug-polymer-salt interactions emerged as the element controlling drug release, rather than drug-polymer interactions alone. Thus, ternary systems, containing atenolol, λ-carrageenan and various salts, were investigated as possible oral controlled delivery systems. The exploitability of the mixture λ-carrageenan-salt to deliver other drugs presenting basic groups, such as methyl L-dopa and buflomedil pyridoxal phosphate, was also evaluated.

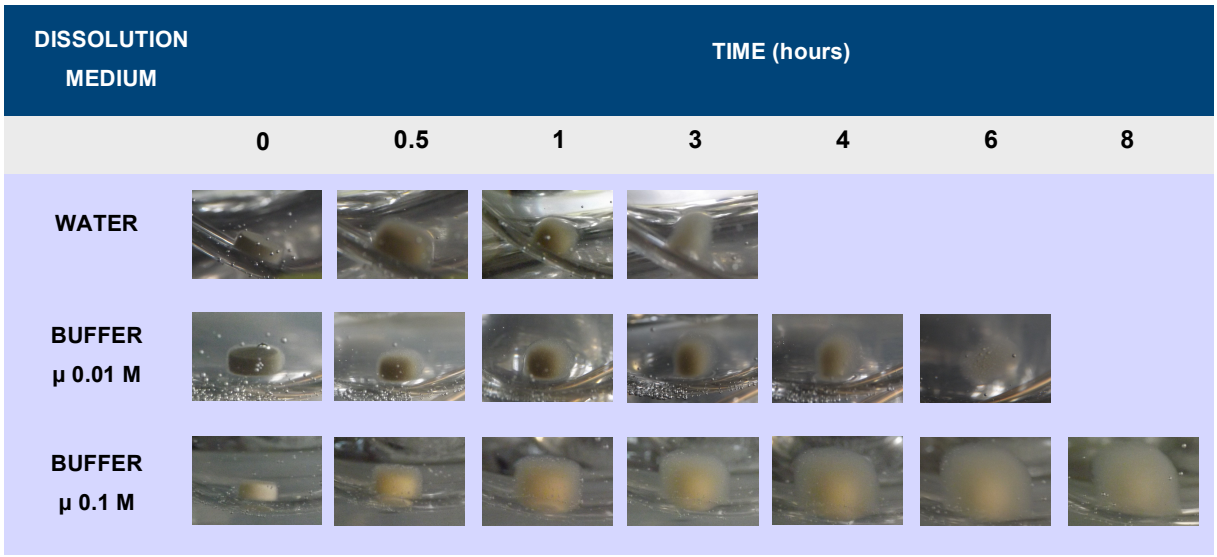

Figure 28. Pictures of atenolol-λ-carrageenan matrices taken during *in vitro* drug release studies in various media in the time interval 0-8 hours.

1. MATERIALS AND METHODS

1.1 Materials

- METHYL L-DOPA (Figure 29) was kindly donated by Chiesi Farmaceutici S.p.A (Italy). The drug has a molecular mass of 211.21 g/mol and a pK_a value of 8.7 [96]. It is a produced by esterification of the carboxylic moiety of the levodopa molecule. The prodrug is more soluble than levodopa, offers a more rapid absorption and onset of action [97].

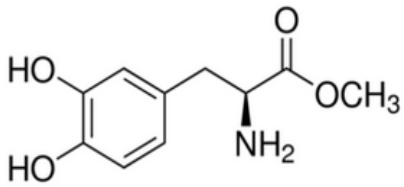

Figure 29. Molecular structure of levodopa methyl ester.

- BUFLOMEDIL PYRIDOXAL PHOSPHATE (Figure 30) was kindly donated by Lisapharma S.p.A (Italy). The drug has a molecular mass of 554.53 g/mol. It is a vasoactive molecule effective in improving blood flow in ischemic tissues in patients with peripheral and/or cerebral disease, by combining different pharmacological effects, such as α-adrenoreceptor antagonism, inhibition of platelet aggregation and weak calcium antagonistic effect [98]. It has been used to treat the symptoms of peripheral arterial occlusive disease. In 2012 the European Medicine Agency recommended the suspension of all the marketing authorizations through the European Union because of serious side effects reported in patients treated. In the present work, the drug has been selected because of its particular structure, in a frame aimed to investigate the effect of the molecular structure on interactions with λ-carrageenan and release kinetics.

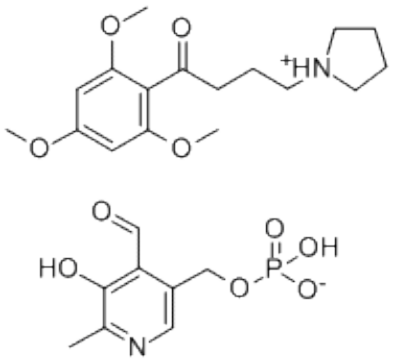

Figure 30. Molecular structure of buflomedil pyridoxal phosphate.

- λ-CARRAGEENAN Viscarin® GP 209 NF was kindly donated by FMC Biopolymer (USA).
- ATENOLOL (Figure 6) was kindly donated by Lisapharma S.p.A (Italy).
- Other chemicals used were: methanol and acetonitrile HPLC grade, acetic acid, dibutylamine, triethylamine, potassium acetate, citrate, oxalate, orthophosphate, sulfate, phthalate monobasic, tartrate (Sigma Aldrich, Germany), acid 1-heptansulphonic acid sodium salt (Alfa Aesar, Germany), anhydrous dibasic sodium phosphate (Riedel-de haën, Germany), potassium dibasic phosphate, potassium dihydrogen phosphate, hydrochloric acid 37% (Carlo Erba, Italy), phosphoric acid 85% (ACEF, Italy), sodium hydroxide pellets (Prolabo, France).
- Phosphate buffers at pH 4.5 and 7.4 and at ionic strength 0.01 and 0.1 M were prepared according to the procedures described in the section 1.1.2 of chapter III.

1.2 Methods

1.2.1 Analytical method for the determination of methyl L-dopa

The quantitative determination of methyl L-dopa was carried out by High Performance Liquid Chromatography (HPLC), using an Agilent 1200 Series (Agilent Technologies, USA) chromatographic system. The analysis was performed on an Alltech Alltima C-18 silica-bonded stationary phase column (150 x 4.6 mm, 5 µm; Grace, USA) using a mobile phase composed of an aqueous solution of potassium dihydrogen phosphate 0.02 M, acetic acid and triethylamine (99.3:0.5:0.2 v/v/v) at pH 3.3, isocratically eluted at a flow rate of 1 mL/min. The UV detector was set at 280 nm and data were analysed using ChemStation B.03.02 software (Agilent).

The HPLC method was validated by considering linearity, precision, limit of detection (LOD) and of quantification (LOQ), according to the ICH Q2(R1) guidelines [77]. In addition, number of theoretical plates, tailing factor, signal-to-noise (S/N) ratio were calculated from a chromatogram obtained from the analysis of a solution 0.01 mg/mL of methyl L-dopa in water.

The linearity of the method was verified by plotting areas obtained from chromatograms of 5 aqueous solutions of methyl L-dopa as a function of their concentration. The concentration range 0.001 – 0.1 mg/mL was used. Precision is expressed as the relative standard deviation (% RSD) of a series of measurements. % RSD of the area of chromatographic peaks was calculated for 5 repeated injections of methyl L-dopa standard solutions in the range of concentration 0.001 – 0.1 mg/mL. % RSD values lower than 2 were considered acceptable. Limit of detection (LOD) and limit of quantification (LOQ) were also determined using the signal-to-noise approach, considering said limits the concentrations of analyte providing S/N ratios of 3 and 10, respectively.

1.2.2 Analytical method for the determination of buflomedil pyridoxal phosphate

The quantitative determination of buflomedil pyridoxal phosphate was carried out by High Performance Liquid Chromatography (HPLC), using an Agilent 1200 Series (Agilent Technologies, USA) chromatographic system. The analysis was performed on an Alltech Alltima C-18 silica-bonded stationary phase column (150 x 4.6 mm, 5 µm; Grace, USA) using an isocratic solvent system consisting of methanol / water / acetonitrile / triethylamine (50:30:20:0.4 v/v/v/v), delivered at a flow rate of 1 mL/min. The UV detector was set at 272 nm and data were analysed using ChemStation B.03.02 software (Agilent).

The HPLC method has been validated by considering linearity, precision, limit of detection (LOD) and of quantification (LOQ), according to the ICH Q2(R1) guidelines [77]. In addition, number of theoretical plates, tailing factor, signal-noise ratio were calculated from a chromatogram obtained from the analysis of a solution 0.01 mg/mL of buflomedil pyridoxal phosphate in water.

The linearity of the method was verified by plotting areas obtained from chromatograms of 5 aqueous solutions of buflomedil pyridoxal phosphate as a function of their concentration. The concentration range 0.001 – 0.1 mg/mL was used. Precision is expressed as the relative standard deviation (% RSD) of a series of measurements. % RSD was calculated of the area of chromatographic peaks for 5 repeated injections of methyl L-dopa standard solutions in the range of concentration 0.001 – 0.1 mg/mL. % RSD values lower than 2 were considered acceptable. Limit of detection (LOD) and limit of quantification (LOQ) were also determined

using the signal-to-noise approach, considering said limits the concentrations of analyte providing S/N ratios of 3 and 10, respectively.

1.2.3 Preparation of matrix tablets

Binary and ternary matrix tablets were prepared. Binary matrices consisted of drug and λ-carrageenan in 1:1 weight ratio, where the drug was either atenolol, methyl L-dopa or buflomedil pyridoxal phosphate. Salts were added to the binary mixtures to prepare ternary tablets. Salts used were: potassium acetate, citrate, dihydrogen phosphate, orthophosphate, oxalate, phthalate monobasic, sulfate, tartrate. Ternary matrices were made up of a mixture of atenolol, λ-carrageenan and each salt in weight ratio 47:47:6 and 45:45:10. Tablets containing methyl L-dopa or buflomedil pyridoxal phosphate, λ-carrageenan and potassium dihydrogen phosphate in weight ratio 47:47:6 were also produced.

All the powders employed were initially sieved (Endecotts Limited, UK) in order to obtain powders with particle size ranging between 180 and 125 μm and mixed in Turbula® (WAB, Switzerland) for 15 min before compression. Tablets were prepared by direct compression of 150 mg of powders mixtures using 7 mm diameter flat faced punches and a fixed cylindrical die, mounted on a reciprocating tablet press Korsch Mod. EKO (Germany) instrumented for the registration of applied compression force (Kistler, Italy). Compression force was maintained in the range of 12-15 kN.

1.2.4 Hydration properties of λ-carrageenan by differential scanning calorimetry (DSC)

DSC experiments were carried out in order to study the interactions between λ-carrageenan and the solvents previously used in *in vitro* dissolution studies. Series of gel samples of λ-carrageenan were prepared with different percentages (from 20 to 97% w/w) of the following solvents: distilled water, phosphate buffer at pH 4.5 and 7.4, both at ionic strength 0.01 M and 0.1 M. Gels were directly prepared in aluminium crucibles with capacity of 40 μL. The polymer was accurately weighed and then wetted with the correct amount of solvent to obtain each concentration. Crucibles were hermetically closed, stored at 37°C for 12 hours and then at room temperature for 4 days, to allow equilibration and uniform liquid distribution in gels. The exact polymer: water ratios were calculated using the initial and final weight of crucibles, in order to account for the water loss during storage. Finally, samples were frozen at -18°C until analysis.

Measures were performed by using an instrument Mettler Toledo DSC 821^e (Mettler Toledo, Switzerland) equipped with a cryostat Heto CBN 18-50 (Heto, USA). STARe software version

11.0 was used to analyse data. Analyses were carried out under nitrogen atmosphere (flow 100 mL/min), each sample was cooled from 25°C to -10°C with a rate of 10°C/minute, then maintained at -10°C for 40 minutes and finally heated up at 30°C at a heating rate of 10°C/minute. Experiments were conducted in three replicates.

1.2.5 Fronts Movement and Drug Release

The position of the fronts and the release behaviour of the atenolol- λ-carrageenan tablets were studied in a USP dissolution apparatus II as a function of time. Cylindrical matrices were placed in a cell consisting of two transparent Plexiglas discs fixed on their bases by screws, as reported by Bettini [66]. Swelling and drug release were accomplished only from the lateral side of the matrix, since the penetration of the dissolution medium was limited to this side. The assembled device, containing the tablet, was introduced into the vessel of the dissolution apparatus filled with 1000 mL of dissolution medium at 37°C. Distilled water, phosphate buffer at pH 4.5 and 7.4, both at ionic strength of 0.01 M and 0.1 M, were used. The paddle rotation speed was set to 200 rpm, in order to avoid any boundary layer effects during drug release. At fixed time intervals, the device was removed from the dissolution apparatus and photographed by means of a video camera (JVC, Japan) connected to a stereomicroscope Citoval 2 (Carl Zeiss Jena, Germany) to follow the swelling phenomenon and the front movement. Atenolol release was quantified by using the HPLC-UV method previously described in the section 1.2.3 of chapter III. Experiments were repeated in triplicate.

1.2.6 In vitro dissolution studies

Drug release from binary and ternary tablets was studied for up to 12 h. The experiments were conducted at 37 ± 0.5°C on a USP dissolution apparatus II (Agilent VK 7025, Agilent Technologies, USA) equipped with a peristaltic pump (Agilent 810, Agilent Technologies) and an autosampler (Agilent 8000, Agilent Technologies) for automatic sampling. Dissolution studies were performed at 50 rpm in 1000 mL of distilled water. Samples of 1.5 mL were withdrawn at defined time intervals and the amount of the released drug was quantified by HPLC-UV. All experiments were done in triplicate. Peppas' empirical power law (eq. 4) was used to characterize drug release mechanism from the matrix tablets prepared [14, 15].

2. RESULTS AND DISCUSSION

2.1 Validation of the HPLC analytical method for the determination of methyl L-dopa

The chromatographic peak related to methyl L-dopa was detected at the retention time of 8.4 minutes. In Figure 31 the concentration of aqueous solutions of methyl L-dopa was plotted against areas obtained from their chromatograms. The equation of the regression line, calculated with the method of least square, was y = 11930x – 2.06, with a correlation coefficient R^2 of 0.9998. The linear relationship between the chromatogram signals and the analyte concentration was then demonstrated. The signal-to-noise ratio calculated for the standard solution at concentration 0.01 mg/mL was 155. The method had a limit of quantification of 8.4 x 10^{-4} mg/mL and a limit of detection of 1.9 x 10^{-4} mg/mL.

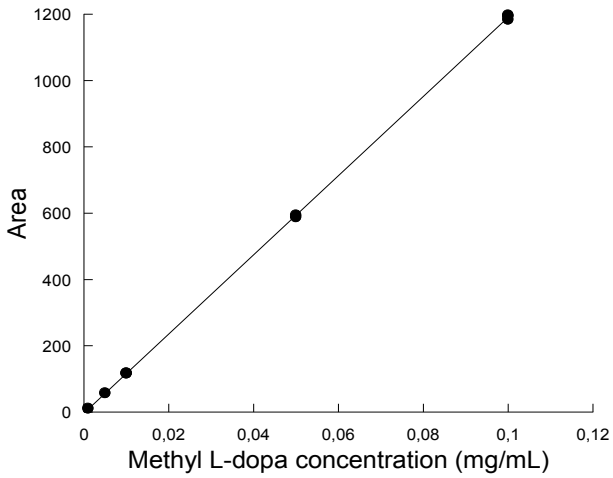

Figure 31. Area of chromatographic peaks obtained from methyl L-dopa solutions plotted vs their concentration.

Table 10 reports the values of % relative standard deviations obtained from chromatographic areas of 5 injections of methyl L-dopa standard solutions. Since all the % RSD values calculated were lower than 2, the method was considered precise and reliable. The number of theoretical plates and the tailing factor were also calculated, resulting 9772 and 0.87, respectively.

Table 10. Mean peak areas, standard deviations (SD) and % relative standard deviations (%RSD) calculated for standard solution of methyl L-dopa at various concentrations.

CONCENTRATION (mg/mL)	MEAN PEAK AREA	SD	% RSD
0.001	11.08	0.16	1.47
0.005	57.90	0.14	0.24
0.01	117.45	1.20	1.02
0.05	591.05	4.88	0.83
0.1	1192.03	6.75	0.57

2.2 Validation of the HPLC analytical method for the determination of buflomedil pyridoxal phosphate

The chromatographic peak related to buflomedil pyridoxal phosphate was detected at the retention time of 7.4 minutes. In Figure 32 the concentration of aqueous solutions of buflomedil pyridoxal phosphate was plotted against areas obtained from their chromatograms. The equation of the regression line, calculated with the method of least square, was y = 9738x – 3.583, with a correlation coefficient R^2 of 0.9999. The linear relationship between the chromatogram signals and the analyte concentration was then demonstrated. The signal-to-noise ratio calculated for the standard solution at concentration 0.01 mg/mL was 120. The method had a limit of quantification of 8.3 x 10^{-4} mg/mL and a limit of detection of 2.5 x 10^{-4} mg/mL.

Table 11 reports the values of % relative standard deviations obtained from chromatographic areas of 5 injections of buflomedil pyridoxal phosphate standard solutions. Also in this case, since all the % RSD values calculated were lower than 2, the method proved to be precise and reliable. The number of theoretical plates and the tailing factor were also calculated, resulting 5000 and 0.85, respectively.

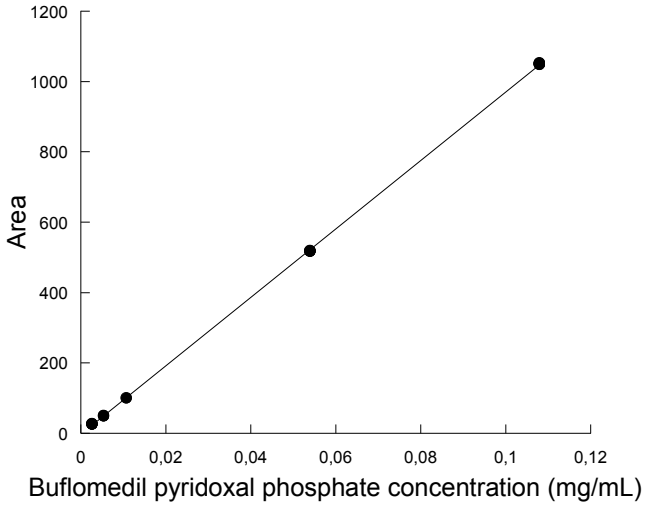

Figure 32. Area of chromatographic peaks obtained from buflomedil pyridoxal phosphate solutions plotted vs their concentration.

Table 11. Mean peak areas, standard deviations (SD) and % relative standard deviations (%RSD) calculated for standard solution of buflomedil pyridoxal phosphate at various concentrations.

CONCENTRATION (mg/mL)	MEAN PEAK AREA	SD	% RSD
0.0027	25.77	0.42	1.62
0.0054	49.03	0.15	0.31
0.0108	99.88	0.28	0.28
0.054	517.77	1.10	0.21
0.108	1049.90	2.04	0.19

2.3 Hydration properties of λ-carrageenan by differential scanning calorimetry (DSC)

DSC analysis was used to study the interactions between λ-carrageenan and the solvents used in *in vitro* dissolution studies, previously described in the section 2.5 of chapter III. It is generally accepted that there are three different types of water interacting with hydrophilic polymers: free or unbound water, freezing bound water and non-freezing bound water. Free water does not interact with polymer and its transition enthalpy and peak shape, detected by

DSC analysis, correspond to the ones observed with pure water. Freezing bound water weakly interacts with the polymer and its phase-transition temperature is lower than that of pure water. Non-freezing water strongly interacts with the polymer binding sites and it does not freeze [99, 100].

Enthalpy values related to the melting of frozen free water, calculated by DSC analysis, were plotted against the percentage of λ-carrageenan content in each series of gel samples, as shown in Figures 33-35. The values of the melting enthalpy decreased as the concentration of the polymer increased. In particular, a linear relationship was found between the two variables in gel samples containing pure water, as shown in Figure 33. As to gels containing phosphate buffers, deviations from linearity was observed (Figures 34 and 35). The plots were extrapolated to zero enthalpy through the lines of best fit. The concentration at this point represents the minimum ratio of λ-carrageenan: water that is required for water to occupy the binding sites of the polymer, giving complete hydration of λ-carrageenan. Once all binding sites are occupied, any excess of water present is free or lightly bounded [100]. Table 12 reports, for each solvent used, the amount of bound water extrapolated at zero enthalpy. The amount of pure water required to completely hydrate λ-carrageenan was 18.9 % w/w, indicating that the polymer had high affinity for water. The presence of salt in the solvent used to hydrate λ-carrageenan did not significantly influence the polymer : water compositions extrapolated to zero enthalpy, which resulted very similar to that observed when pure water was used. However, when higher concentration of salt was present, such as in phosphate buffers at ionic strength 0.1 M, much water (about 23-25% w/w) was required for the complete hydration of the polymer. Thus, the presence of salt slightly decreased the λ-carrageenan affinity for water. Since the composition of the fully hydrated λ-carrageenan was related to its affinity for each solvent investigated, the values found could be somehow considered indicative of the polymer solubility in each solvent. Hence, DSC analyses showed that λ-carrageenan was, as expected, more soluble in pure water and in buffers at lower ionic strength, while the presence of higher concentration of salt lowered its solubility.

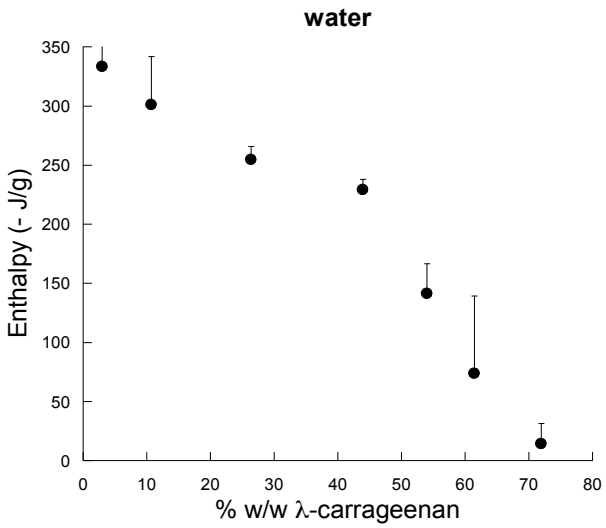

Figure 33. Enthalpy of melting water as a function of λ-carrageenan gels hydrated with pure water. The bars represent the standard deviation (n=3).

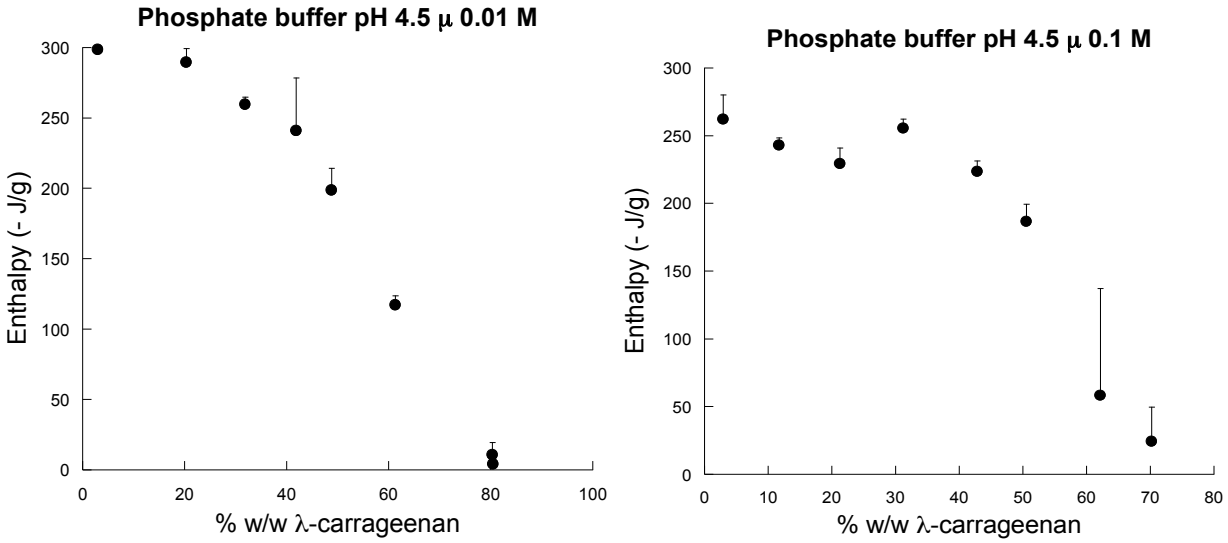

Figure 34. Enthalpy of melting water as a function of λ-carrageenan gels hydrated with phosphate buffer pH 4.5 at different ionic strength. The bars represent the standard deviation (n=3).

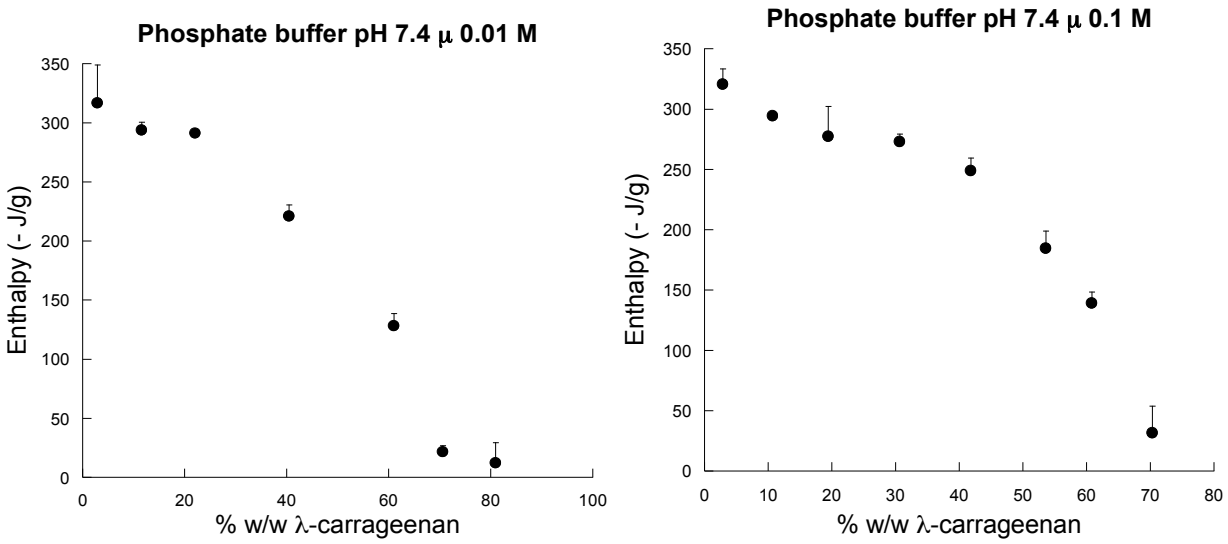

Figure 35. Enthalpy of melting water as a function of λ-carrageenan gels hydrated with phosphate buffer pH 7.4 at different ionic strength. The bars represent the standard deviation (n=3).

Table 12. Amount of bound water (% w/w) in gels of λ-carrageenan prepared with different solvents.

SOLVENT	% w/w of bound water (± SD)
Distilled water	18.9 (3.06)
Phosphate buffer pH 4.5 μ 0.01 M	18.2 (0.6)
Phosphate buffer pH 7.4 μ 0.01 M	20.7 (1.0)
Phosphate buffer pH 4.5 μ 0.1 M	24.9 (2.0)
Phosphate buffer pH 7.4 μ 0.1 M	22.7 (0.9)

2.2 Fronts Movement and Drug Release

Fronts movement in matrix tablets consisting of atenolol and λ-carrageenan was studied in the different dissolution media selected, in order to better understand the relative contribution of polymer hydration properties and of drug-polymer ionic interaction on atenolol release profiles.

Figure 36 reports the fraction of atenolol released from λ-carrageenan tablets in different dissolution media. In water and at lower ionic strength, atenolol was released completely in 5

and 7 hours, while slower release was observed at higher ionic strength, with about 70% of atenolol dose delivered within 10 hours.

Analysis of release kinetics by comparing the n exponent of Peppas' equation (eq. 4), reported in Table 13, revealed super Case II kinetics in water and at the acidic pH at low ionic strength; whereas at pH 7.4 and at acidic pH at higher ionic strength linear kinetics were observed, confirming the drug release profiles obtained in *in vitro* dissolution studies described in the section 2.5.2 of the present work.

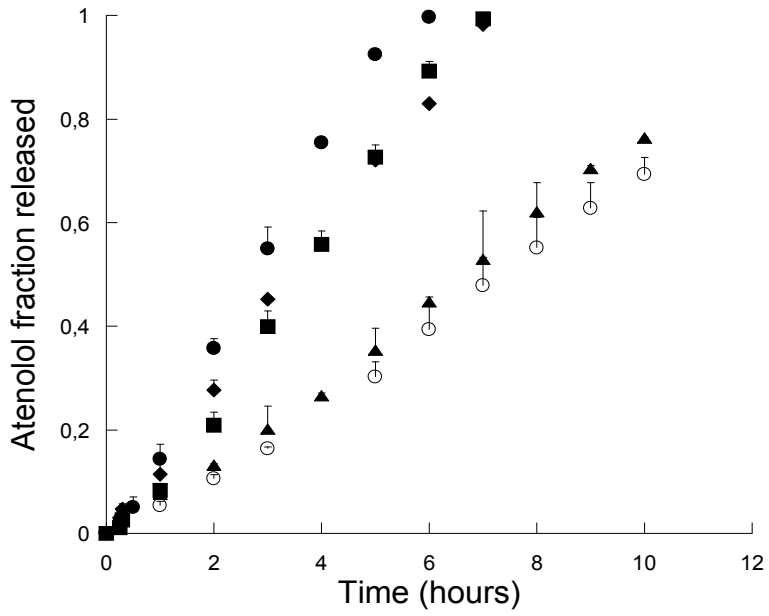

Figure 36. Fraction of atenolol released as a function of time from λ-carrageenan matrices in different dissolution media. Filled circle: water; filled square: phosphate buffer pH 4.5 μ 0.01 M; filled diamond: phosphate buffer pH 7.4 μ 0.01 M; empty circle: phosphate buffer pH 4.5 μ 0.1 M; filled triangle: phosphate buffer pH 7.4 μ 0.1 M. The bars represent the standard deviation (n=3).

Table 13. Diffusional exponent n, calculated by using Peppas' equation (eq. 4). Standard deviation in parenthesis (n=3).

SOLVENT	*n*
Distilled water	1.39 (0.15)
Phosphate buffer pH 4.5 μ 0.01 M	1.31 (0.01)
Phosphate buffer pH 7.4 μ 0.01 M	1.02 (0.07)
Phosphate buffer pH 4.5 μ 0.1 M	0.94 (0.03)
Phosphate buffer pH 7.4 μ 0.1 M	1.04 (0.08)

A swellable matrix system, upon contact with a thermodynamically compatible solvent, exhibits three fronts, starting from the centre of the matrix: the *swelling front*, which is the boundary between the glassy and dry polymer and its gelled state; the *diffusion front*, which indicates the boundary between the undissolved drug and its solution in the gel layer; the *erosion front*, which represents the boundary between the polymeric gel layer and the dissolution medium [8, 9]. A fourth, although less sharp interface can be evidenced into the gel layer between the swelling and the erosion front [101].

The observation of the matrix tablets during the dissolution test showed a different aspect from those observed in HMPC matrices [9] or in matrices consisting of λ-carrageenan and diltiazem or metoprolol, reported by Bettini [65].

In fact, the region comprised between the swelling and the erosion fronts was not a uniform layer of hydrated gel but consisted of two different regions, irrespectively of the solvent used, as shown in Figure 37. The inner layer, in contact with the swelling front, consisted of not fully hydrated polymeric particles; the outer layer, in contact with the erosion front, was transparent and, therefore, fully hydrated. The interface between these two layer is here defined as polymer gelling front and corresponds the above mentioned fourth front described by Bettini [101].

The partially hydrated particles persisted after each solvent reached the matrix centre, up to the complete matrix dissolution, although occupying a progressively reducing space. It may be speculated that the small amount of solvent penetrating the matrix gradually dissolved the atenolol present in this region. Since atenolol-λ-carrageenan interactions mainly occurred in solution, likely drug-polymer complexes formed within this region, which acted as a reservoir of drug.

In the matrix system considered here, the diffusion front was not observed in any of the solvents studied. Based on the above-mentioned hypothesis of the complex formation upon contact with water, it is possible to assume the observed not fully hydrated polymer particles were drug-polymer complex particles. Thus the polymer gelling front can be assumed here as the actual diffusion front of the drug.

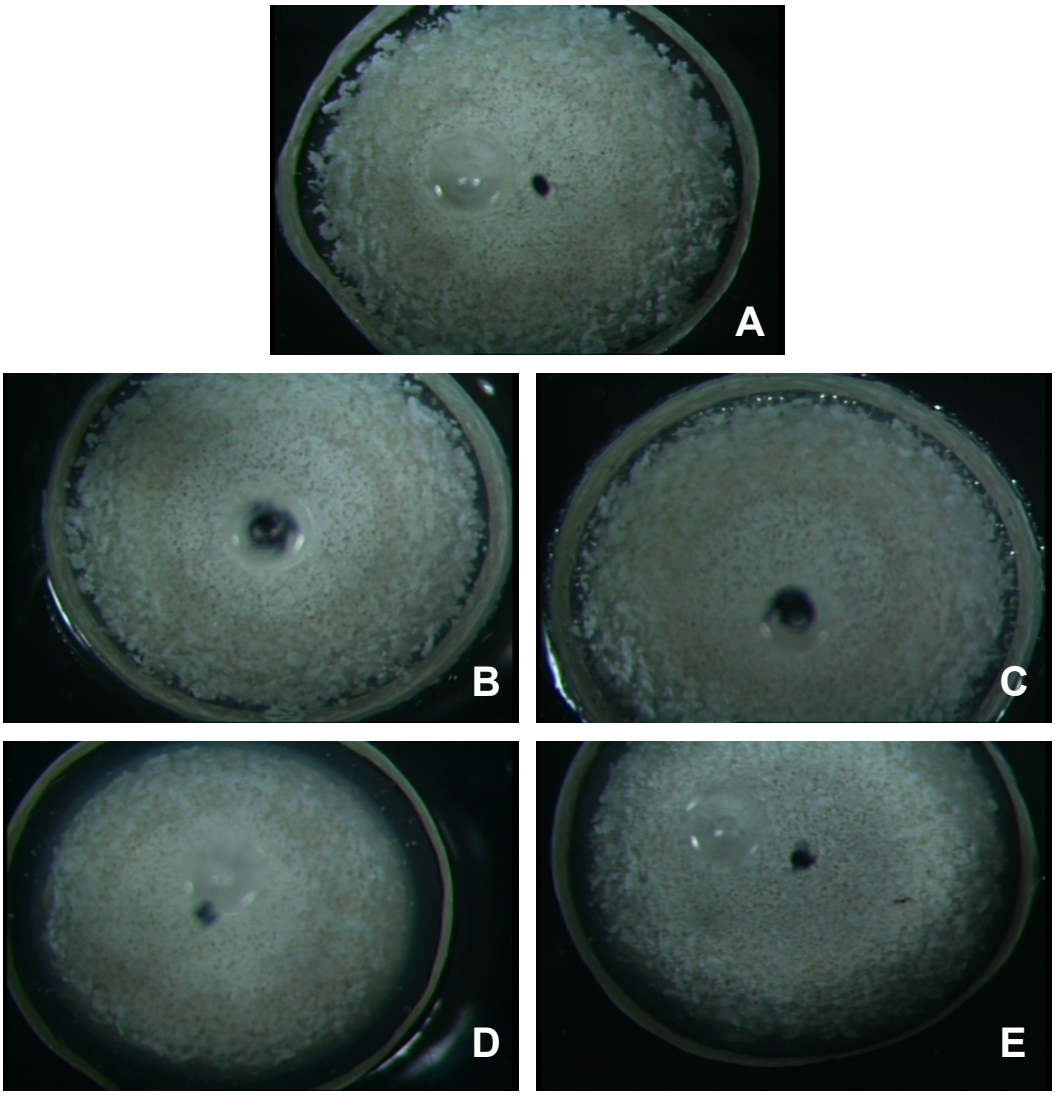

Figure 37. Pictures of atenolol-λ-carrageenan matrix tablets taken after 30 minutes in different dissolution media: A) water; B) phosphate buffer pH 4.5 μ 0.01 M; C) phosphate buffer pH 7.4 μ 0.01 M; D) phosphate buffer pH 4.5 μ 0.1 M; E) phosphate buffer pH 7.4 μ 0.1 M.

The positions of the three fronts observed in atenolol-λ-carrageenan tablets in the studied dissolution media are reported in Figures 38-40. The interface between the matrix and the dissolution medium at the beginning of the experiments is indicated by position 0;0.

The swelling front, moved toward the centre of the matrix within 2 hours when water was used as dissolution medium (Figure 38), while phosphate buffers penetrated within 3 hours (Figures 39 and 40).

The position of the erosion front moved outward during the first hour in distilled water and in buffers at ionic strength 0.01 M. Afterword, matrices showed a gradual dissolution, as demonstrated by the inwards movement of the erosion front. At higher ionic strength, the erosion front moved outward for the first three hours and then levelled off, confirming the swelling behaviour already observed in the USP apparatus II (Figure 28). The different swelling/erosion behaviour of atenolol-λ-carrageenan tablets was explained by the different solubility of the polymer in each solvent. As resulted from DSC analyses, λ-carrageenan was more soluble in water and at lower ionic strength, so that matrices dissolved in these solvents, whereas the lower solubility of λ-carrageenan afforded a more persisting swollen layer at higher ionic strength. Only after 6 hours the erosion front started moving inwards. As previously stated (section 2.5.1 of chapter III) the observed behaviour is somehow unusual with respect to the common know-how; as a matter of fact we linear kinetics was observed in swelling system where the gel layer expanded over time (at least for the first 6 hours).

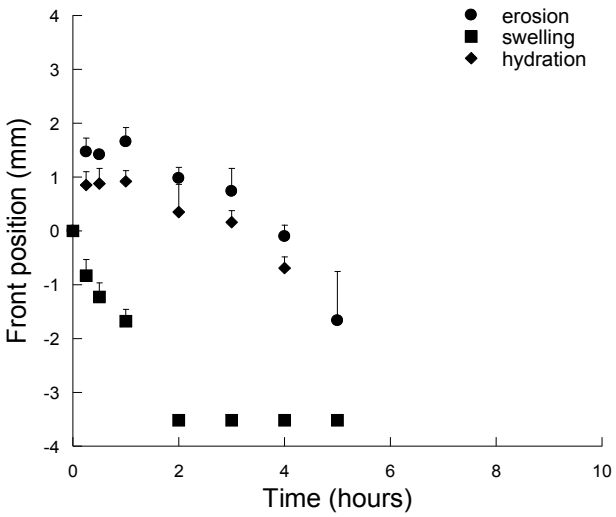

Figure 38. Erosion, swelling and hydration fronts position as a function of time in atenolol-λ-carrageenan matrices in water. The bars represent the standard deviation (n=3).

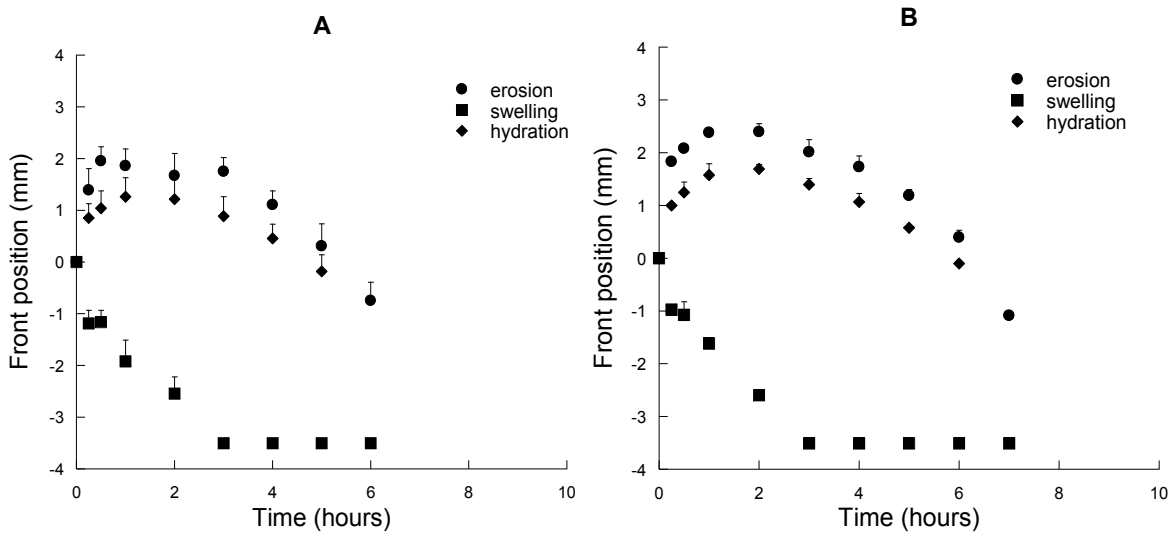

Figure 39. Erosion, swelling and hydration fronts position as a function of time in atenolol-λ-carrageenan matrices in A) phosphate buffer pH 4.5 μ 0.01 M and B) phosphate buffer pH 7.4 μ 0.01 M. The bars represent the standard deviation (n=3).

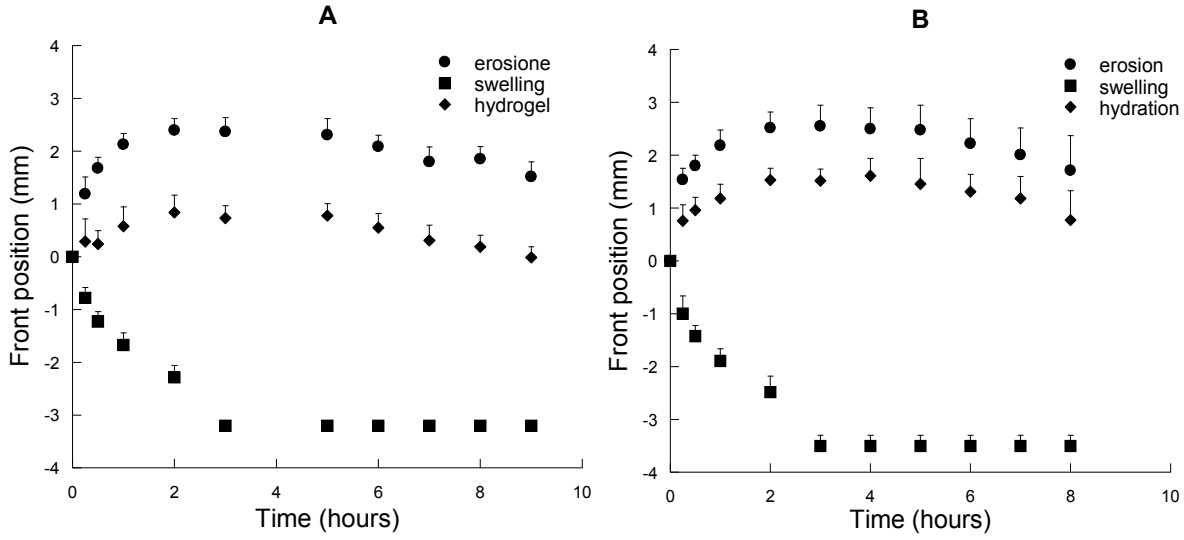

Figure 40. Figure 39. A) Erosion, swelling and hydration fronts position as a function of time in atenolol-λ-carrageenan matrices in A) phosphate buffer pH 4.5 μ 0.1 M and B) phosphate buffer pH 7.4 μ 0.1 M. The bars represent the standard deviation (n=3).

The reason of this behaviour may rely on the different thickness of the gel layer that represented the actual barrier for molecular diffusion. This gel layer was represented by the distance between the erosion and the polymer gelling front. In water and at lower ionic strength, after an initial rapid increase, the gel layer showed reducing thickness, whereas at higher ionic strength the gel layer remained fairly constant, due to the synchronization between the movement of the erosion and the polymer gelling fronts. With respect to the behaviour of the systems at higher ionic strength, the mentioned front synchronization allows explaining the lack of effect of drug solubility on drug release rate [102]. On the other hand the progressive reduction of the gel layer observed in water and at lower ionic strength accounted for the relevant increase in drug release rate reported in Figure 36, namely for the noticed super Case II kinetics.

In conclusion, DSC analyses and the study of fronts position in different solvents confirmed that atenolol-λ-carrageenan interaction played a role in the drug release from polymeric matrices, since drug-polymer complexes represented the diffusing species, independently on the solvent used. Afterward, the polymer properties became more important in determining delivery rates and kinetics. In fact, λ-carrageenan, less soluble at lower ionic strength, eroded rapidly affording a faster atenolol release with super Case II kinetics. Differently, the increase of the ionic content of the dissolution medium determined a reduction of the polymer solubility which implied the formation of a more stable and constant gel layer that ultimately resulted in a slower release rate and a liner release kinetics.

Since λ-carrageenan properties depended on the concentration of potassium dihydrogen phosphate in the dissolution medium, it is clear that the overall release mechanism was governed by atenolol-λ-carrageenan-salt interaction.

2.5 *In vitro* drug release studies

2.5.1 Ternary atenolol-λ-carrageenan-salt matrix systems: effect of different salts

Atenolol delivery from λ-carrageenan matrix tablets was controlled by its interaction with the polymer and influenced by the concentration of potassium dihydrogen phosphate present in the dissolution media. In particular, different concentration of salt mainly affected the drug release rate. In order to make the drug release independent from the ionic strength of the dissolution medium, potassium dihydrogen phosphate was added directly to the drug-polymer powder mixture prior the compression. This approach was meant to create a microenvironment with high ionic strength within the matrix during the dissolution process.

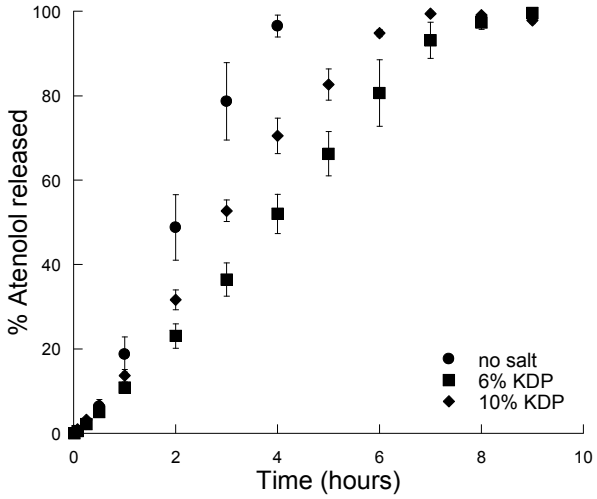

Figure 41. Atenolol release profiles in water from λ-carrageenan tablets containing 6 and 10% of potassium dihydrogen phosphate (KDP).

Figure 41 reports atenolol release profiles in water from λ-carrageenan tablets containing 6 and 10% of potassium dihydrogen phosphate. As a matter of a fact, the presence of the salt within the matrix significantly lowered atenolol drug release rate with respect to tablets not containing salt. 6% amount of potassium dihydrogen phosphate was particularly effective, providing the complete release of atenolol dose within 8 hours.

The study of fronts position was carried out with tablets containing 6% of potassium dihydrogen phosphate. As shown in Figure 42 B, the swelling front moved inward, reaching the centre of the matrix within 2 hours. The erosion front moved outward during the first hour, remaining in the same position for the following 3 hours. Then, the erosion front started to gradually move inward and tablets dissolved completely within 9 hours. The amount of water penetrating the matrix did not promote the complete hydration of the polymer present in the region comprised between the swelling and the erosion front, as already observed in tablets without salt (see Figure 37). Therefore, also in tablets with salt, a hydration front, separating the core containing solid particles from the dissolution medium, was observed. As shown in Figure 42 A, the addition of potassium dihydrogen phosphate to the drug-polymer mixture did not determine the formation of the thick gel layer observed in tablets dissolving in 0.1 M media (Figure 37 D and E). However the salt did reduce the solubility of the polymer within the matrix, decreasing its dissolution rate and affording a more prolonged atenolol release rate.

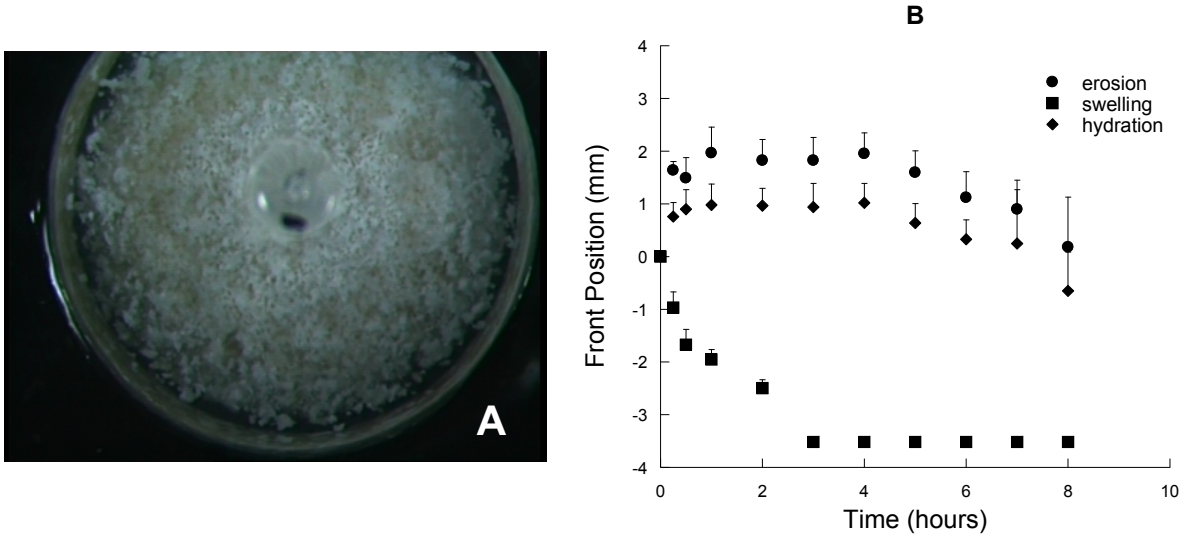

Figure 42. Front position study in water of atenolol-λ-carrageenan tablets containing 6% of potassium dihydrogen phosphate. A) Picture taken after 30 minutes; B) Erosion, swelling and hydration front position as a function of time. The bars represent the standard deviation (n=3).

Given the observed specific influence of potassium dihydrogen phosphate on atenolol release from λ-carrageenan matrix tablets the effect of various potassium salts, having solubility in water ranging in a large interval of values, (Table 14), on atenolol release rate and kinetics was then evaluated.

Table 14. Potassium salts solubility values in water at 20°C [103-108].

SALT	SOLUBILITY (% w/w)
Potassium hydrogen tartrate	0.62
Potassium phthalate monobasic	8
Potassium sulfate	12
Potassium dihydrogen phosphate	22
Potassium oxalate	36.4
Potassium orthophosphate	94
Potassium citrate	154
Potassium acetate	256

Figure 43 and 44 report atenolol release profiles obtained from λ-carrageenan matrix tablets containing 6 and 10% of different potassium salt. In general, drug release profiles obtained in water from tablets containing different potassium salts were not significantly different from that obtained from tablets without salt, independently from the amount of salt added. This implied that salt solubility did not have any effect on drug release. However, very soluble salts, such as potassium acetate and orthophosphate, likely attracting water within the matrix as osmotic effect, determined a slightly faster release in 10% salt-containing tablets.

Any of the salt added to the matrix system prolonged atenolol release over 8 hours, as observed in tablets containing of potassium dihydrogen phosphate. Nevertheless, tablets containing potassium oxalate, phthalate and tartrate decreased to some extent drug release rate, affording the complete release of atenolol dose within 5-6 hours. As shown in Figure 45, salts effective in reducing atenolol release rate presented acidic hydrogen atoms, which might have a role in modifying the microenvironment within the matrix. As previously demonstrated, λ-carrageenan solubility decreased by increasing the concentration of potassium dihydrogen phosphate in water, modifying its hydration properties. Likely this effect was related to the dissociation of the acidic salt and the subsequent localized availability of protons within the matrix.

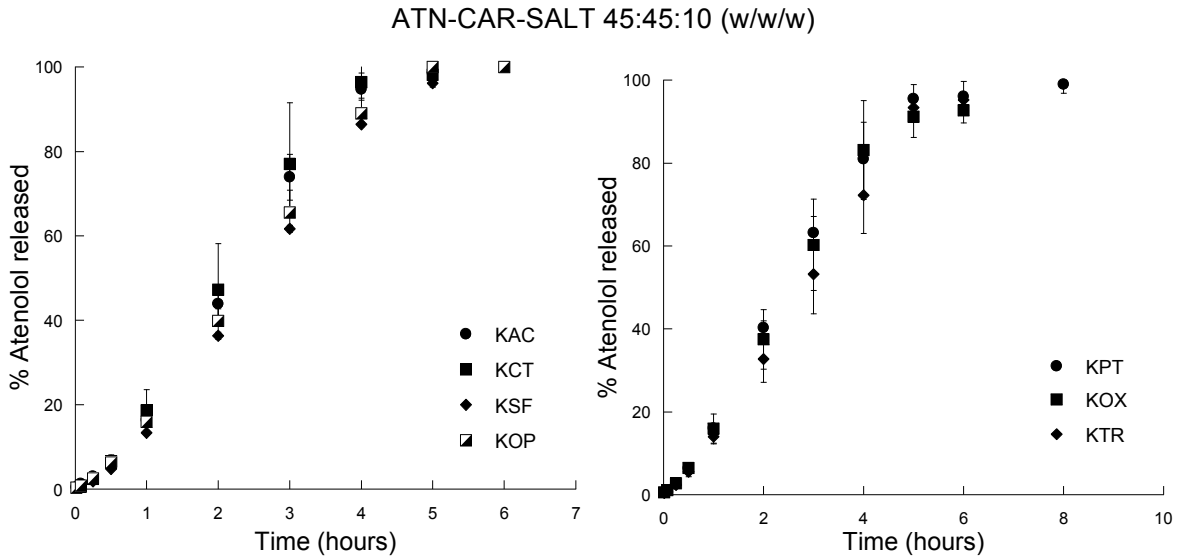

Figure 43. Atenolol release from λ-carrageenan matrix tablets containing 6% of different salts as a function of time. KAC: potassium acetate; KCT: potassium citrate; KSF: potassium sulfate; KOP: potassium orthophosphate; KPT: potassium phthalate monobasic; KTR: potassium hydrogen phosphate. The bars represent the standard deviation (n=3).

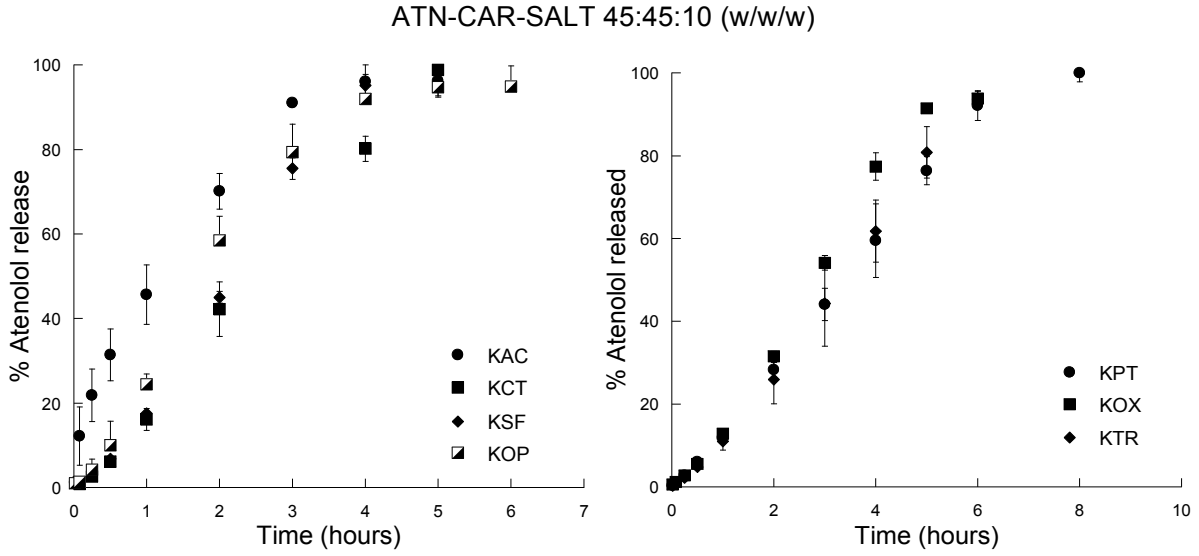

Figure 44. Atenolol release from λ-carrageenan matrix tablets containing 10% of different salts as a function of time. KAC: potassium acetate; KCT: potassium citrate; KSF: potassium sulfate; KOP: potassium orthophosphate; KPT: potassium phthalate monobasic; KTR: potassium hydrogen phosphate. The bars represent the standard deviation (n=3).

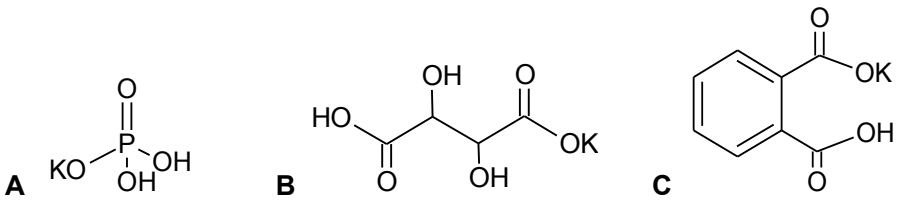

Figure 45. Molecular structure of A: potassium dihydrogen phosphate; B: potassium hydrogen tartrate; C: potassium phthalate.

2.5.2 Ternary drug-λ-carrageenan-salt matrix systems: effect of different basic drugs

The addition of acidic salts to the atenolol-λ-carrageenan formulation was a successful approach to obtain controlled drug delivery. In particular, potassium dihydrogen phosphate afforded the most prolonged release. Thus, the possibility to employ drug-polymer-salt interactions to deliver various drugs having basic characteristics from λ-carrageenan-potassium dihydrogen phosphate matrices was evaluated.

Drugs selected were methyl L-dopa, containing a primary amine group (see Figure 29), and buflomedil pyridoxal phosphate, a salt presenting a charged tertiary amine group included within an aliphatic ring (see Figure 30).

Figure 46 and 47, respectively, report methyl L-dopa and buflomedil pyridoxal phosphate release profiles obtained in water from λ-carrageenan matrix tablets either without salt or containing 6% of potassium dihydrogen phosphate.

Surprisingly, for each drug, no differences were observed between release profiles obtained from tablets with and without salt. These results confirmed that the prolonged release profile observed with atenolol was due not only to the particular properties of the polymer in presence of the salt, but also to its specific interactions with the drug. As a matter of a fact, different release kinetics were shown for the three drug used. Diffusional exponents *n* calculated for methyl L-dopa-λ-carrageenan tablets with and without salt were 0.64 ± 0.02 and 0.62 ± 0.04, respectively, corresponding to an anomalous-Fickian drug release. For buflomedil pyridoxal phosphate, instead, *n* values of 1.09 ± 0.17 (no salt) and 1.07 ± 0.03 (tablets containing salt) indicated a linear release kinetics, while atenolol was released with super Case II kinetics (*n* value of 1.55 ± 0.1 in tablets without salt and of 1.22 ± 0.01 in tablets with salt). Since amine groups of every drug used were positively charged at the slightly acid pH (about 5.5-6) of distilled water used in dissolution studies, they should similarly interact with the negatively charged sulfate groups of λ-carrageenan. Nevertheless, the differences observed in release kinetics suggested that various levels of interactions might occur between each drug and the polymer, probably because of different mutual conformations assumed within the drug-polymer complexes.

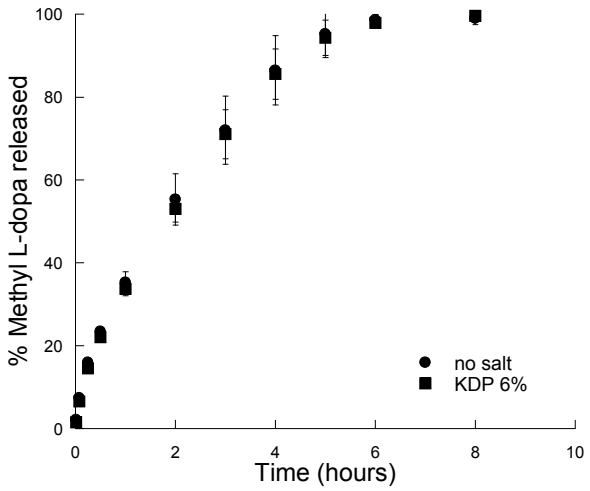

Figure 46. Methyl L-dopa release in water from λ-carrageenan tablets without salt and with 6% of potassium dihydrogen phosphate (KDP) as a function of time. The bars represent the standard deviation (n=3).

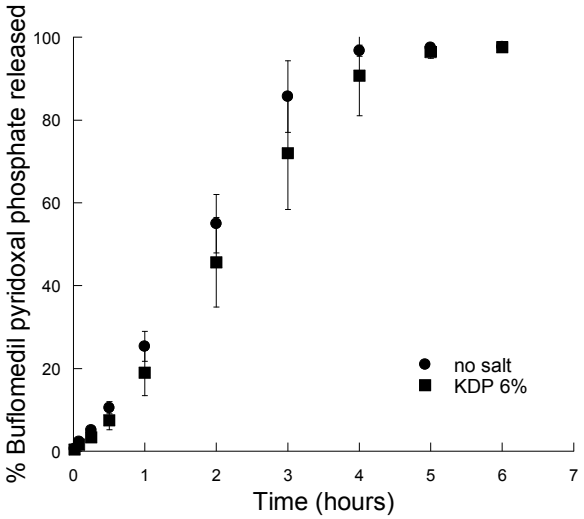

Figure 47. Buflomedil pyridoxal phosphate release profiles in water from λ-carrageenan tablets without salt and with 6% of potassium dihydrogen phosphate (KDP) as a function of time. The bars represent the standard deviation (n=3).

3. CONCLUSIONS

Drug release from atenolol-λ-carrageenan matrix tablets was decreased by the increasing ionic strength of the dissolution medium. Differential scanning calorimetry showed that λ-carrageenan was more soluble in water and in media at lower ionic strength.

The observation of matrices clamped between two transparent discs and introduced in water and phosphate buffers at 0.01 and 0.1 M ionic strength put in evidence the following fronts:

- the erosion front, which delimited the boundary between the matrix and the dissolution medium;
- the swelling front, which separated the region of the matrix penetrated by water from the dry core;
- the polymer gelling front which separated the fully from the not fully hydrated regions within the solvent penetrated matrix.

At lower ionic strength and in water, the progressive erosion of the matrix, due to the higher solubility of the polymer, afforded the super Case II release of the drug. In μ 0.1 M media, λ-carrageenan was less soluble and swelled, forming a layer of gel that remained constant in thickness over 6 hours. Thus, the drug was released with linear kinetics by diffusing through a constant thickness pathway. In conclusion, the overall release rate and kinetics observed in this matrix system was controlled by atenolol-λ-carrageenan-potassium dihydrogen phosphate mutual interactions.

In order to make the atenolol release independent of the environmental conditions, different potassium salts were added to the drug-polymer mixture. Acidic salts, such as potassium dihydrogen phosphate, oxalate, tartrate and phthalate monobasic, were effective in providing more prolonged release rates of atenolol in water with respect to tablets not containing salts. This effect was probably related to a decreased solubility of the polymer, subsequent to the local availability of protons after salt dissociation. Thus, it is here reported an example of how to exploit salts in controlled drug delivery as retarding agents rather than disintegrants or osmotic agents.

Since the ternary system atenolol-λ-carrageenan-potassium dihydrogen phosphate provided the most suitable drug release for controlled delivery, this polymer-salt mixture was investigated to obtain controlled delivery of different basic drugs, such as methyl L-dopa and buflomedil pyridoxal phosphate. Release profiles obtained in water showed that the salt was not effective in reducing release rate for both of the drugs selected, confirming that the results obtained with atenolol were due to specific and mutual interactions among atenolol-polymer and salt. Moreover, different release kinetics were observed for the three drugs

used, suggesting that each drug interacted with λ-carrageenan to different extent. Further investigations, for instance with computer assisted molecular modelling, will surely help to better clarify these aspects.

V. THIRD PART

V. THIRD PART

The third part of the present research work has been carried out at UCL School of Pharmacy in London, under the supervision of Professor Duncan Craig and Doctor Min Zhao.

The project has been focused on the evaluation of the possibility to produce ionic liquid-like systems from oppositely charged drugs and polymers by hot melt extrusion, as a new approach to develop medicinal products for the oral route.

1. INTRODUCTION

1.1 Hot Melt Extrusion

Extrusion is the process of converting a raw material into a product of uniform shape and density by forcing it through a die under controlled temperature and pressure [109].

Hot melt extrusion was first introduced at the end of the eighteenth century for the manufacture of lead pipes. Since then, it has been widely used in the plastic, rubber and food manufacturing industry.

Extruders generally consist of a cylindrical stationary barrel containing one or two screws. They are defined as single-screw or twin-screw extruders, depending on the number of screws in the barrel. In twin-screw extruders, screws can rotate either in the same direction or in the opposite sense.

The extrusion channel is usually divided into three sections: feeding zone, compression zone and metering zone (Figure 48). The depth and the pitch of the screw flights differ within each zone, generating dissimilar pressures along the screw length. Solid or liquid raw material is introduced, manually or by an opportune device, into the feeding zone. The pressure in this section is generally low in order to mix and convey the raw materials to the compression zone. Within the compression zone, the pressure is increased to melt or soften the material. In fact, although the barrel is heated up, almost 80% of the heat required to melt or soften the material is provided by friction as the material is sheared between the rotating screws and the wall of the barrel. The material reaches the metering zone in the form of a homogeneous plastic melt suitable for extrusion. The function of the metering zone is to reduce pulsatile flow through the die in order to obtain a uniformly extruded product. Further equipment may be present for down-stream processes on the extrudate, such as cooling, pelleting, in-line analysis. [109, 110].

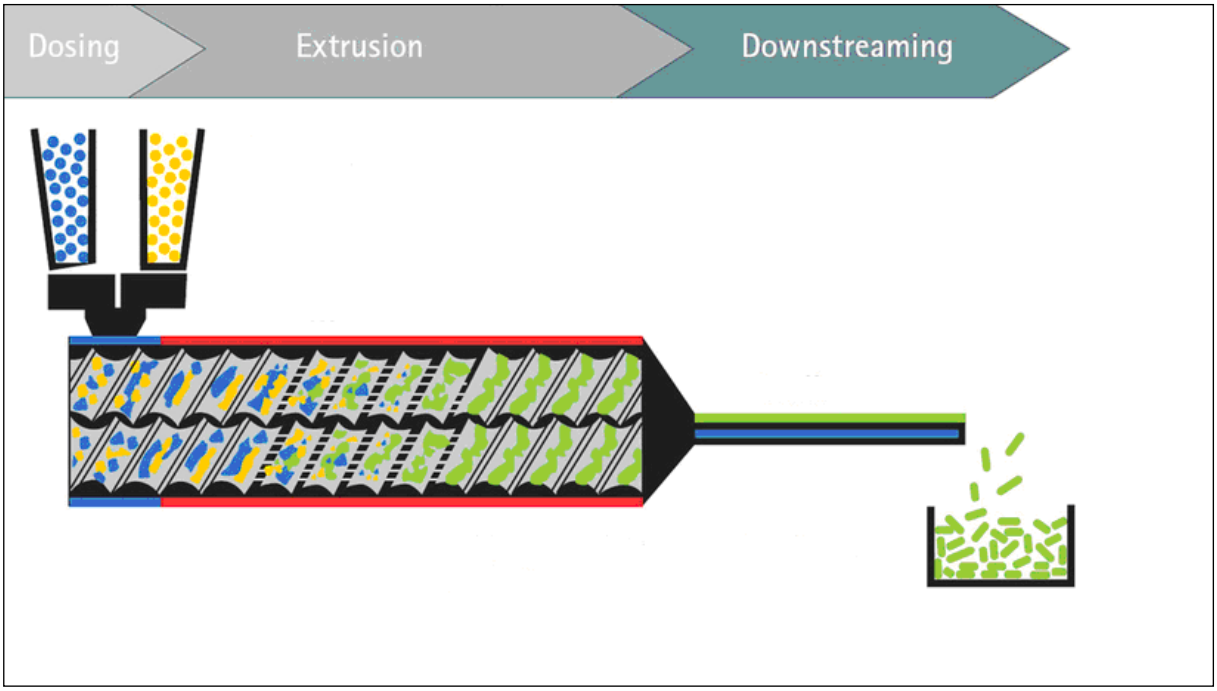

Figure 48. Schematic overview of the hot melt extrusion process [111].

Hot melt extrusion technology in pharmaceutical industry has been employed in the preparation of granules or pellets of uniform size, shape and density, containing one or more drugs. Lately, hot melt extrusion has been successfully employed to disperse drug in polymeric matrices at a molecular level. Solid solutions produced by hot melt extrusion may enhance the dissolution rate and the bioavailability of poorly soluble drugs [112], control or modify drug delivery [113], mask the bitter taste of active substances [114].

The technique offers several advantages, especially for the production of solid dispersions. It is a solvent-free process that guarantees a better content uniformity in extrudates. Moreover, the instrument can operate continuously, with reduced time of production and fewer operation steps. On the other hand, extrusion is carried out at high temperatures, thus only thermostable polymers and drugs can be processed. Polymers must have also good rheological and flow properties, therefore the number of suitable molecules is limited. Polymers usually employed are polyvinylpyrrolidone, polyoxyethylene, cellulose esters and polymethacrylates.

Despite the increasing interest of academic and industrial research in this technique, the number of currently marketed products obtained by hot melt extrusion is limited. Kaletra HME (Abbvie) is a combination product of ritonavir and lopinavir indicated for the treatment of

human immunodeficiency virus infections. It demonstrated a significantly enhanced oral bioavailability with respect to the soft capsules, previously authorised by FDA [115]. Additionally, sustained release formulations of itraconazole (Onmel, Merz) and verapamil (Isoptin SR-E, SOLIQS) and fast dissolving tablets of ibuprofen (Nurofen Meltlets Lemon, Reckitt Benckiser) are available on the market.

1.2 The role of drug-polymer interactions in hot melt extrusion

Drug-polymer interactions in extrudates play an important role in determining drug-polymer miscibility, in improving the operative conditions in the extrusion process and in enhancing physical stability of amorphous solid dispersions [116].

Solid dispersions are classified as solid crystalline dispersions, solid glassy suspensions and solid solutions. In solid crystalline dispersions, the drug is suspended in a crystalline state within a polymeric matrix. In solid glassy suspensions, the amorphous drug is a separate phase from the amorphous polymer. Solid solutions consist of a drug molecularly dispersed within the polymer [117].

The dispersion at molecular level requires a high degree of interaction between the drug and the polymer involved. Solid solutions are formed when the existing crystalline lattice of the drug is broken and the polymeric intermolecular interactions are overcome, permitting the intimate mixing of the two molecules with the subsequent establishment of new drug-polymer interactions.

The Flory-Huggins theory was developed for describing polymer-solvent or polymer-polymer miscibility on the basis of Gibbs free energy before and after mixing [118-120]. If an amorphous drug is assumed to behave similarly to a solvent, then the Flory-Huggins theory can be applied to describe the thermodynamics of drug-polymer systems.

The thermodynamics of mixing in polymeric systems is described by the Gibbs free energy (eq. 7):

$$\Delta G_M = \Delta H_M - T\Delta S_M \qquad \text{(eq. 7)}$$

Where ΔG_M is the free energy of mixing, ΔH_M is the enthalpy of mixing and ΔS_M is the entropy of mixing.

Miscibility is assumed if ΔG_M becomes negative. The entropy of mixing is generally positive but, for polymeric systems, its contribution to achieve miscibility can be insufficient, since entropy gain is not large for high molecular weight polymers. Thus, miscibility is clearly dependent on the contribution of the enthalpy of mixing [117]. Changes in enthalpy are

determined by interactions between the structural units of the polymer and the drug molecules.

In the framework of the Flory-Huggins theory, enthalpic interactions are described by the interaction parameter χ, linked to the Gibbs free energy of mixing by the following equation:

$$\frac{\Delta G_M}{RT} = n_{drug} \ln \Phi_{drug} + n_{polymer} \ln \Phi_{polymer} + n_{drug} \Phi_{polymer} \chi \qquad \text{(eq. 8)}$$

Where n_{drug} is the number of moles of drug, $n_{polymer}$ is the number of moles of polymer, Φ_{drug} is the volume fraction of the drug, $\Phi_{polymer}$ is the volume fraction of the polymer, R is the gas constant and T is the absolute temperature.

The interaction parameter χ describes the relative strength of cohesive forces, established between molecules of the same specie, and adhesive interactions, occurring between different molecules. Negative interaction parameters defines systems which show strong and numerous adhesive interactions, favouring miscibility and dispersion at molecular level, whereas positive χ characterizes systems exhibiting stronger cohesive forces, predicting immiscibility [121].

One of the main limitations in the exploitation of the hot melt extrusion technique is the high temperature often required for the process, which may led to thermal degradation of the molecules employed. In general, it is necessary to work at temperature above the glass transition temperature of the polymer (T_g), in order to promote the softening of the material, and it is preferable to use a temperature above the melting point of the drug to convert the crystalline drug into the liquid form. Nevertheless, intermolecular interaction between drugs and polymers may lower the operative temperature through the reduction of the T_g of the polymer or the depression of the drug melting point [116].

A drug interacting with a polymer can promote its plasticization by reducing the cohesive interaction among polymeric chains and decreasing the friction, which result in an increased mobility and reduction of the glass transition temperature.

The melting point of a pure drug is the temperature at which the chemical potential of the crystalline drug is equal to the chemical potential of the liquid drug. If a drug is miscible with a polymer, then its chemical potential will be lowered, resulting in a reduction of the temperature of melting.

An important concern about the employment of amorphous phases in pharmaceutical products is their limited physical stability. However, the decreased chemical potential of an amorphous drug, as a result of molecular interactions with a polymer, determines a reduction

of the driving force for the crystallization with respect to the pure amorphous drug, promoting an improvement of the physical stability of the system.

2. AIM OF THE SUBPROJECT

Ionic liquids are salts that melt at temperatures below 100°C and whose melts consist of discrete cations and anions, such as lidocaine docusate and ranitine docusate, prepared by Hough et al. via metathesis reaction between lidocaine hydrochloride or ranitidine hydrochloride and sodium docusate [122].

The aim of this subproject was to verify the applicability of the hot melt extrusion technique for the production of ionic liquid-like systems using oppositely charged drug and polymers, such as the anionic drug sodium ibuprofen and the cationic polymer Eudragit RS 100.

The extrudates produced were characterized in the solid state and the potential occurrence of ionic interactions between the oppositely charged groups was verified by FT-IR analysis.

3. MATERIALS AND METHODS

3.1 Materials

- SODIUM IBUPROFEN (Figure 49) was purchased from Sigma Aldrich (Germany).
  The drug has a molecular mass of 228.26 and is the sodium salt of ibuprofen. Ibuprofen is a non-steroidal anti-inflammatory drug (NSAID) used as analgesic for the treatment of several pain conditions as self-medication.
  Ibuprofen is marketed as a racemate. S-enantiomer is the active form, however R-enantiomer is partially converted in the S-form by metabolic processes. The drug in its acidic form presents several formulation problems, particularly a low water solubility (less than 1 mg/mL). The sodium salt is more soluble in water than ibuprofen, allowing the production of fast dissolving formulation, indicated in the treatment of pain conditions where a rapid onset of action is required. Also sodium ibuprofen is marketed as a racemic mixture and its dihydrate phase is stable under ambient conditions, while the anhydrous form is highly hygroscopic [123].

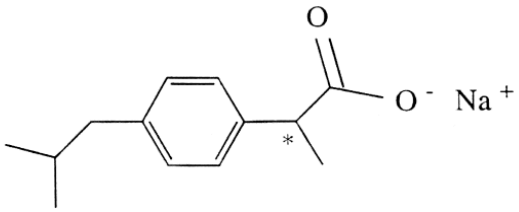

Figure 49. Molecular structure of sodium ibuprofen.
The asterisk indicates the chiral carbon atom.

- EUDRAGIT RS 100 (Figure 50) was kindly donated by Evonik Industries AG (Germany).
  It is a copolymer of ethyl acrylate, methyl methacrylate and methacrylic acid ester with quaternary ammonium groups in molar ratio of 1:2:0.1. It is a water insoluble polymer, showing high permeability and pH-independent swelling, which make it suitable as a coating agent and for the preparation of matrix systems to obtain sustained release formulations [124].

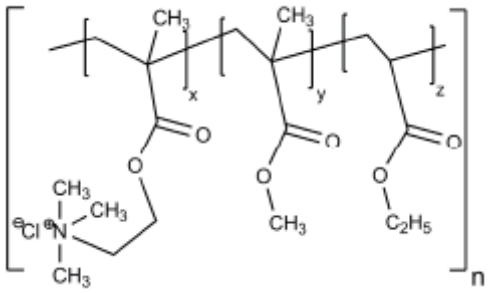

Figure 50. Molecular structure of Eudragit RS 100.

- PEG 200 (Figure 51) was purchased from Sigma Aldrich (Germany). It is a liquid, water miscible polymer, prepared by polymerization of ethylene oxide [125].

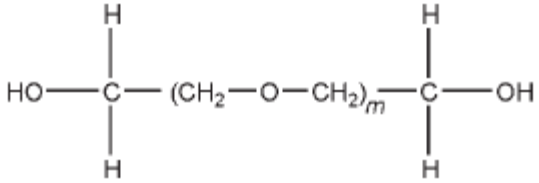

Figure 51. Molecular structure of PEG 200.

3.2 Methods

3.2.1 Hot Melt Extrusion (HME)

Hot melt extrudates were prepared using a co-rotating twin-screw extruder Process 11, Thermo Fisher Scientific (USA).

Eudragit RS 100 was initially milled using mortar and pestle. Polymer and drug powders were then sieved in order to obtain powders with particle size ranging between 63 and 250 µm.

Binary mixtures of sodium ibuprofen and Eudragit RS 100 in 10:90, 20:80 and 30:70 weight ratio were extruded at 130°C with the screws speed set at 50 rpm. A round die with a diameter of 2 mm was attached to the extruder. Since sodium ibuprofen rapidly converts in the dehydrate form at room temperature, the type of form of sodium ibuprofen was verified before the preparation before the extrusion and the amount of drug was taken accordingly.

Extrusion was carried out also on ternary mixtures consisting of anhydrous ibuprofen sodium, PEG 200 and Eudragit at 10:23:67 weight ratio. The mixture was prepared by moistening the Eudragit powder with the solution of sodium ibuprofen in PEG 200. The following temperature profile was set from the feeding zone to the die: 60-90-130°C. Screw were co-rotated at the speed of 50 rpm. Again, a round die with a diameter of 2 mm was attached to the extruder.

3.2.2 Cristallinity Quantification

The amount of crystalline sodium ibuprofen present in the fresh extrudates was estimated by constructing a calibration curve where the enthalpy of fusion of sodium ibuprofen in the presence of Eudragit RS 100 was plotted versus the amount of drug in the mixture. This was performed in order to take into account changes in the melting behaviour and enthalpy caused by the presence of the polymer. Physical mixtures were prepared by mixing sodium ibuprofen and Eudragit in ratios of 5:95, 10:90, 20:80, 40:60, 80:20, 100:0 (w/w) and analyzed in MTDSC.

3.2.3 Modulated Temperature Differential Scanning Calorimetry (MTDSC)

MTDSC experiments were carried out on raw materials, physical mixtures and extrudates using a Q2000 instrument (TA Instruments, USA) at the heating rate of 2°C/min, amplitude ± 0.318 °C and a period of 60 s. Scans were conducted within the temperature range 0-230°C in aluminium sealed and pierced pans. In order to remove the effect of the previous thermal history, a heating-cooling-heating cycle in the same temperature range was used for the analysis of raw materials. Dry nitrogen purge gas was used with a flow rate of 50 ml/minute. Calibration was performed using n-octadecane, indium and tin. For each sample, analysis were conducted in three replicates repeated three times.

3.2.4 Thermogravimetric Analysis (TGA)

TGA experiments were used to detect the degradation temperature of raw materials on a HiRES TGA 2950 equipment (TA Instrument, USA). Analyses were conducted at 10°C/min from room temperature to 250°C in aluminium open pan.

3.2.5 X-Ray Powder Diffraction (XRPD)

XRPD spectra were collected from raw materials, physical mixtures and freshly prepared extrudates with a Rigaku Miniflex 600 instrument (Rigaku Corporation, Japan) in the range 3-60° 2θ with a step size of 0.02° and a rate of 2°/min. The X-ray source used was Cu Kα with

a voltage of 40kV and current of 15 mA. Extrudates were gently milled by mortar and pestle prior to the analysis.

3.2.6 Scanning Electron Microscopy

Scanning electron microscopy was used to acquire microphotographs of the surface and the cross section of the freshly prepared extrudates with a scanning electron microscope FEI Quanta 200F (USA). To improve conductivity prior the examination, samples were coated with gold using a Polacron SC7640 sputter gold coater (Quorum Technologies, UK).

3.2.7 Fourier Transform Infrared Attenuated Total Reflectance (ATR- FT-IR) analysis

FT-IR spectra of raw materials, physical mixtures and freshly prepared extrudates were acquired with a Bruker Vertex 70 (USA) spectrometer equipped with a Specac Golden Gate (UK) zinc selenide accessory. Spectra were recorded by collecting 32 scans with a resolution of 2 cm^{-1} over the wavenumber range 4000-400 cm^{-1}.

4. RESULTS AND DISCUSSION

4.1 Characterization of raw materials

4.1.1 Sodium ibuprofen

Sodium ibuprofen was characterized by TGA, MTDSC, XRPD and ATR-FT-IR.

TGA analysis (Figure 52) showed a weight loss (%) of 13.57 ± 0.03, which complied with the theoretical content of two molecules of water (13.62%), confirming that sodium ibuprofen was in the dihydrate form. Anhydrous form of sodium ibuprofen was easily obtained by heating the powder at 70°C overnight. However, the salt was highly hygroscopic and quickly converted in the dihydrate [123].

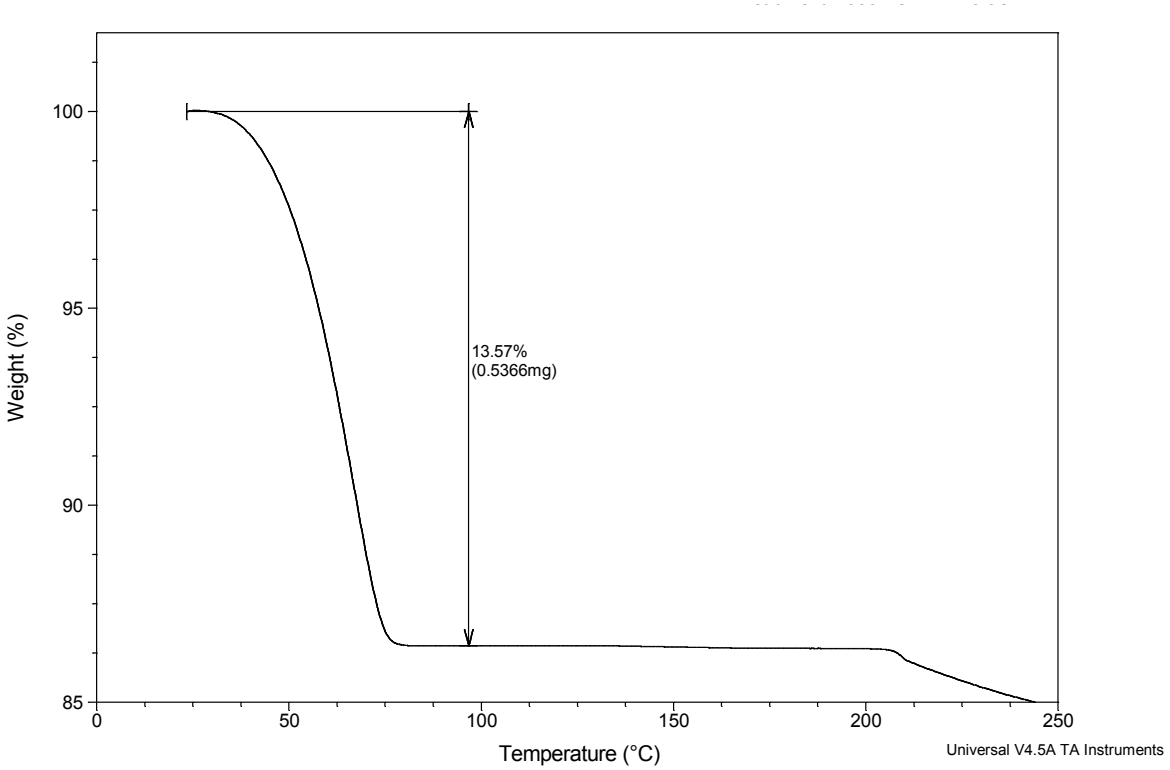

Figure 52. TGA analysis of sodium ibuprofen.

According to Zhang et al. [126], sodium ibuprofen, as a racemic mixture, can crystallize as a racemic compound, racemic conglomerate or pseudoracemate. A racemic conglomerate is an equimolar physical mixture of the individual enantiomeric species, such that only one

enantiomer is present in each crystal and in each unit cell of the crystal lattice (Figure 53 A). A racemic compound consists of crystals in which the two enantiomers are paired up in the unit cell of the crystal lattice, thus they coexist in the same unit cell that differs from that of the corresponding enantiomers (Figure 53 B). In a pseudoracemate crystal, the two opposite enantiomeric molecules are randomly arranged in the same crystal lattice (Figure 53 C).

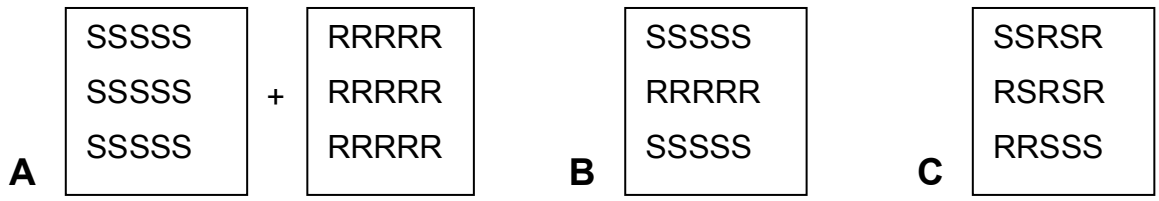

Figure 53. Modes of arrangement of chiral molecules: A) Racemic compound; B) Racemic conglomerate; C) Pseudoracemate.

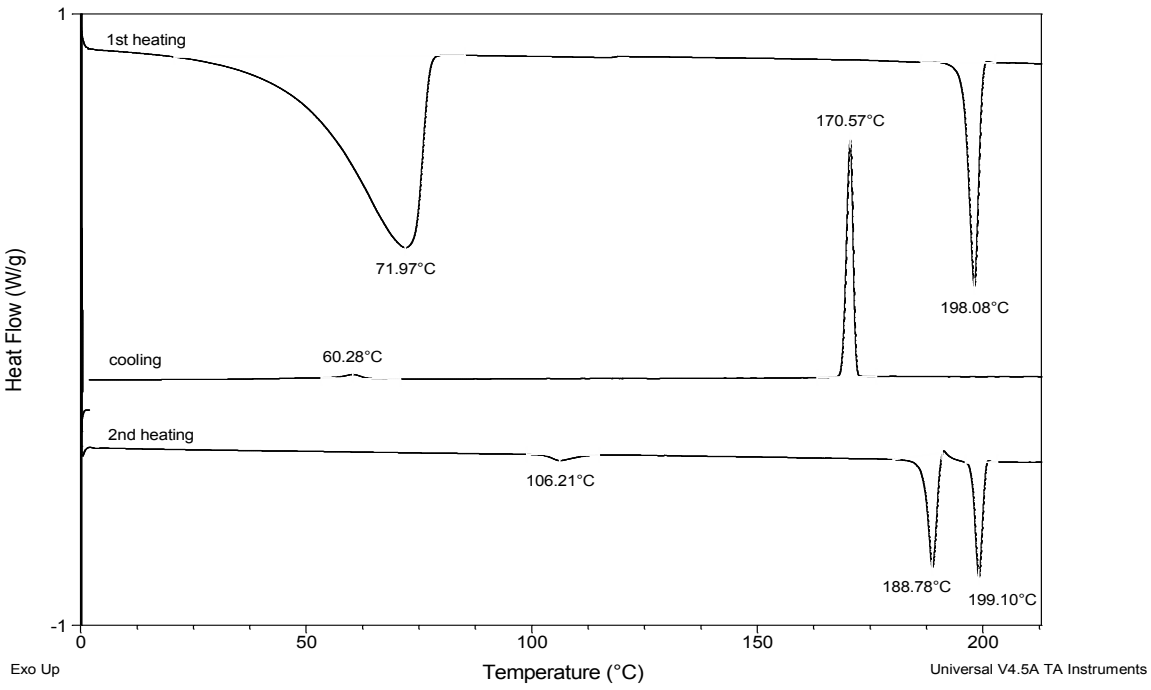

Figure 54. MTDSC analysis of sodium ibuprofen.

Figure 54 reports the MTDSC curves obtained from sodium ibuprofen, treated with the heating-cooling-heating cycle.

According to Zhang et al. [126], sodium ibuprofen is stable as racemic conglomerate, named as γ form, which melts at 198°C. As a matter of fact, the MTDSC analysis carried out on the raw sodium ibuprofen showed a melting peak at 198.1°C in the curve relative to the first heating cycle, as shown in Figure 54. The endothermic peak at 72°C represented water loss, as found in TGA analysis (Figure 52). When the melt was cooled, the drug recrystallized in a form called β at 170.6°C, that converted in the α form at 60.3°C. During the second heating process, the small transition observed at 106.2°C corresponded to the conversion of the α form into the β. The second endotherm at 189°C represented the melting of the β form, which then recrystallized as γ form and melted at 198°C. Zhang et al. found that both α and β forms were racemic compounds. Metastable α and β forms were enantiontropically related, α being more stable at lower temperatures, while β was more stable at higher temperature. Both of them were monotropic with respect to γ form.

The crystalline nature of sodium ibuprofen in its dihydrate and anhydrous state was confirmed also by XRPD, as shown in Figure 55. It is interesting to note that in the region of high angles, peaks of anhydrous sodium ibuprofen were broader and less intense, implying that water removal provoked a perturbation into the crystal leading to a less organized and less crystalline structure.

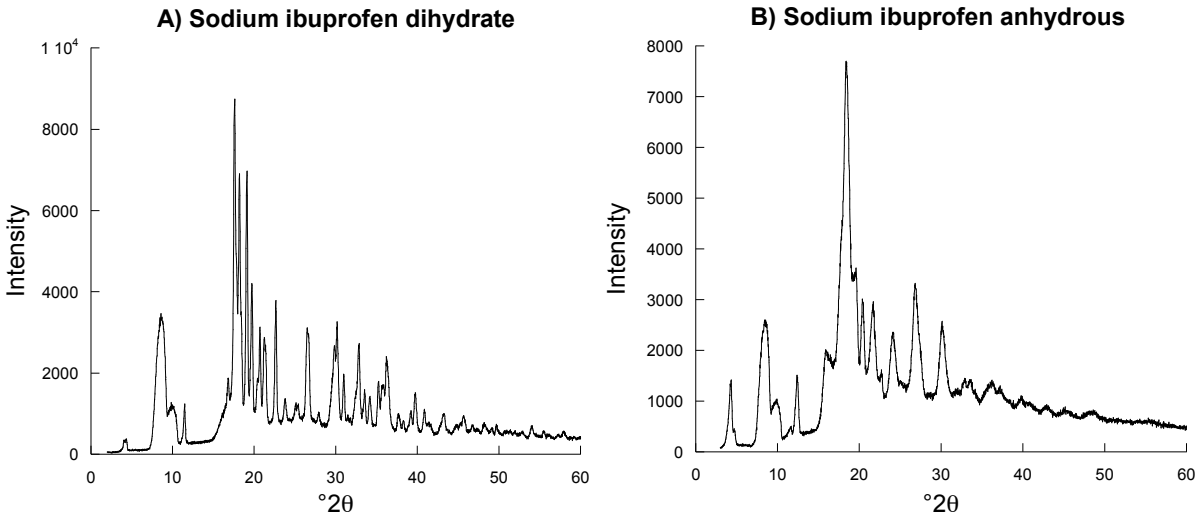

Figure 55. XRPD spectra of sodium ibuprofen dihydrate and anhydrous.

The different organization of sodium ibuprofen molecules in the crystal lattice of the dihydrate and anhydrous form was also confirmed by ATR-FT-IR analysis. Figure 56 reports spectra collected from the drug before and after overnight heating at 70°C. In the spectrum A), the band 1 at 3346 cm^{-1} was attributed to the –OH stretching of water molecules contained in the dihydrate drug, since it disappeared in the spectrum B), relative to the anhydrous form. The band 2, relative to the stretching of the C=O contained in the carboxylate group of the drug, showed a strong shift from 1546 cm^{-1} in the dihydrate form to 1581 cm^{-1} after water removal, confirming that sodium ibuprofen carboxylate groups interacted via hydrogen bond with water, as already reported in the literature [127, 128].

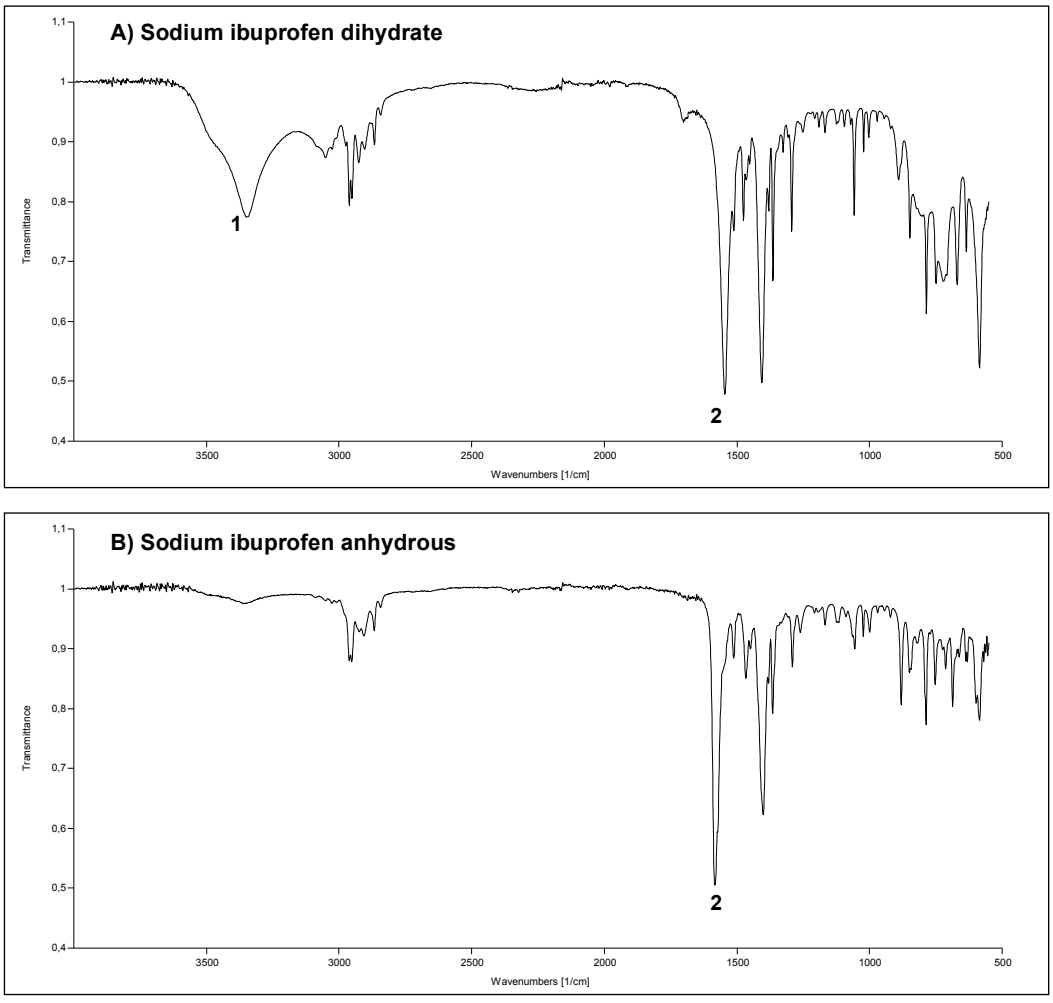

Figure 56. ATR-FT-IR spectra of A) sodium ibuprofen dihydrate and B) sodium ibuprofen anhydrous.

4.1.2 Eudragit RS 100

Hot melt extrusion is generally conducted at a temperature higher than the T_g of the polymer and lower than its degradation temperature.

TGA and MTDSC analyses were carried out on Eudragit RS 100 to evaluate its degradation temperatures and T_g, respectively, in order to select the more appropriate operative temperature for the hot melt extrusion process.

Eudragit did not exhibit any significant degradation when heated up to 180°C, as shown in Figure 57, that reports the massive weight loss of the polymer above this temperature.

MTDSC analysis (Figure 58) demonstrated the amorphous nature of the polymer, since only a T_g value of 53.46 °C ± 1.04 was recorded. This figure differs from the T_g value of 65 °C reported by the supplier. This is not surprising as the glass transition of a polymer is not as sharp and well defined as the melting point and depends much more on the method of measurement and on the rate of heating or cooling during the measurement [129].

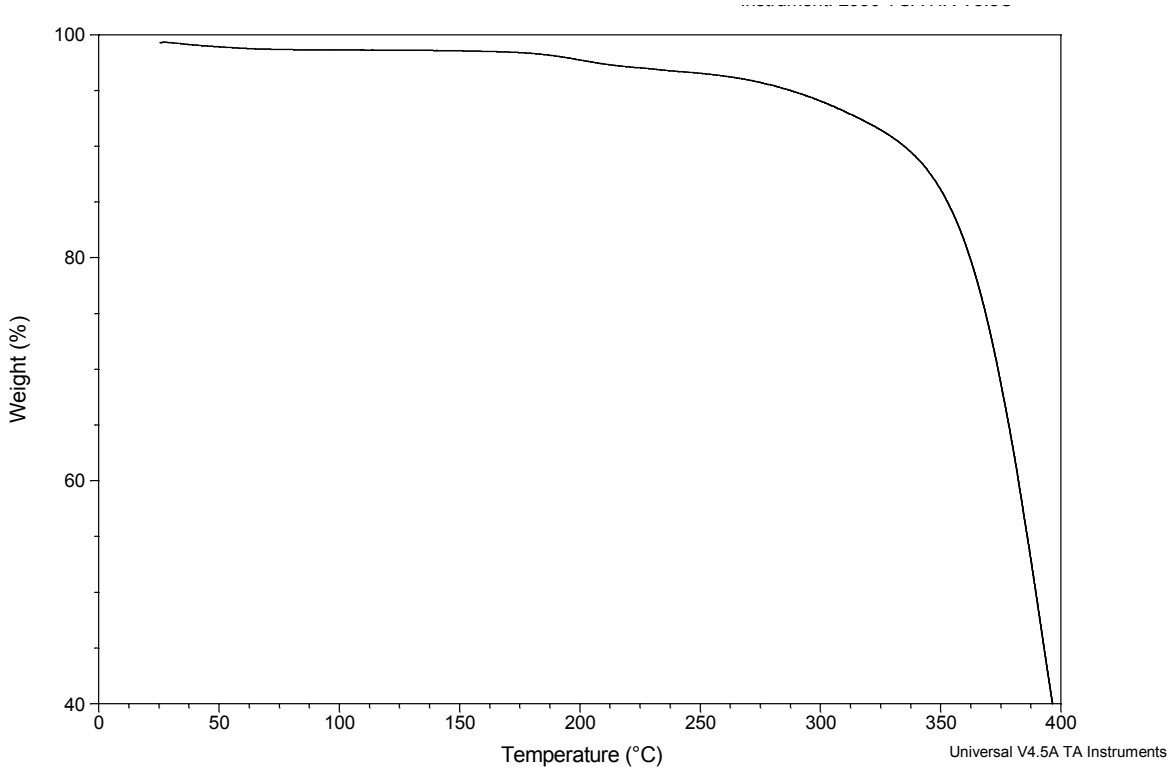

Figure 57. TGA analysis of Eudragit RS 100.

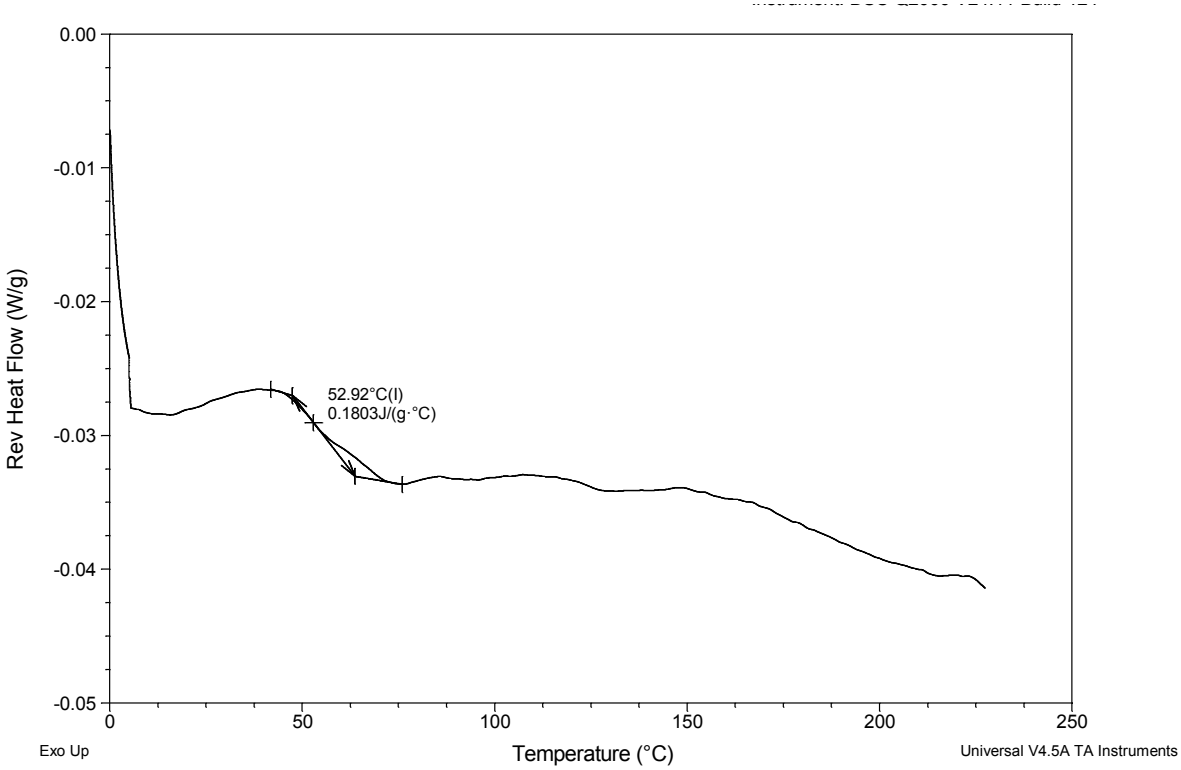

Figure 58. MTDSC analysis of Eudragit RS 100.

The amorphous nature of the polymer was also confirmed by XRPD analysis. The spectrum, reported in Figure 59, presented the halo pattern, typical of amorphous materials.

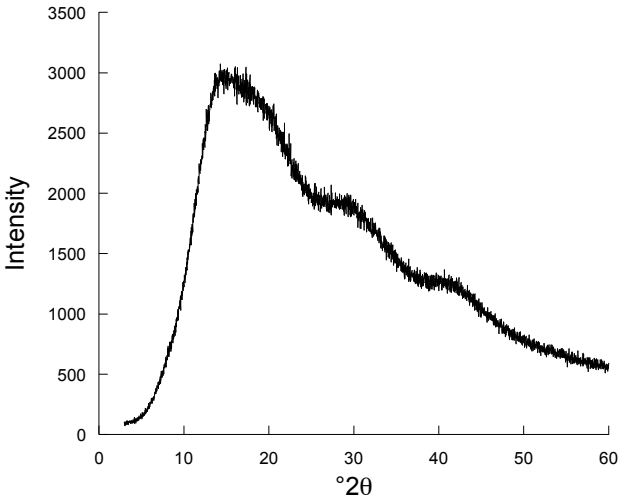

Figure 59. XRPD spectrum of Eudragit RS 100.

Figure 60 reports the ATR-FT-IR spectrum recorded from Eudragit RS 100. Characteristic peak, relative to the stretching vibrations of the C=O groups contained in the acrylic and methacrylic esters, were discerned at 1724, 1236 and 1145 cm^{-1} (band 1, 2, 3, respectively).

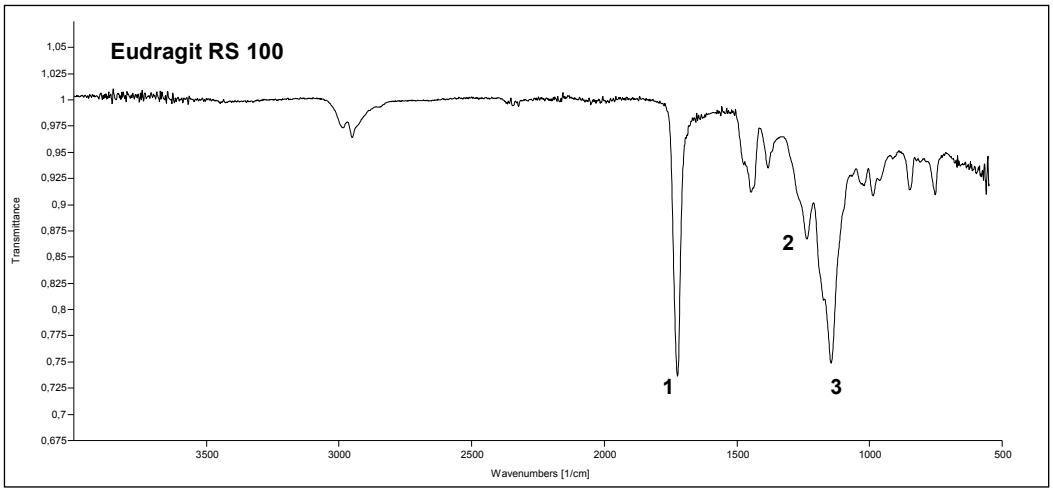

Figure 60. ATR-FT-IR spectrum of Eudragit RS 100.

4.2 Characterization of binary physical mixtures and extrudates

Binary extrudates freshly prepared were studied by MTDSC and XRPD in order to characterize the physical state of the dispersions obtained.

Table 15 summarizes the melting temperature (T_m) of sodium ibuprofen and the T_g of Eudragit RS 100 in the extrudates produced (HME) as well as the relevant physical mixtures (PM).

The extrudate containing 10% of drug exhibited only a T_g of about 50°C, slightly lower that the temperature found for the raw material, whereas the melting peak of the drug was not observed. These results might suggest that in the 10% extrudate, the drug was molecularly dispersed in the polymer, thus forming a solid solution, or was present as solid amorphous within the polymer chains.

Differently, 20 and 30% extrudates contained crystalline drug suspended within the amorphous polymer. The quantification of crystalline sodium ibuprofen in these extrudates was calculated using the calibration curve of the melting enthalpy of drug when physically mixed with Eudragit in different rations, as described in the section 3.2.2 and reported in Figure 61. The percentage of drug crystallinity was found to be 10.90 ± 0.21% and 22.92 ± 0.16% for extrudates with drug loading of 20% and 30%, respectively. The obtained results

indicated that the extrusion process determined the partial transition of the crystalline sodium ibuprofen in its amorphous state, or the partial dissolution of the drug within the polymer. The T_g found was slightly lower in these extrudated than the correspondent physical mixtures, suggesting that the part of drug could be molecularly dispersed into the Eudragit, exerting a plasticizing effect on the polymer.

Table 15. Melting temperature (T_m) of sodium ibuprofen and glass transition temperature (T_g) of Eudragit in fresh extrudates (HME) and their relative physical mixtures (PM).

DRUG AMOUNT % (w/w)		Tm (°C)	Tg (°C)
10%	**PM**	191.99 (0.16)	55.97 (2.37)
	HME	n.d*	50.36 (1.91)
20%	**PM**	192.94 (0.36)	55.25 (3.04)
	HME	183.64 (0.23)	48.52 (3.52)
30%	**PM**	193.34 (0.18)	58.17 (1.88)
	HME	190.23 (0.14)	52.64 (1.40)
*n.d.: not detectable			

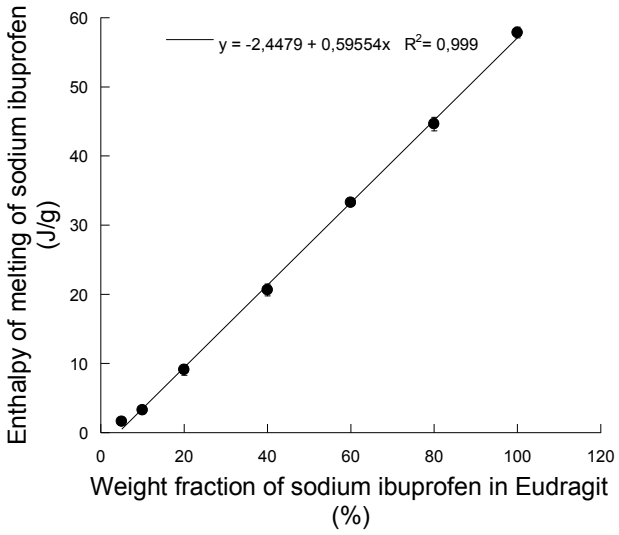

Figure 61. Calibration curve of the enthalpy of melting of sodium ibuprofen in the presence of Eudragit versus the ratio of crystalline drug in the physical mixtures. The bars represent the standard deviation (n=3).

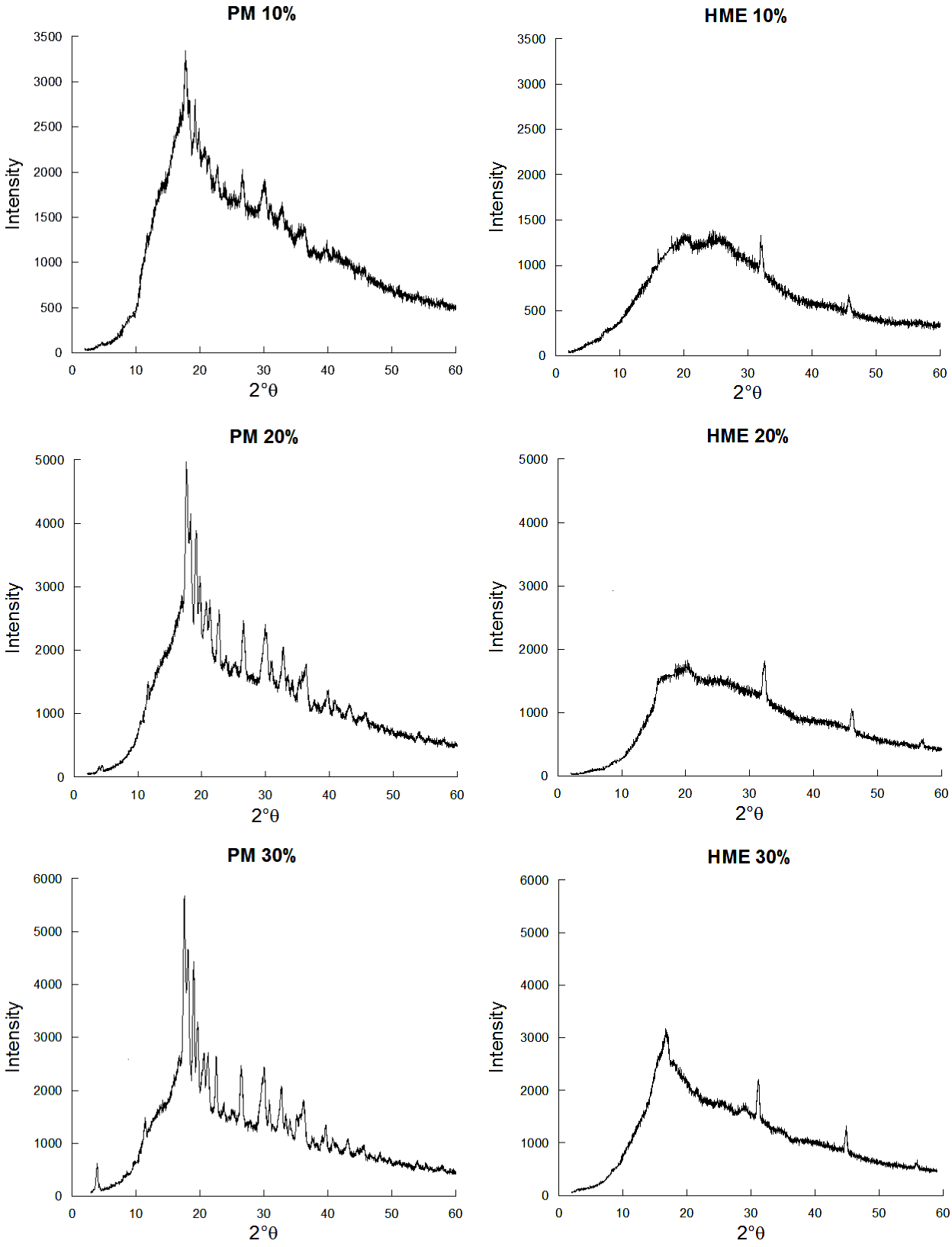

Figure 62. XRPD patterns obtained from physical mixtures and freshly prepared extrudates containing different drug loading.

As shown in Figure 62, XRPD spectra collected from all the prepared extrudates showed two sharp peaks at 31° 2θ and 44° 2θ, which were likely due to impurities stemming in the extruder. In fact, no peaks related to sodium ibuprofen were found in the same positions neither in the spectra collected from the physical mixtures nor in that of the pure drug.

Thus, spectra of extrudates with 10% and 20% of drug loading did not present crystalline peaks. Only the spectrum of extrudate containing the 30% of drug presented small peaks in the region 10-30° 2θ. These results partially confirmed DSC data, particularly concerning HME products containing 10% and 30% of drug. The lack of crystalline peaks in extrudates with 20% of drug loading was quite surprising. The crystallinity in extrudates containing the 30% of drug was actually of the 23% and the intensity of peaks in the spectrum was rather limited. Thus it is likely that the technique was not enough sensitive to detect lower amounts of crystalline drug, as the case of extrudate at 20% of drug, where the actual crystallinity was around the 10%.

Microphotographs of the cross section and external surface of freshly prepared HME product, reported in Figures 63-65, showed compact and smooth structures for all the prepared extrudates. No crystals were observed in extrudates containing the 20% and 30% of drug.

Figure 66 reports FT-IR spectra recorded from extrudates containing 10, 20 and 30% of sodium ibuprofen. Possible changes in the position of the peak assigned to the C=O contained in the carboxylic groups of the drug were monitored in order to detect the potential interaction with the amine groups of Eudragit RS 100. In extrudate containing 10 and 20% of sodium ibuprofen, said peak was observed at 1579 cm^{-1}, a wavenumber value not significantly different from that observed in the pure drug in the anhydrous state. In extrudates containing the 30% of drug, the peak relative to the vibration of C=O was located at 1561 cm^{-1}. In this case, the position of the peak was intermediate with respect to that observed in the anhydrous pure drug and the dihydrate form (1546 cm^{-1}). Thus, the shift observed with respect to the original position in the dihydrate drug, used in the production of extrudates, was attributed to the dehydration of sodium ibuprofen during the process, since the latter was conducted at 130°C. The wider shift observed in extrudates containing 10 and 20% of sodium ibuprofen was due to the complete dehydration of the drug. As opposite, in extrudates with 30% of drug loading, the shift toward an intermediate position between the limit values of 1581 and 1546 cm^{-1} was due to the partial dehydration of the molecules of drug. Thus ATR-FT-IR analysis did not demonstrate any evidence of ionic interactions between sodium ibuprofen and Eudragit RS 100 in the extrudates produced.

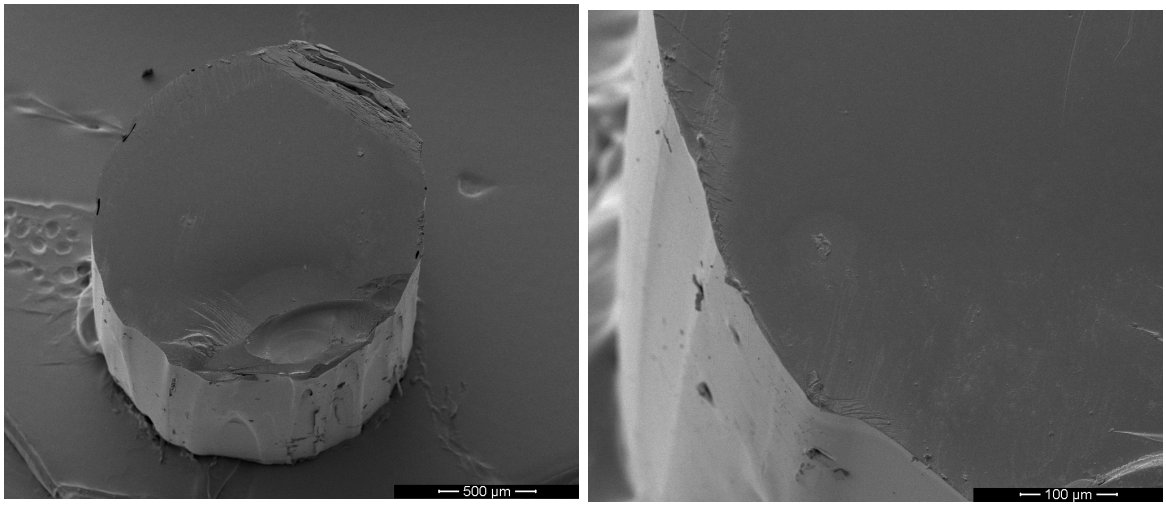

Figure 63. Microphotographs of extrudates with 10% of drug loading.

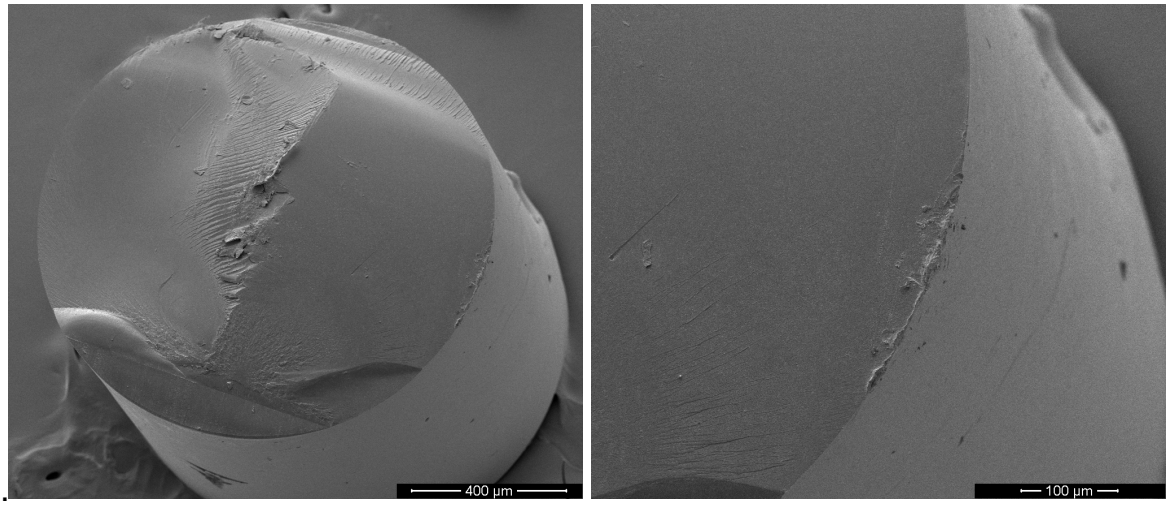

Figure 64. Microphotographs of extrudates with 20% of drug loading

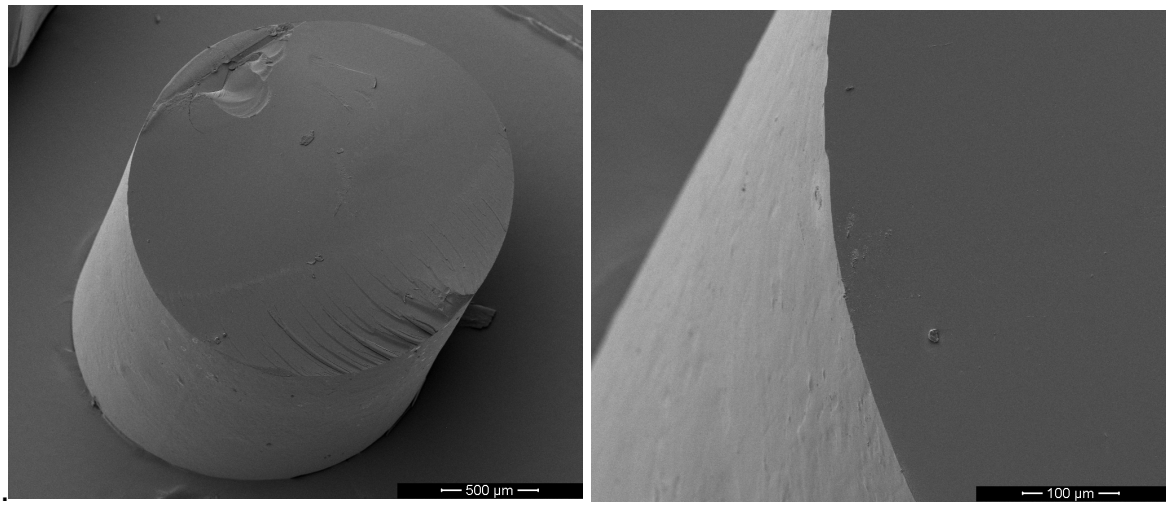

Figure 65. Microphotographs of extrudates with 30% of drug loading.

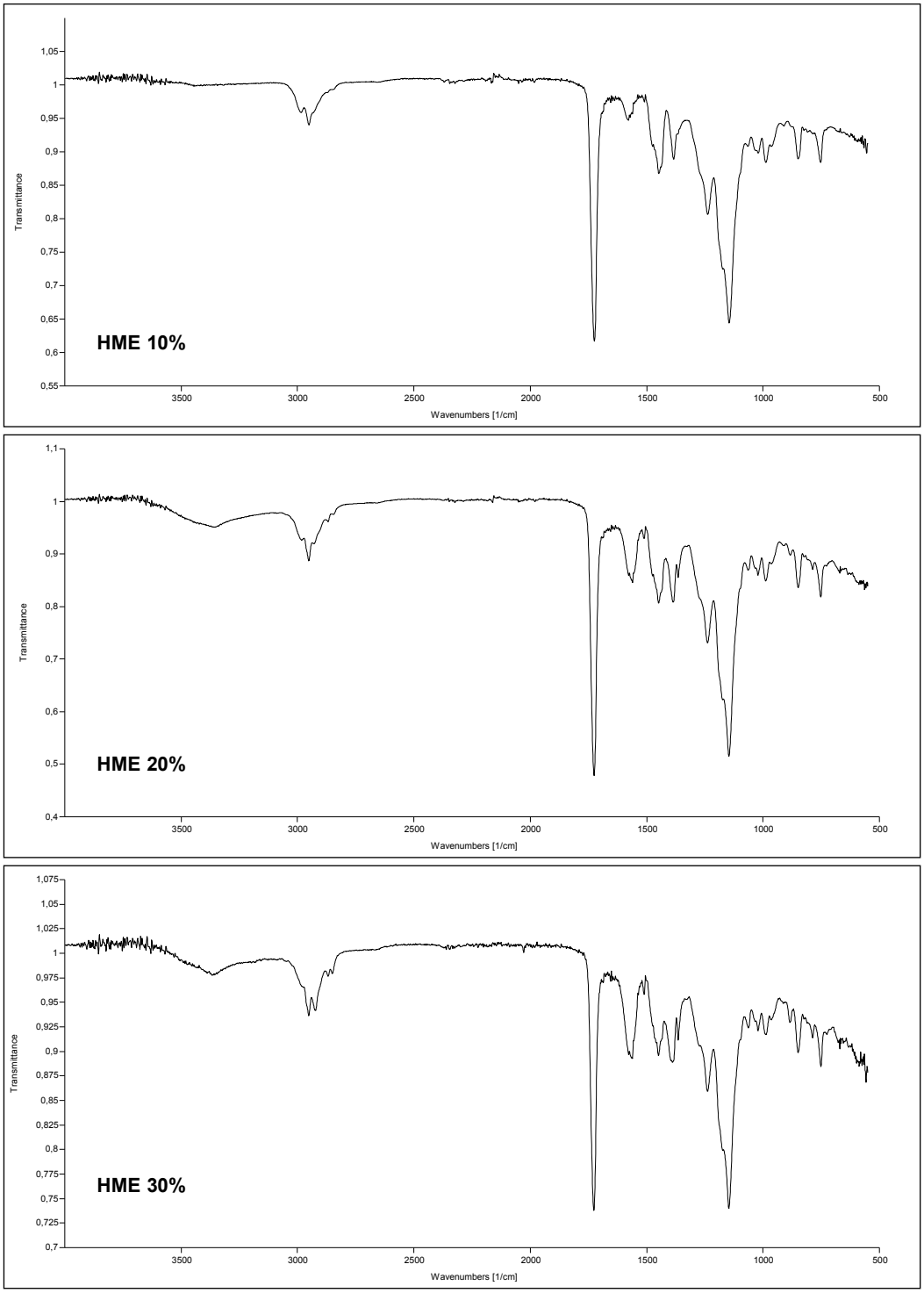

Figure 66. ATR-FT-IR spectra of extrudates containing different amount of sodium ibuprofen.

4.3 Characterization of ternary mixture and extrudate

The lack of interaction between the oppositely charged groups of the molecules employed was likely due to an incomplete melting of sodium ibuprofen within the softened polymer, especially for extrudates with the highest drug loading, presenting still crystalline drug after the extrusion process.

In order to promote the interaction with Eudragit RS 100, the crystal lattice of anhydrous sodium ibuprofen was broken by dissolving the drug in PEG 200, prior the mixing with the polymer and the extrusion process. A semi-solid physical mixture, with the composition 10:23:67 sodium ibuprofen/PEG 200/Eudragit RS 100, was obtained. It was not possible to produce mixture with a greater drug loading because of the limited solubility of sodium ibuprofen in PEG 200.

DSC analysis, carried out on the physical mixture, supported the disruption of the crystal lattice of the drug, since the melting peak of the crystalline sodium ibuprofen was not detected. The physical mixture exhibited a T_g value of 59.03 ± 0.68°C.

The absence of crystalline drug in the physical mixture was also confirmed by XRPD analysis, as shown in Figure 67.

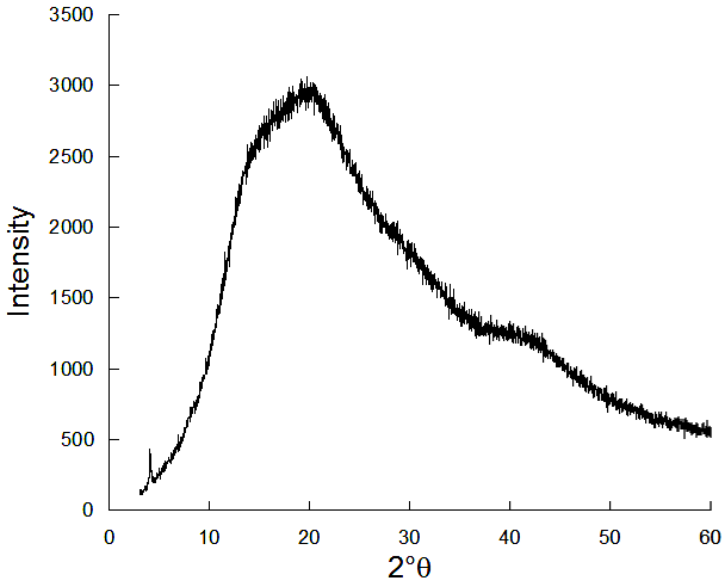

Figure 67. XPRD pattern of the ternary physical mixture containing sodium ibuprofen/PEG 200/Eudragit RS 100 (10:23:67).

The ternary extrudate, analysed by MTDSC, exhibited a T_g value of 52.85 ± 0.81°C, and no melting of the crystalline sodium ibuprofen, suggesting the formation of a solid solution, since no melting of the crystalline sodium ibuprofen was detected.

DSC data were supported by XRPD analysis, since the halo pattern, typical of amorphous materials was detected in the ternary extrudate, as shown in Figure 68.

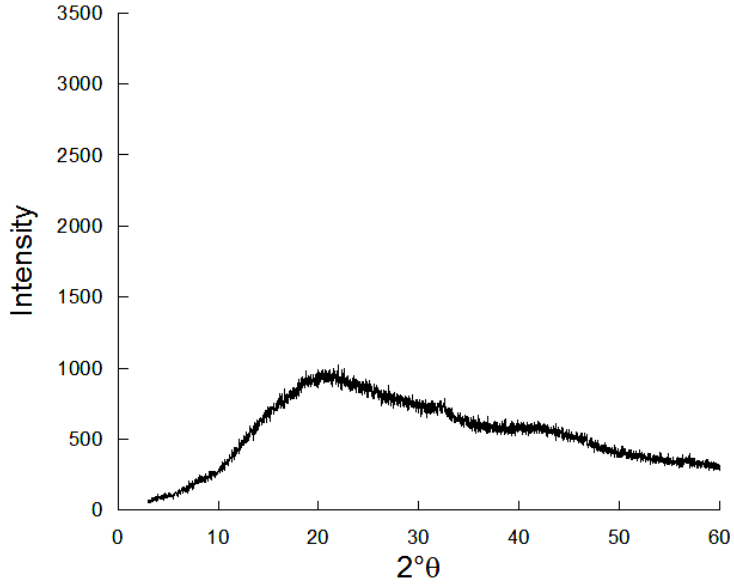

Figure 68. XRPD pattern of the ternary extrudate.

SEM microphotographs, reported in Figure 69, showed that the introduction of the PEG 200 modified the structure of the extrudate, which resulted more rough and porous.

ATR-FT-IR analysis, again, did not provide any evidence of ionic interaction occurring between the two oppositely charged sodium ibuprofen and Eudragit RS 100, since the peak assigned to the carboxylic group of the drug maintained, both in the physical mixture and in the extrudate, the same position with respect to the pure drug (1579 cm^{-1}). ATR-FT-IR spectra collected from the ternary physical mixture and the extrudate are reported in Figure 70. It may be assumed that other kind of interactions were involved in the stabilization of the amorphous drug within the ternary and the binary extrudate with 10% of drug. It is evident that the ATR-FT-IR technique used here did not permit the identification of the type of intermolecular forces established.

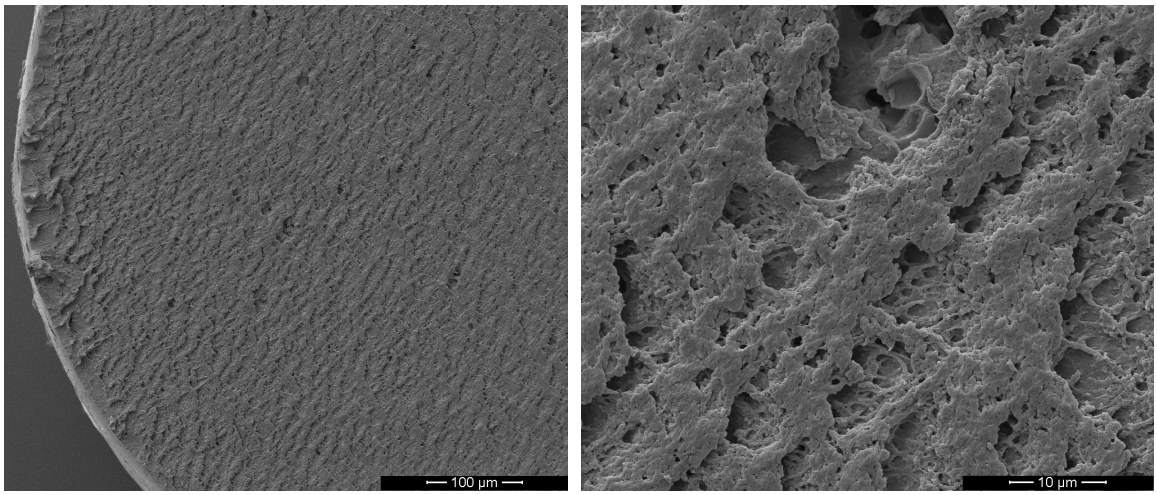

Figure 69. SEM microphotographs of the cross section of the ternary extrudate.

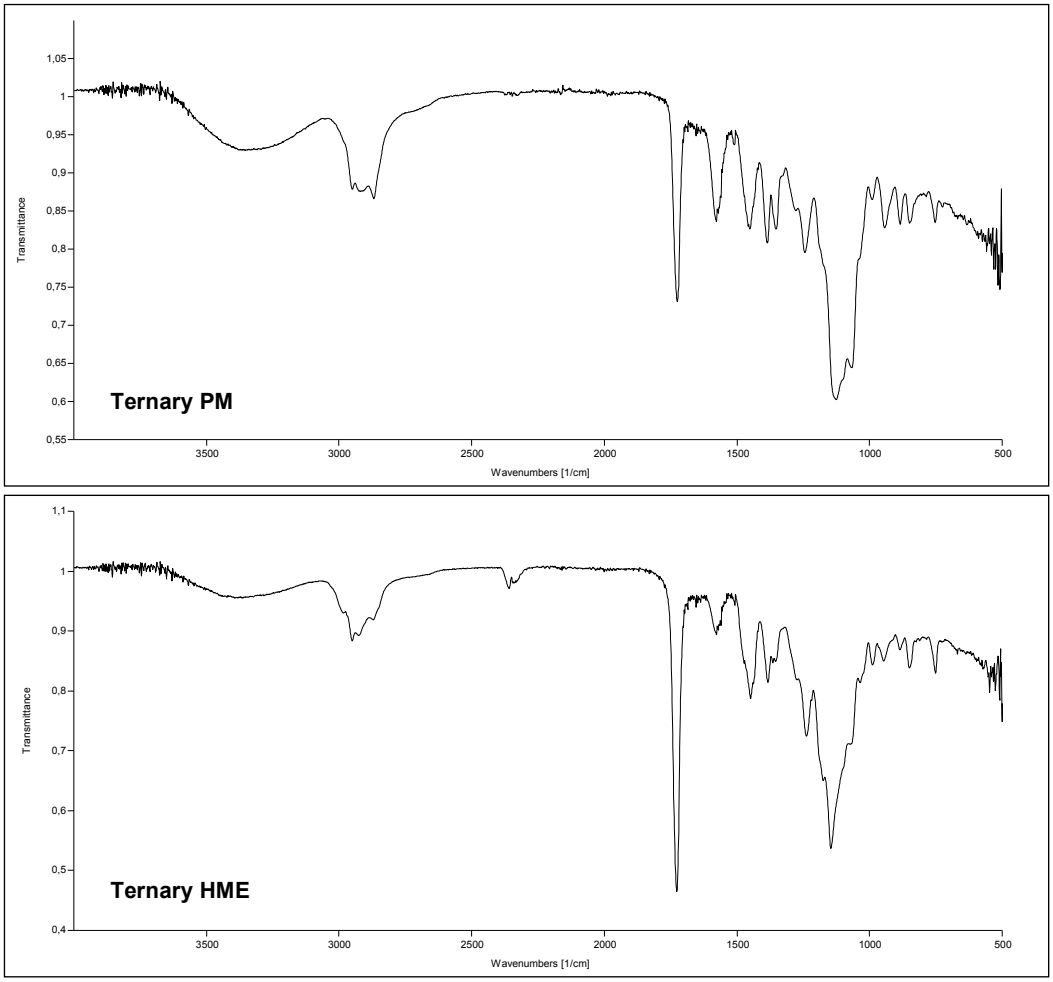

Figure 70**.** ATR-FT-IR spectrum of the ternary physical mixture and extrydates containing sodium ibuprofen/PEG 200/Eudragit RS 100 (10:23:67).

5. CONCLUSIONS

Hot melt extrusion was employed for the production of extrudates containing sodium ibuprofen and Eudragit RS 100 in different weight ratios.

The physical state of the drug within the extrudates depended on their drug loading. In particular, HME products containing drug amount greater than 10% presented partially crystalline sodium ibuprofen, while the solid dispersion at a molecular level was obtained only in the mixture with the 10% of drug loading.

The presence of a co-solvent, namely PEG 200, facilitated the formation of the solid solution, as the breaking of the crystal lattice of the drug permitted to molecularly disperse the drug directly in the physical mixture. This approach was not evaluated for higher drug loadings because of the solubility of sodium ibuprofen in PEG 200. The presence of the co-solvent also modified the micro-structure of the extudate, which resulted more rough and porous with respect to the binary HME products.

ATR-FT-IR did not provide any evidence of ionic interaction between the oppositely charged molecules in any of the systems produced. It is evident that other kinds of intermolecular forces were involved in the stabilization of sodium ibuprofen within the extrudates produced, although the ATR-FT-IR technique did not permit to better identify them.

In conclusion, this preliminary study evidenced that the hot melt extrusion technique might not be suitable to produce solid solutions, where the drug and the polymer are electrostatically bonded. Nevertheless, a further investigation, by using different molecules and operative conditions, may permanently clarify the applicability of the technique to obtain ionically bonded solid solutions.

VI. CONCLUSIONS

VI. CONCLUSIONS

The present research work has been focused on the study of non covalent interactions between drugs and polymer in oral controlled drug delivery with the aim to provide new insights and more systematic approach for the prediction of desired release profile, depending on the chemical functions and the interactions involved.

The interactions of a model drug having basic characteristics, such as atenolol, with polymers carrying different functional groups, were investigated by ATR-FT-IR and H^1 NMR techniques.

Electrostatic interactions were found between atenolol and chondroitin sulfate, sodium alginate and λ-carrageenan, while hydrogen bonds were established with chitosan.

In vitro dissolution studies carried out on matrix systems, consisting of atenolol and each polymer selected, put into evidence that both drug-polymer interactions and polymer characteristics play a key role in drug release.

The interaction of the polymer with the dissolution media was more important in controlling atenolol release in the case of matrix tablets containing chondroitin sulfate and chitosan. In fact, chondroitin sulfate tablets dissolved within two hours, independently of the solvent used, affording a non controlled atenolol release. Differently, chitosan tablets did not dissolve completely in any media used, thus atenolol release was controlled by its dissolution/diffusion in the solvent penetrated matrix.

Ionic interactions were more effective in determining atenolol release from matrix tablets made by sodium alginate and λ-carrageenan, as demonstrated by different release rates observed in dissolution medium having different ionic strength. Curiously, and as opposite than expected, drug release rate was lowered by increasing ionic strength.

These results were also confirmed by analysis conducted on tablets containing atenolol and each polymer selected by desorption electrospray ionization mass spectrometry, here reported as an innovative technique to investigate drug-polymer interactions.

The DESI-MS technique allowed studying the mechanisms involved in drug release from polymeric matrices in a localized area of the tablet surface in contact with a small volume of solvent. These particular operative conditions permitted to indentify an interval of time where polymer-solvent interactions were negligible, so that only the contribution of drug-polymer interactions on drug release could be evidenced and evaluated. DESI-MS data confirmed that drug-polymer non-covalent interactions were important in atenolol release only in the case of sodium alginate and λ-carrageenan, while polymer-solvent interactions and drug-

solvent interactions mainly controlled drug release from chondroitin sulfate and chitosan matrices respectively.

Atenolol-λ-carrageenan tablets were the most suitable matrix systems for oral controlled drug delivery. The tablets exhibited different behaviours in each solvent used, showing erosion at lower ionic strength and swelling at higher ionic strength. As a consequence, super Case II and zero order release kinetics were observed at lower and higher ionic strength, respectively.

Atenolol-λ-carrageenan ionic interactions play a role in preventing drug diffusion through the swollen polymer at higher ionic strength, affording a linear kinetics rather than the expected Fickian kinetics.

The observation of matrices clamped between transparent discs and introduced either in water or phosphate buffers at 0.01 and 0.1 M ionic strength put in evidence the swelling and the erosion fronts of a typical matrix systems. The region comprised between the two fronts presented an interface that separated an inner zone, consisting of not fully hydrated particles, from the outer fully hydrated region. This interface was called “polymer gelling front”. Since it was demonstrated that drug and polymer interacted in solution, the inner partially hydrated region likely consisted of atenolol-λ-carrageenan complexes, which represented the diffusing species. Thus, the polymer gelling front corresponded actually to the diffusion front and drug delivery rates and kinetics were determined by the variations of the thickness of the gel layer over time.

The thickness of the gel layer was influenced by λ-carrageenan solubility in the solvents used. DSC studies demonstrated that λ-carrageenan was more soluble in water and in solvent at low ionic strength. The increase of ionic concentration in the solvent determined a reduction of the polymer solubility. As consequence, in μ 0.1 M media, λ-carrageenan swelled, forming a layer of gel that remained constant in thickness over 6 hours. Thus, the drug was released with linear kinetics by diffusing through a constant thickness pathway.

In water and in media at lower ionic strength, the gel layer thickness rapidly decreased, affording a super Case II release kinetics of the drug

These considerations highlighted that mutual interactions among atenolol, λ-carrageenan and potassium dihydrogen phosphate, present in the dissolution media, controlled the overall drug release from λ-carrageenan tablets.

Salt interactions with atenolol and λ-carrageenan were exploited to make the atenolol release independent of the environmental conditions. In this respect, different potassium salts were added to the drug-polymer mixture prior the tablets production. Acidic salts, such as potassium dihydrogen phosphate, oxalate, tartrate and phthalate monobasic, were effective

in providing more prolonged release rates of atenolol in water with respect to tablets not containing salts. This effect was probably related to a decreased solubility of the polymer, stemming to the local availability of protons after salt dissociation.
Since the ternary system atenolol-λ-carrageenan-potassium dihydrogen phosphate provided the most suitable drug release for controlled delivery, this polymer-salt mixture was investigated to obtain controlled delivery of different basic drugs, such as methyl L-dopa and buflomedil pyridoxal phosphate.
Release profiles obtained in water showed that the salt was not effective in reducing release rate for both of the drugs selected, confirming that the results obtained with atenolol were due to specific and mutual interactions among atenolol-polymer and salt. Moreover, different release kinetics were observed for the three drugs used, suggesting that each drug interacted with λ-carrageenan to different extent.
In conclusion, it is evident that, in the matrix systems investigated in the present research work, drug-polymer-salt interactions controlled the drug delivery.
We put into evidence here that many properties of drug and polymer, especially the solubility in the solvents used, play an important role in determining drug release rates and kinetics, in the studied systems, overcoming in some cases also strong interactions.
We also demonstrated that it is not sufficient to refer simply to specific functional moieties in the drug molecules in order to get to a generalised description of the drug-polymer-solvent behaviour. For these reasons, it is difficult, at the moment, to provide a general and systematic model for the prediction of the performances obtained from oral controlled drug delivery systems based on non-covalent interactions between drug and polymers.

The research project carried out during the 6 months spent as a visiting student at UCL-School of Pharmacy in London, was aimed to obtain solid dispersion of ionically bonded drugs and polymers, as a novel approach to deliver active molecules via the oral route, by hot melt extrusion.
Solid solutions of Eudragit RS 100 and sodium ibuprofen were successfully obtained with the 10% of drug loading, with and without the presence of PEG 200, which acted as co-solvent for the drug. Differently, extrudates containing more than 10% of drug presented partially crystalline sodium ibuprofen.
However, no evidences of ionic bonds between the oppositely charged molecules were found, suggesting that the technique was not suitable for the production of ionic liquid-like extrudates, at least with the two molecules selected.

VII. PUBLICATIONS AND CONFERENCE ATTENDANCE

VII. LIST OF PUBLICATIONS AND CONFERENCE ATTENDANCE

PUBLICATIONS

- L. Elviri, S. De Robertis, S. Baldassarre, R. Bettini. *Desorption electrospray ionization high-resolution mass spectrometry for the fast investigation of natural polysaccharide interactions with a model drug in controlled drug release systems.*
  Rapid Communications in Mass Spectrometry, 2014. **28**, 1544-1552.
- S. De Robertis, M.C. Bonferoni, L. Elviri, G. Sandri, C. Caramella, R. Bettini. *Advances in oral controlled drug delivery: the role of drug – polymer and intrepolymer non-covalent interactions.*
  Expert Opinion on Drug Delivery, 2014. **12** (3). (Review).

CONFERENCE PROCEEDINGS

- S. De Robertis, A. Luchena, L. Elviri, R. Bettini. *Interactions between atenolol and polysaccharides by H^1-NMR and ATR .* 7th AiTUN, March 2013, Perugia, Italy.
- L. Elviri, S. De Robertis, S. Baldassarre, R. Bettini. *A DESI-MS technique to investigate atenolol-polysaccharide matrices behaviour.* 3rd Conference Innovation in Drug Delivery, Advances in Local Drug Delivery, September 2013, Pisa, Italy.
- L. Elviri, S. De Robertis, S. Baldassarre, R. Bettini. *DESI-MS and FTIR-HATR techniques to investigate atenolol-polysaccharide interactions*. AAPS, November 2013, San Antonio, Texas, USA.
- S. De Robertis, A. Luchena, L. Elviri, R. Bettini. *Drug-polymer interactions as a tool for oral controlled drug release*. AAPS, November 2013, San Antonio, Texas, USA.
- S. De Robertis, L. Elviri, R. Bettini. *Influence of atenolol – λ-carrageenan electrostatic interactions on drug release from polymeric matrices.* UKPharmSci, September 2014, Hatfield, UK.
- L. Elviri, S. De Robertis, R. Bettini. *Salt effect in the DESI-HMRS analysis of a model drug in λ-carrageenan tablets*. AAPS, November 2014, San Diego, California, USA

VIII. BIBLIOGRAPHY

VIII. BIBLIOGRAPHY

1. *European Pharmacopoeia, 8th Edition*. 2014, Strasbourg: Council of Europe. 707.
2. Hoffman, A.S., *The origins and evolution of "controlled" drug delivery systems.* Journal of Controlled Release, Proceedings of the Tenth European Symposium on Controlled Drug Delivery, 2008. **132**(3): p. 153-163.
3. MP-Advisors, *Innovative Drug Delivery Systems Oppotunities for Generic & Specialty Pharmaceutical Companies.* Available from:http://www.reportsnreports.com/reports/275193-innovative-drug-delivery-systems-opportunities-for-generic-specialty-pharmaceutical-companies.html, 2014.
4. Das, N.G. and S.K. Das, *Controlled-Release of Oral Dosage Forms.* Formulation, Fill & Finish, 2003: p. 10-16.
5. Coffin, M. and M. Burke, *Controlling Release by Gastroretention*, in *Controlled Release in Oral Drug Delivery SE - 17*, C.G. Wilson and P.J. Crowley, Editors. 2011, Springer US DA - 2011/01/01. p. 361-383.
6. Basit, A. and E. McConnell, *Drug Delivery to the Colon*, in *Controlled Release in Oral Drug Delivery SE - 18*, C.G. Wilson and P.J. Crowley, Editors. 2011, Springer US DA - 2011/01/01. p. 385-399.
7. Tiwari, S., J. DiNunzio, and A. Rajabi-Siahboomi, *Drug-Polymer Matrices for Extended Release*, in *Controlled Release in Oral Drug Delivery SE - 7*, C.G. Wilson and P.J. Crowley, Editors. 2011, Springer US DA - 2011/01/01. p. 131-159.
8. Colombo, P., *Swelling-controlled release in hydrogel matrices for oral route.* Advanced Drug Delivery Reviews, Modern Hydrogel Delivery Systems, 1993. **11**(1-2): p. 37-57.
9. Colombo, P., et al., *Drug Diffusion Front Movement Is Important in Drug Release Control from Swellable Matrix Tablets.* Journal of Pharmaceutical Sciences, 1995. **84**(8): p. 991-997.
10. Colombo, P., R. Bettini, and N.A. Peppas, *Observation of swelling process and diffusion front position during swelling in hydroxypropyl methyl cellulose (HPMC) matrices containing a soluble drug.* Journal of Controlled Release, 1999. **61**(1-2): p. 83-91.

11. Burnette, R.R., *Theory of Mass Transfer*, in *Controlled Drug Delivery: Fundamentals and Applications, Second Edition*, J. Robinson and V.H.L. Lee, Editors. 1987, Taylor & Francis. p. 96-138.
12. Higuchi, T., *Rate of release of medicaments from ointment bases containing drugs in suspension.* Journal of Pharmaceutical Sciences, 1961. **50**(10): p. 874-875.
13. Siepmann, J. and N.A. Peppas, *Modeling of drug release from delivery systems based on hydroxypropyl methylcellulose (HPMC).* Advanced Drug Delivery Reviews, Mathematical Modeling of Controlled Drug Delivery, 2001. **48**(2-3): p. 139-157.
14. Peppas, N.A., *Analysis of Fickian and non-Fickian drug release from polymers.* Pharmaceutica acta Helvetiae, 1985. **60**(4): p. 110-111.
15. Peppas, N.A. and R.W. Korsmeyer, *Dinamically swelling hydrogels in controlled release applications*, in *Hydrogels in Medicine and Pharmacy*, N.A. Peppas, Editor. 1986, CCR Press. p. 109-136.
16. Peppas, N.A. and J. Sahlin, *A simple equation of for the description of solute release. III. Coupling of diffusion and relaxation.* International Journal of Pharmaceutics, 1989. **57**: p. 169-172.
17. Colombo, P., et al., *Drug release modulation by physical restrictions of matrix swelling.* International Journal of Pharmaceutics, 1990. **63**(1): p. 43-48.
18. Colombo, P., G. Colombo, and C. Cahyadi, *Geometric Release Systems: Principles, Release Mechanisms, Kinetics, Polymer Science, and Release-Modifying Material*, in *Controlled Release in Oral Drug Delivery SE - 11*, C.G. Wilson and P.J. Crowley, Editors. 2011, Springer US DA - 2011/01/01. p. 221-237.
19. Conte, U., et al., *Multi-layered hydrophilic matrices as constant release devices (GeomatrixTM Systems).* Journal of Controlled Release, 1993. **26**(1): p. 39-47.
20. *Geomatrix:customisable oral drug delivery platform. Available from: http://www.skyepharma.com/Technologies/Oral_drug_delivery_technologies/Geomatrix%E2%84%A2/Default.aspx?id=62.*
21. Conte, U. and L. Maggi, *Modulation of the dissolution profiles from Geomatrix® multi-layer matrix tablets containing drugs of different solubility.* Biomaterials, 1996. **17**(9): p. 889-896.
22. Conte, U. and L. Maggi, *A flexible technology for the linear, pulsatile and delayed release of drugs, allowing for easy accommodation of difficult in vitro targets.* Journal of Controlled Release, 2000. **64**(1-3): p. 263-268.

23. Losi, E., et al., *Assemblage of novel release modules for the development of adaptable drug delivery systems.* Journal of Controlled Release, 2006. **111**(1-2): p. 212-218.
24. Strusi, O.L., et al., *Module assemblage technology for floating systems: In vitro flotation and in vivo gastro-retention.* Journal of Controlled Release, 2008. **129**(2): p. 88-92.
25. Strusi, O.L., et al., *Artesunate-clindamycin multi-kinetics and site-specific oral delivery system for antimalaric combination products.* Journal of Controlled Release, 2010. **146**(1): p. 54-60.
26. Pifferi, G. and P. Restani, *The safety of pharmaceutical excipients.* Il Farmaco, 2003. **58**: p. 541-550.
27. Tsuchida, E., *Formation of polyelectrolyte complexes and their structures.* Journal of Macromolecular Science, 1994. **31**(1): p. 1-15.
28. Thunemann, A., et al., *Polyelectrolyte Complexes*, in *Polyelectrolytes with Defined Molecular Architecture II SE - 0004*, M. Schmidt, Editor. 2004, Springer Berlin Heidelberg. p. 113-171.
29. Khutoryanskiy, V.V., *Hydrogen-bonded interpolymer complexes as materials for pharmaceutical applications.* International Journal of Pharmaceutics, 2007. **334**(1-2): p. 15-26.
30. Moustafine, R.I., et al., *Drug release modification by interpolymer interaction between countercharged types of Eudragit RL 30D and FS 30D in double-layer films.* International Journal of Pharmaceutics, 2012. **439**(1-2): p. 17-21.
31. Mustafin, R.I., et al., *Synthesis and characterization of a new carrier based on Eudragit® EPO/S100 interpolyelectrolyte complex for controlled colon-specific drug delivery.* Pharmaceutical Chemistry Journal, 2011. **45**: p. 568-574.
32. Mustafin, R.I., et al., *Comparative study of structural and compositional changes of polycomplex matrices based on Eudragit® EPO and Eudragit® L100.* Pharmaceutical Chemistry Journal, 2011. **45**: p. 114-117.
33. Moustafine, R.I., et al., *Structural transformations during swelling of polycomplex matrices based on countercharged (meth)acrylate copolymers (Eudragit® EPO/Eudragit® L 100-55).* Journal of Pharmaceutical Sciences, 2011. **100**(3): p. 874-885.
34. Moustafine, R.I., et al., *Interpolyelectrolyte complexes of Eudragit® E PO with sodium alginate as potential carriers for colonic drug delivery: monitoring of structural*

transformation and composition changes during swellability and release evaluating. Drug Development and Industrial Pharmacy, 2009. **35**(12): p. 1439-1451.

35. Prado, H.J., et al., *Basic butylated methacrylate copolymer/kappa-carrageenan interpolyelectrolyte complex: Preparation, characterization and drug release behaviour.* European Journal of Pharmaceutics and Biopharmaceutics, 2008. **70**(1): p. 171-178.
36. Torre, P.M.d.l., et al., *Release of amoxicillin from polyionic complexes of chitosan and poly(acrylic acid). study of polymer/polymer and polymer/drug interactions within the network structure.* Biomaterials, 2003. **24**(8): p. 1499-1506.
37. de la Torre, P.M., G. Torrado, and S. Torrado, *Poly (acrylic acid) chitosan interpolymer complexes for stomach controlled antibiotic delivery.* Journal of Biomedical Materials Research Part B: Applied Biomaterials, 2005. **72B**(1): p. 191-197.
38. de la Torre, P.M., S. Torrado, and S. Torrado, *Interpolymer complexes of poly(acrylic acid) and chitosan: influence of the ionic hydrogel-forming medium.* Biomaterials, 2003. **24**(8): p. 1459-1468.
39. Torrado, S., et al., *Chitosan-poly(acrylic) acid polyionic complex: in vivo study to demonstrate prolonged gastric retention.* Biomaterials, 2004. **25**(5): p. 917-923.
40. Clausen, A.E. and A. Bernkop-Schnurch, *Direct compressible polymethacrylic acid-starch compositions for site-specific drug delivery.* Journal of Controlled Release, 2001. **75**(1-2): p. 93-102.
41. Kim, B. and N.A. Peppas, *Complexation Phenomena in pH-Responsive Copolymer Networks with Pendent Saccharides.* Macromolecules, 2002. **35**: p. 9545-9550.
42. Peppas, N.A. and J. Klier, *Controlled release by using poly(methacrylic acid-g-ethylene glycol) hydrogels.* Journal of Controlled Release, 1991. **16**: p. 203-214.
43. Bell, C. and N.A. Peppas, *Water, solute and protein diffusion in physiogically responsive hydrogels of poly(methacrylic acid-g-ethylene glycol).* Biomaterials, 1996. **17**: p. 1203-1218.
44. Madsen, F. and N.A. Peppas, *Complexation graft copolymer networks: Swelling properties, calcium binding and proteolytic enzyme inhibition.* Biomaterials, 1999. **20**: p. 1701-1708.
45. De Robertis, S., et al., *Advances in oral controlled drug delivery: the role of drug-polymer and interpolymer non-covalent interactions.* Expert Opinion on Drug Delivery, 2014. **12**(3): p. 1-13.

46. Papageorgiou, G., S. Papadimitriou, and E. Karavas, *Improvement in chemical and physical stability of fluvastatin drug through hydrogen bonfing intractions with different polymer matrices.* Current Drug Delivery, 2009. **6**(1): p. 101-112.
47. Alvarez-Fuentes, J., et al., *Study of a complexation process between naltrexone and Eudragit® L as an oral controlled release system.* International Journal of Pharmaceutics, 1997. **148**(2): p. 219-230.
48. Alvarez-Fuentes, J., et al., *Morphine Polymeric Coprecipitates for Controlled Release: Elaboration and Characterization.* Drug Development and Industrial Pharmacy, 1994. **20**(15): p. 2409-2424.
49. Holgado, M.A., et al., *Development and in vitro evaluation of a controlled release formulation to produce wide dose interval morphine tablets.* European Journal of Pharmaceutics and Biopharmaceutics, 2008. **70**(2): p. 544-549.
50. Coughlan, D.C., F.P. Quilty, and O.I. Corrigan, *Effect of drug physicochemical properties on swelling/deswelling kinetics and pulsatile drug release from thermoresponsive poly(N-isopropylacrylamide) hydrogels.* Journal of Controlled Release, 2004. **98**(1): p. 97-114.
51. Coughlan, D.C. and O.I. Corrigan, *Drug-polymer interactions and their effect on thermoresponsive poly(N-isopropylacrylamide) drug delivery systems.* International Journal of Pharmaceutics, 2006. **313**(1-2): p. 163-174.
52. Le Tien, C., et al., *N-acylated chitosan: hydrophobic matrices for controlled drug release.* Journal of Controlled Release, 2003. **93**(1): p. 1-13.
53. Berknop-Schnurch, A., et al., *Development of a Sustained Release Dosage Form for alpha-Lipoic Acid I. Design and in vitro evaluation.* Drug development & Industrial Pharmacy, 2004. **30**(1): p. 27-34.
54. Amidon, G., et al., *A theoretical basis for a biopharmaceutic drug classification - the correlation of in-vitro drug product dissolution and in-vivo bioavailability.* Pharmaceutical Research, 1995. **12**(3): p. 413-420.
55. Jintapattanakit, A., et al., *Peroral delivery of insulin using chitosan derivatives: A comparative study of polyelectrolyte nanocomplexes and nanoparticles.* International Journal of Pharmaceutics, 2007. **342**(1-2): p. 240-249.
56. Heinen, C., et al., *Mechanistic basis for unexpected bioavailability enhancement of polyelectrolyte complexes incorporating BCS class III drugs and carrageenans.* European Journal of Pharmaceutics and Biopharmaceutics, 2013. **85**(1): p. 26-33.

57. Ramirez-Rigo, M.V., et al., *Enhanced intestinal permeability and oral bioavailability of enalapril maleate upon complexation with the cationic polymethacrylate Eudragit E100.* European Journal of Pharmaceutical Sciences, 2014. **55**: p. 1-11.
58. Jimenez-Kairuz, A.F., et al., *Swellable drug-polyelectrolyte matrices (SDPM): Characterization and delivery properties.* International Journal of Pharmaceutics, 2005. **288**(1): p. 87-99.
59. Rigo, M.V.R., D.A. Allemandi, and R.H. Manzo, *Swellable drug-polyelectrolyte matrices (SDPM) of alginic acid: Characterization and delivery properties.* International Journal of Pharmaceutics, 2006. **322**(1-2): p. 36-43.
60. Quinteros, D.A., et al., *Interaction between a cationic polymethacrylate (Eudragit E100) and anionic drugs.* European Journal of Pharmaceutical Sciences, 2008. **33**(1): p. 72-79.
61. Bonferoni, M., et al., *On the employmet of lambda-carrageenan in a matrix system. I. Sensitivity to dissolution medium and comparison with Na carboxymethylcellulose and xanthan gum.* Journal of Controlled Release, 1993. **26**: p. 119-127.
62. Aguzzi, C., et al., *Influence of complex solubility on formulations based on lambda carrageenan and basic drugs.* AAPS PharmSciTech, 2002. **3**(3): p. 83-89.
63. Bonferoni, M.C., et al., *Characterization of a diltiazem-lambda carrageenan complex.* International Journal of Pharmaceutics, 2000. **200**(207-216).
64. Bonferoni, M.C., et al., *Development of Oral Controlled Release Tablet Formulations Based on Diltiazemâ€“Carrageenan Complex.* Pharmaceutical Development and Technology, 2004. **9**(2): p. 155-162.
65. Bettini, R., et al., *Drug Release Kinetics and Front Movement in Matrix Tablets Containing Diltiazem or Metoprolol/lambda-Carrageenan Complexes.* BioMed Research International, 2014. **2014**: p. 1-8.
66. Bettini, R., et al., *Swelling and drug release in hydrogel matrices: polymer viscosity and matrix porosity effects.* European Journal of Pharmaceutical Sciences, 1994. **2**(3): p. 213-219.
67. Pavli, M., et al., *Doxazosin-carrageenan interactions: A novel approach for studying drug-polymer interactions and relation to controlled drug release.* International Journal of Pharmaceutics, 2011. **421**(1): p. 110-119.
68. Pavli, M., F. Vrecer, and S. Baumgartner, *Matrix tablets based on carrageenans with dual controlled release of doxazosin mesylate.* International Journal of Pharmaceutics, 2010. **400**(1-2): p. 15-23.

69. Gruetter, C.A., *Atenolol xPharm: The Comprehensive Pharmacology Reference*, S.J. Enna and D.B. Bylund, Editors. 2007, Elsevier: New York. p. 1-6.
70. Mikami, T. and H. Kitagawa, *Biosynthesis and function of chondroitin sulfate.* Biochimica et Biophysica Acta (BBA) - General Subjects, 2013. **1830**(10): p. 4719-4733.
71. Rowe, R., P. Sheskey, and M. Quinn, *Alginic Acid*, in *Handbook of Pharmaceutical Excipients*, R. Rowe, P. Sheskey, and M. Quinn, Editors. 2009, Pharmaceutical Press and American Pharmacists Association. p. 20-22.
72. Rowe, R., P. Sheskey, and M. Quinn, *Chitosan*, in *Handbook of Pharmaceutical Excipients*, R. Rowe, P. Sheskey, and M. Quinn, Editors. 2009, Pharmaceutical Press and American Pharmacists Association. p. 159-161.
73. Li, L., et al., *Carrageenan and its applications in drug delivery.* Carbohydrate Polymers, 2014. **103**(0): p. 1-11.
74. *4.1 Reattivi, Soluzioni standard, Soluzioni tampone*, in *Farmacopea Ufficiale della Repubblica Italiana XII edizione*. 2008, Istituto Poligrafico e Zecca dello Stato. p. 521-664.
75. *2.9.3 Saggio di dissoluzione per le forme farmaceutiche solide*, in *Farmacopea Ufficiale della Repubblica Italiana*. 2008, Istituto Poligrafico e Zecca dello Stato. p. 343-356.
76. *Atenolol Official Monograph*, in *United State Pharmacopoeia (USP 38 NF 34)*. 2015, The United States Pharmacopeial Convention. p. 2306-2307.
77. *ICH Validation of Analytical Procedures: Text and Methodology Q2(R1).* 2005.
78. Takats, Z., et al., *Mass Spectrometry Sampling Under Ambient Conditions with Desorption Electrospray Ionization.* Science, 2004. **306**: p. 471-473.
79. Takats, Z., J. Wiseman, and R. Cooks, *Ambient mass spectrometry using dersorption electrospray ionization (DESI): instrumentation, mechanism and applications in forensics, chemistry and biology.* Journal of Mass Spectrometry, 2005. **40**: p. 1261-1275.
80. Cozar, O., et al., *Spectroscopic and DFT stufy of atenolol and metoprolol and their copper complexes.* Journal of Molecular Structure, 2011. **993**: p. 357-366.
81. Esteves de Castro, R., et al., *Infrared Spectroscopy of racemic and enantiomeric forms of atenolol.* Spectrochimica Acta Part A, 2007. **67**: p. 1194-1200.
82. Servaty, R., et al., *Hydration of polymeric components of cartilage - an infrared spectroscopic study on hyaluronic acid and chondroitin sulfate.* International Journal of Biological Maromolecules, 2001. **28**: p. 121-127.

83. Gomez-Ordonez, E. and P. Ruperez, *FTIR-ATR spectroscopy as a tool for polysaccaride identification in edible brown and red seaweeds.* Food Hydrocolloids, 2011. **25**: p. 1541-1520.
84. Pawlak, A. and M. Mucha, *Thermogravimentric and FTIR studies of chitosan blends.* Thermochimica Acta, 2003. **396**: p. 153-166.
85. CPKelco, *Genu, Carrageenan Book.*
86. Chandran, P.L. and F. Horkay, *Aggrecan, an Unusual Polyelectrolyte: Review of Solution Behavior and Physiological Implications.* Acta biomaterialia, 2012. **8**(1): p. 3-12.
87. O'Sullivan, L., et al., *Prebiotics from Marine Macroalge for Human and Animal Health Application.* Marine Drugs, 2010. **8**(2038-2064).
88. Gu, Y.S., E.A. Decker, and D.J. McClements, *Influence of pH and iota-Carrageenan Concentration on Physicochemical Properties and Stability of beta-Lactoglobulin-Stabilized Oil-in-Water Emulsions.* Journal of Agricultural and Food Chemistry, 2004. **52**(11): p. 3626-3632.
89. Wander, G., S. Chhabra, and K. Kaur, *Atenolol Drug Profile.* Supplement of JAPI, 2009. **57**: p. 13-17.
90. Etherson, K., et al., *Determination of excipient based solubility increases using the CheqSol method.* International Journal of Pharmaceutics, 2014. **465**(1-2): p. 202-209.
91. Barhate, L.N.Y.a.V.D., *Kinetic and intrinsic solubility determination of some b-blockers and antidiabetics by potentiometry*, in *2011*. 2011.
92. Dash, M., et al., *Chitosan - A versatile semi-synthetic polymer in biomedical applications.* Progress in Polymer Science, 2011. **36**(8): p. 981-1014.
93. Colombo, P., et al., *Drug volume fraction profile in the gel phase and drug release kinetics in hydroxypropylmethyl cellulose matrices containing a soluble drug.* European Journal of Pharmaceutical Sciences, 1999. **9**(1): p. 33-40.
94. Ebube, N.K., et al., *Sustained Release of Acetaminophen from Heterogeneous Matrix Tablets: Influence of Polymer Ratio, Polymer Loading, and Co-active on Drug Release.* Pharmaceutical Development and Technology, 1997. **2**(2): p. 161-170.
95. Li, H., R.J. Hardy, and X. Gu, *Effect of Drug Solubility on Polymer Hydration and Drug Dissolution from Polyethylene Oxide (PEO) Matrix Tablets.* AAPS PharmSciTech, 2008. **9**(2): p. 437-443.
96. Gorton, J. and R. Jameson, *Complexes of doubly chelating ligands. Part I. Proton and copper (II) complexes of L-beta-(3,4-dihydroxyphemyl)alanine (DOPA).* Journal of the Chemical Society A, 1968: p. 2615-2618.

97. Zangaglia, R., et al., *Clinical Experiences with Levodopa Methyl Ester (Melevodopa) in Patiens with Parkinson Disease Experiencing Motor Fluctuations: an open-label observational study.* Clinical Neuropharmacology, 2010. **33**(2): p. 61-66.
98. Clissold, S., S. Lynch, and E. Sorkin, *Buflomedil.* Drugs, 1987. **33**(5): p. 430-460.
99. McCrystal, C., J. Ford, and A. Rajabi-Siahboomi, *A study on the interaction of water and cellulise ethers using differential scanning calorimetry.* Thermochimica Acta, 1997. **294**: p. 91-98.
100. Ford, J. and K. Mitchell, *Thermal analysis of gels and matrix tablets containing cellulose ethers.* Thermochimica Acta, 1995. **248**: p. 329-345.
101. Bettini, R., *Water as activating agent in swelling controlled drug delivery systems.* Proceeding of Frontiers in Water Biophysics, 2010.
102. Conte, U., et al., *Swelling-activated drug delivery systems.* Biomaterials, 1988. **9**: p. 489-493.
103. *Potassium Hydrogen Tartrate.* Available from: https://pubchem.ncbi.nlm.nih.gov/compound/23681127#section=Top.
104. *Potassium Hydrogen Phthalate.* Available from: http://www.chemicalbook.com/ChemicalProductProperty_EN_CB1132397.htm.
105. *Potassium Sulfate from ILO-ICSC 1451.* Available from: http://www.ilo.org/dyn/icsc/showcard.display?p_card_id=1451, 2006.
106. *Potassium Dihydrogen Phosphate from ILO-ICSC 1608.* Available from: http://www.ilo.org/dyn/icsc/showcard.display?p_card_id=1608, 2006.
107. *Potassium Oxalate.* Available from: http://www.chemicalbook.com/ChemicalProductProperty_EN_CB2162722.htm.
108. *Potassium Citrate.* Available from: https://pubchem.ncbi.nlm.nih.gov/compound/13344#section=Top.
109. Breitenbach, J., *Melt extrusion: from process to drug delivery tecnhology.* European Journal of Pharmaceutics and Biopharmaceutics, 2002. **54**: p. 107-117.
110. Maniruzzaman, M., et al., *A Review of Hot-Melt Extrusion: Process Technology to Pharmaceutical Products.* ISRN Pharmaceutics, 2012. **2012**: p. 9.
111. *http://www.rottendorf.com/index.php/hot-melt-extrusion.html.*
112. Hulsmann, S., et al., *Melt extrusion - an alternative method for enhancing the dissolution rate of 17beta-estradiol hemihydrate.* European Journal of Pharmaceutics and Biopharmaceutics, 2000. **49**(3): p. 237-242.

113. Munch, U., et al., *Orally administered solvent-free pharmaceutical preparation with delayed active-substance release, and a method of preparing the preparation*. 1995, Google Patents.
114. Gryczke, A., et al., *Development and evaluation of orally disintegrating tablets (ODTs) containing Ibuprofen granules prepared by hot melt extrusion.* Colloids and Surfaces B: Biointerfaces, 2011. **86**(2): p. 275-284.
115. Klein, C.E., et al., *The Tablet Formulation of Lopinavir/Ritonavir Provides Similar Bioavailability to the Soft-Gelatin Capsule Formulation With Less Pharmacokinetic Variability and Diminished Food Effect.* JAIDS Journal of Acquired Immune Deficiency Syndromes, 2007. **44**(4): p. 401-410 10.1097/QAI.0b013e31803133c5.
116. Li, Y., et al., *Interactions between drugs and polymers influencing hot melt extrusion.* Journal of Pharmacy and Pharmacology, 2013. **66**: p. 148-166.
117. Gryczke, A., *Solubility Parameters for Predictions of Drug/Polymer Miscibility in Hot-Melt Extruded Formulations*, in *Hot-melt Extrusion: Pharmaceutical Applications*, D. Douroumis, Editor. 2012, John Wiley & Sons Ltd.
118. Flory, P., *Thermodynamics of high polymer solutions.* Journal of Chemical Physics, 1941. **9**: p. 660-661.
119. Huggins, M., *Solutions of Long Chain Compounds.* Journal of Chemical Physics, 1941. **9**: p. 440.
120. Flory, P., *Principles of polymer chemistry*. 1953: Cornell University Press.
121. Marsac, P., S. Shamblin, and L. Taylor, *Theoretical and Practical Approaches for Predictions of Drug-Polymer Miscibility and Solubility.* Pharmaceutical Research, 2006. **23**(10): p. 2417-2426.
122. Hough, W., et al., *The third evolution of ionic liquids: active pharmaceutical ingredients.* New Journal of Chemistry, 2007. **31**: p. 1429-1436.
123. Censi, R., et al., *Sodium ibuprofen dihydrate and anhydrous. Study of the dehydration and hydration mechanisms.* Journal of Thermal Analysis and Calorimetry, 2013. **111**: p. 2009-2018.
124. Evonik, *EUDRAGIT RL 110, EUDRAGIT RL PO, EUDRAGIT RS 100 and EUDRAGIT RS PO. Technical information.*
125. Rowe, R., P. Sheskey, and M. Quinn, *Polyethylene Glycol*, in *Handbook of Pharmaceutical Excipients*, R. Rowe, P. Sheskey, and M. Quinn, Editors. 2009, Pharmaceutical Press and American Pharmacists Association.

126. Zhang, G., et al., *Racemic Species of Sodium Ibuprofen: Characterization and Polymorphic Relationships.* Journal of Pharmaceutical Sciences, 2003. **92**(7): p. 1356-1366.

127. Zhang, Y. and D. Grant, *Similarity in structures of racemic and enantiomeric ibuprofen sodium dihydrate.* Acta Crystallographica, 2005. **C61**: p. m435-m438.

128. Rossi, P., et al., *Solid-Solid Transition between Hydrated Racemic Compound and Anhydrous Conglomerate in Na-Ibuprofen: A combined X-Ray Diffraction, Solid-State NMR, Calorimetric and Computational Study*. Crystal Growth & Design, 2014. **14**: p. 2441-2452.

129. *Martin's Physical Pharmacy and Pharmaceutical Sciences*, ed. P. Sinko. 2006: Lippincott Williams & Wilikins. 612.